Journal of Optimization, Differential Equations and Their Applications

ISSN (print) 2617-0108

ISSN (online) 2663-6824

Volume 29

Issue 1

2021

Online Edition at http://model-dnu.dp.ua

Journal of Optimization, Differential Equations and Their Applications

Editor-in-Chief
Peter I. Kogut
Department of Differential Equations
Oles Honchar Dnipro National University
72, Gagarin av., Dnipro 49010, Ukraine
(+380) 67631-6755

p.kogut@i.ua

EDITORIAL BOARD

Journal of Optimization, Differential Equations and Their Applications welcomes application-oriented articles with strong mathematical content in scientific areas such as deterministic and stochastic ordinary and partial differential equations, mathematical control theory, modern optimization theory, variational, topological and viscosity methods, qualitative analysis of solutions, approximation and numerical aspects. JODEA also provides a forum for research contributions on nonlinear differential equations and optimal control theory motivated by applications to applied sciences.
JODEA is published twice a year (in June and December).
ISSN (print) 2617–0108, ISSN (on-line) 2663–6824, DOI 10.15421/14212901.

JOURNAL OF OPTIMIZATION, DIFFERENTIAL EQUATIONS AND THEIR APPLICATIONS (JODEA)
Volume **29**, Issue **1**, June **2021**, pp. 1–31, DOI 10.15421/142101

ISSN (print) 2617–0108
ISSN (on-line) 2663–6824

SOLUTIONS TO A SIMPLIFIED INITIAL BOUNDARY VALUE PROBLEM FOR 1D HYPERBOLIC EQUATION WITH INTERIOR DEGENERACY

Vladimir L. Borsch*, Peter I. Kogut†

Communicated by Prof. G. Leugering

Abstract. A 1-parameter initial boundary value problem (IBVP) for a linear homogeneous degenerate wave equation (JODEA, 28(1), 1 вЂ“ 42) in a space-time rectangle is considered. The origin of degeneracy is the power law coefficient function with respect to the spatial distance to the symmetry line of the rectangle, the exponent being the only parameter of the problem, ranging in (0,1) and (1,2) and producing the weak and strong degeneracy respectively. In the case of weak degeneracy separation of variables is used in the rectangle to obtain the unique bounded continuous solution to the IBVP, having the continuous flux. In the case of strong degeneracy the IBVP splits into the two derived IBVPs posed respectively in left and right half-rectangles and solved separately using separation of variables. Continuous matching of the obtained left and right families of bounded solutions to the IBVPs results in a linear integro-differential equation of convolution type. The Laplace transformation is used to solve the equation and obtain a family of bounded solutions to the IBVP, having the continuous flux and depending on one undetermined function..

Key words: degenerate wave equation, separation of variables, linear integro-differential equation of convolution type, Laplace transformation.

2010 Mathematics Subject Classification: 35L05, 35L35, 35L80.

1. Introduction and Setting of the Problem

The current study is a sequel to [2] and deals with the following 1-parameter simplified initial boundary value problem (IBVP) for the degenerate wave equation in the space-time rectangle $[0, T] \times [-1, +1]$

$$\left\{\begin{array}{ll} \dfrac{\partial^2 u(t,x;\alpha)}{\partial t^2} = \dfrac{\partial}{\partial x}\left(a(x;\alpha)\,\dfrac{\partial u(t,x;\alpha)}{\partial x}\right), & (t,x) \in (0,T]\times(-1,+1)\,, \\ \left.\begin{array}{l} u(t,-1;\alpha) = h_2(t;\alpha) \\ u(t,+1;\alpha) = h_1(t;\alpha) \end{array}\right\}, & t \in [0,T]\,, \\ \left.\begin{array}{l} \dfrac{\partial u(0,x;\alpha)}{\partial t} = \overset{**}{u}(x;\alpha) \\ u(0,x;\alpha) = \overset{*}{u}(x;\alpha) \end{array}\right\}, & x \in [-1,+1]\,, \end{array}\right. \tag{1.1}$$

*Dept. of Differential Equations, Faculty of Mech & Math, Oles Honchar Dnipro National University, 72, Gagarin av., Dnipro, 49010, Ukraine, bvl@dsu.dp.ua

†Dept. of Differential Equations, Faculty of Mech & Math, Oles Honchar Dnipro National University, 72, Gagarin av., Dnipro, 49010, Ukraine, p.kogut@i.ua

where known control functions $h_1(t;\alpha), h_2(t;\alpha) \in \mathscr{C}^1[0,T]\bigcap\mathscr{C}^2(0,T]$ obey the compatibility conditions: $h_1(0;\alpha) = \overset{*}{u}(+1;\alpha)$, $h_1'(0;\alpha) = \overset{**}{u}(+1;\alpha)$, $h_2(0;\alpha) = \overset{*}{u}(-1;\alpha)$, and $h_2'(0;\alpha) = \overset{**}{u}(-1;\alpha)$, and the 1-parameter family of coefficient functions is defined as follows

$$a(x;\alpha) = |x|^\alpha, \qquad x \in [-1,+1]\,, \tag{1.2}$$

the parameter $\alpha \in (0,2)$, and all the dependent and independent variables are non-dimensional. Simplification of the IBVP (1.1) compared to that of [2] is in extending the power law for the coefficient function to the segment $[-1,+1]$. One should refer to [2] to find out more details on the problem formulation.

The degenerate wave equation of the IBVP (1.1) has non-unique one-sided solutions, obtained in [2] as the following power series

$$\begin{cases} u_{1,j}(t,x;\alpha) = \displaystyle\sum_{\gamma=0}^{\infty} U_{1,j,\gamma}(t;\alpha)\,|x|^{\gamma\theta}, \\ u_{3,j}(t,x;\alpha) = U_{3,j}(t;\alpha) + |x|^\nu\, U_{3,j,0}(t;\alpha)\,, \\ u_{5,j}(t,x;\alpha) = U_{5,j}(t;\alpha) + |x|^\nu \displaystyle\sum_{\gamma=0}^{\infty} U_{5,j,\gamma}(t;\alpha)\,|x|^{\gamma\theta}, \end{cases} \tag{1.3}$$

where $\nu = 1-\alpha$, $\theta = 2-\alpha$, the values $\{1,3,5\}$ of the first subscript k refer to the kind of the above solutions, and the values $\{1,2\}$ of the second subscript j refer to the values $x>0$ and $x<0$ respectively. The coefficient functions of the solutions $u_{1,j}(t,x;\alpha)$ and $u_{5,j}(t,x;\alpha)$ obey the following recurrence relations

$$\begin{cases} U''_{1,j,\gamma-1}(t;\alpha) = \gamma\theta\,[\gamma\theta-\nu]\,U_{1,j,\gamma}(t;\alpha)\,, \\ U''_{5,j,\gamma-1}(t;\alpha) = \gamma\theta\,[\gamma\theta+\nu]\,U_{5,j,\gamma}(t;\alpha)\,, \end{cases} \qquad \gamma\in\mathbb{N}\,.$$

and the function $U_{5,j}(t;\alpha)$ is linear: $U''_{5,j}(t;\alpha)=0$, whereas both coefficient functions $U_{3,j}(t;\alpha)$, $U_{3,j,0}(t;\alpha)$ are linear: $U''_{3,j}(t;\alpha) = 0$, $U''_{3,j,0}(t) = 0$. Note, that the solution of the third kind is derived from the fifth one when $U''_{5,j,0}(t;\alpha)=0$.

The solution of the first kind is bounded for $\alpha\in(0,2)$, whereas the solutions of the third and fifth kind are bounded for $\alpha\in(0,1]$ and unbounded for $\alpha\in(1,2)$. An other representation of the solutions of the first and fifth kinds, showing their relation to the Bessel functions of the first kind and orders $\mp\varrho$, reads as follows

$$\begin{cases} u_{1,j}(t,x;\alpha) = |x|^{\frac{\nu}{2}}\left(s^{-\varrho}\displaystyle\sum_{\gamma=0}^{\infty} U_{1,j,\gamma}(t;\alpha)\,s^{2\gamma}\right), \\ u_{5,j}(t,x;\alpha) = U_{5,j}(t;\alpha) + |x|^{\frac{\nu}{2}}\left(s^{+\varrho}\displaystyle\sum_{\gamma=0}^{\infty} U_{5,j,\gamma}(t;\alpha)\,s^{2\gamma}\right), \end{cases} \tag{1.4}$$

where $\varrho\theta = \nu$ and the auxiliary variable $s = |x|^{\frac{\theta}{2}}$ is used.

The spatial derivatives of the solutions (1.3)

$$q_{k,j}(t,x;\alpha) = \frac{\partial u_{k,j}}{\partial x} = \mathrm{sign}\,(x) \begin{cases} |x|^{\nu}\,\theta \displaystyle\sum_{\gamma=1}^{\infty} \gamma\, U_{1,j,\gamma}(t;\alpha)\,|x|^{(\gamma-1)\theta}, \\ |x|^{-\alpha}\,\nu\, U_{3,j,0}(t;\alpha)\,, \\ |x|^{-\alpha} \displaystyle\sum_{\gamma=0}^{\infty} [\nu+\gamma\theta]\, U_{5,j,\gamma}(t;\alpha)\,|x|^{\gamma\theta} \end{cases} \tag{1.5}$$

are bounded in the case of weak degeneracy ($\alpha \in (0,1)$) and unbounded in the case of strong degeneracy ($\alpha \in (1,2)$) for the first kind, and always unbounded for the third and fifth kinds. The fluxes of the solutions (1.3)

$$-f_{k,j}(t,x;\alpha) = a\, q_{k,j} = \begin{cases} x\,\theta \displaystyle\sum_{\gamma=1}^{\infty} \gamma\, U_{1,j,\gamma}(t;\alpha)\,|x|^{(\gamma-1)\theta}, \\ \mathrm{sign}\,(x)\,\nu\, U_{3,j,0}(t;\alpha)\,, \\ \mathrm{sign}\,(x) \displaystyle\sum_{\gamma=0}^{\infty} [\nu+\gamma\theta]\, U_{5,j,\gamma}(t;\alpha)\,|x|^{\gamma\theta} \end{cases} \tag{1.6}$$

are bounded, but have quite different nature at the interior degeneracy: the flux of the first kind is vanishing at the degeneracy and, therefore, continuous; whereas the two others have generally non-vanishing values of opposite signs. The odd-behavior of the one-sided fluxes of the fifth kind prompts us the way of their continuous matching.

In the current study we shall try to continuously match the one-sided solutions (1.3) of the first and fifth kinds (therefore, the subscript k takes values $\{1,5\}$) to find bounded solutions to the IBVP (1.1) using the method of separation of variables (SV) and implying an analogy of the required solutions with a continuous imaginary 'string'. The current study is arranged as follows.

In Section 2 we: 1) give some preliminaries on SV in relation to the original IBVP in the case of weak degeneracy and based on the one-sided solutions of kinds $1,5$, both continuous and improving to have the continuous fluxes; 2) split the original IBVP posed in the space-time rectangle $[0,T]\times[-1,+1]$ and describing the behavior of the continuous 'string', into the derived IBVP_2 posed in the left space-time rectangle $[0,T]\times[-1,0]$) and the IBVP_1 posed in the right space-time rectangle $[0,T]\times[0,+1]$), describing respectively the behaviour of the left and the right parts of the 'string' separately in the case of strong degeneracy; 3) formulate the conditions for continuous matching the bounded solutions $u_{1,j}(t,x;\alpha)$ to the IBVP_j and expressing the integrity of the 'string' and continuity of the flux; 4) apply the method of SV to find the unique bounded solutions $u(t,x;\alpha)$ to the IBVP in the case of weak degeneracy, continuous and having the continuous flux; 5) apply the method of SV to find families of bounded solution $u_{1,j}(t,x;\alpha)$ to the IBVP$_j$ in the case of strong degeneracy, having the continuous flux and depending on undetermined functions $h_{j+2}(t;\alpha)\in\mathscr{C}^1[0,T]\bigcap\mathscr{C}^2(0,T]$; 6) apply the continuity condition to the solutions $u_{1,j}(t,x;\alpha)$ to derive a linear integro-differential equation of convolution type with respect to the required functions $h_{j+2}(t;\alpha)$.

In Section 3 we solve the above integro-differential equation with respect to the difference $h_3(t;\alpha)-h_4(t;\alpha)$ and show that one of the two functions can be chosen quite freely, that is, the bounded solutions to the IBVP of the resulting family are continuous and have the continuous fluxes.

In Section 4 we summarize the results obtained and some observations on the procedures applied.

In Section 2 we place some useful rules to calculate the coefficients of expansions in the series of the eigenfunctions used in Section 2.

2. Method of Separation of Variables

2.1. Preliminaries to SV

Implementing SV to the IBVP (1.1) is essentially based on the following two assertions.

Proposition 2.1. *Let the following incomplete 1-parameter boundary value problems be given*

$$\begin{cases} \big[a(x;\alpha)\,Z_j'(x;\alpha)\big]' + \lambda_j(\alpha)\,Z_j(x;\alpha) = 0\,, & 0<|x|<1\,, \\ Z_j(\mp 1;\alpha) = 0\,, \end{cases} \tag{2.1}$$

then: 1) *the eigenvalues and the eigenfunctions of the problems of the two kinds* $\big(\lambda_{k,j,\mu}(\alpha), Z_{k,j,\mu}(x;\alpha)\big) \equiv \big(\lambda_{k,\mu}(\alpha), Z_{k,\mu}(x;\alpha)\big)$ (*marked with the first subscript* $k\in\{1,5\}$) *are defined as follows*

$$\begin{cases} \lambda_{1,\mu}(\alpha) = \left(\dfrac{\theta}{2}\,s_{1,\mu}\right)^2 \equiv \sigma_{1,\mu}^2\,, & Z_{1,\mu}(x;\alpha) = |x|^{\frac{\nu}{2}}\,\mathsf{J}_{-\varrho}\!\left(s_{1,\mu}\,|x|^{\frac{\theta}{2}}\right), \\ \lambda_{5,\mu}(\alpha) = \left(\dfrac{\theta}{2}\,s_{5,\mu}\right)^2 \equiv \sigma_{5,\mu}^2\,, & Z_{5,\mu}(x;\alpha) = |x|^{\frac{\nu}{2}}\,\mathsf{J}_{+\varrho}\!\left(s_{5,\mu}\,|x|^{\frac{\theta}{2}}\right), \end{cases} \tag{2.2}$$

where ν,θ,ϱ *are the* α*-dependent quantities*

$$\nu(\alpha) = 1-\alpha\,, \qquad \theta(\alpha) = 2-\alpha\,, \qquad \varrho(\alpha) = \frac{\nu}{\theta} = \frac{1-\alpha}{2-\alpha}\,; \tag{2.3}$$

$\mathsf{J}_{\mp\varrho}(s)$ *are the Bessel functions of the first kind and orders* $\mp\varrho$ [7]; $\big\{s_{k,\mu}\big\}_{\mu=1}^{\infty}$ *are the unbounded monotonically increasing sequences of the zeros of functions*

$\mathtt{J}_{\mp\varrho}(s)$; 2) *the eigenfunctions* (2.2) *of each kind are orthogonal in* $\mathscr{L}_2(-1,0)$ *and* $\mathscr{L}_2(0,+1)$ *respectively, that is*

$$\mp\int_0^{\mp 1} Z_{k,\mu}(x;\alpha)\, Z_{k,\gamma}(x;\alpha)\,\mathrm{d}x = \frac{1}{\theta}\,\mathtt{J}^2_{\mp\varrho+1}(s_{k,\mu})\,\delta_{\mu,\gamma} \equiv \|Z_{k,\mu}\|^2\delta_{\mu,\gamma}\,, \tag{2.4}$$

where $\mu,\gamma\in\mathbb{N}$, *and* $\delta_{\mu,\gamma}$ *is the Kronecker delta.*

Proof. We start proving the first part of the proposition from representing the eigenfunctions (2.2) in such a generic formulation

$$Z_{k,\mu}(x;\alpha) = |x|^{\frac{\nu}{2}}\,\mathtt{Z}_\varrho(s)\,, \qquad s = s_{k,\mu}\,|x|^{\frac{\theta}{2}}\,, \tag{2.5}$$

where the generic Bessel function $\mathtt{Z}_\varrho(s)$ stands for the Bessel functions $\mathtt{J}_{\mp\varrho}(s)$ of the first kind and satisfies the ordinary differential equation

$$s^2\,\mathtt{Z}''_\varrho(s) + s\,\mathtt{Z}'_\varrho(s) + \left(s^2-\varrho^2\right)\mathtt{Z}_\varrho(s) = 0\,.$$

Differentiating the generic eigenfunction (2.5) with respect to x yields to

$$Z'_{k,\mu}(x;\alpha) = \operatorname{sign}(x)\left[\frac{\nu}{2}\,|x|^{\frac{\nu}{2}-1}\,\mathtt{Z}_\varrho(s) + \frac{\theta}{2}\,s_{k,\mu}\,|x|^{\frac{\nu}{2}+\frac{\theta}{2}-1}\,\mathtt{Z}'_\varrho(s)\right],$$

$$a(x;\alpha)Z'_{k,\mu}(x;\alpha) = \operatorname{sign}(x)\left[\frac{\nu}{2}\,|x|^{-\frac{\nu}{2}}\,\mathtt{Z}_\varrho(s) + \frac{\theta}{2}\,s_{k,\mu}\,|x|^{-\frac{\nu}{2}+\frac{\theta}{2}}\,\mathtt{Z}'_\varrho(s)\right],$$

$$\begin{aligned}\left[a(x;\alpha)Z'_{k,\mu}(x;\alpha)\right]' &= |x|^{-\frac{\nu}{2}-1}\left[-\left(\frac{\nu}{2}\right)^2\mathtt{Z}_\varrho(s) + \left(\frac{\theta}{2}\right)^2\left(s^2\,\mathtt{Z}''_\varrho(s) + s\,\mathtt{Z}'_\varrho(s)\right)\right]\\ &= -\left(\frac{\theta}{2}\,s_{k,\mu}\right)^2|x|^{\frac{\nu}{2}}\,\mathtt{Z}_\varrho(s) = -\sigma^2_{k,\mu}\,Z_{k,\mu}(x)\,,\end{aligned}$$

wherefrom we conclude, that the functions (2.2) indeed satisfy the differential equation of the problems (2.1). This completes the proof of the first part of the proposition.

To prove the second part of the proposition, we use:

1) the variable transformation $s = x^{\frac{\theta}{2}}$ when calculating the integral

$$\int_0^1 Z_{k,\mu}(x;\alpha)\,Z_{k,\gamma}(x;\alpha)\,\mathrm{d}x = \frac{2}{\theta}\int_0^1 s\,\mathtt{Z}_\varrho\left(s_{k,\mu}\,s\right)\mathtt{Z}_\varrho\left(s_{k,\gamma}\,s\right)\mathrm{d}s\,;$$

2) the known value of the last integral [7]

$$\int_0^1 s\,\mathtt{Z}_\varrho\left(s_{k,\mu}\,s\right)\mathtt{Z}_\varrho\left(s_{k,\gamma}\,s\right)\mathrm{d}s = \frac{1}{2}\,\mathtt{Z}^2_{\varrho+1}(s_{k,\mu})\,\delta_{\mu,\gamma}\,.$$

This completes the proof of the second part of the proposition. □

Proposition 2.2. *Let the following composite 1-parameter boundary value problem be given*

$$\begin{cases} \big[a(x;\alpha)\,X'(x;\alpha)\big]' + \lambda(\alpha)\,X(x;\alpha) = 0\,, \qquad 0 < |x| < 1\,, \\ X(\mp 1;\alpha) = 0\,, \qquad \big[X(x;\alpha)\big]\big|_{x=0-0} = \big[X(x;\alpha)\big]\big|_{x=0+0}\,, \\ \big[a(x;\alpha)\,X'(x;\alpha)\big]\big|_{x=0-0} = \big[a(x;\alpha)\,X'(x;\alpha)\big]\big|_{x=0+0}\,, \end{cases} \tag{2.6}$$

then: 1) *in the case of weak degeneracy, the eigenvalues and the eigenfunctions of the problem of the two kinds* (*marked with the first subscript* $k \in \{1,5\}$) *are defined as follows*

$$\begin{cases} \lambda_{1,\mu}(\alpha) = \sigma^2_{1,\mu}\,, \qquad X_{1,\mu}(x;\alpha) = \qquad\qquad Z_{1,\mu}(x;\alpha)\,, \\ \lambda_{5,\mu}(\alpha) = \sigma^2_{5,\mu}\,, \qquad X_{5,\mu}(x;\alpha) = \operatorname{sign}(x)\,Z_{5,\mu}(x;\alpha)\,, \end{cases} \tag{2.7}$$

where $\sigma^2_{k,\mu}$ *and* $Z_{k,\mu}(x;\alpha)$ *are given in* (2.2) *of Proposition 2.1;* 2) *the eigenfunctions* (2.7) *of both kinds are orthogonal in* $\mathscr{L}_2(-1,+1)$, *that is*

$$\begin{cases} \displaystyle\int_{-1}^{+1} X_{k,\mu}(x;\alpha)\,X_{k,\gamma}(x;\alpha)\;dx = 2\,\|Z_{k,\mu}\|^2\delta_{\mu,\gamma} \equiv \|X_{k,\mu}\|^2\delta_{\mu,\gamma}\,, \\ \displaystyle\int_{-1}^{+1} X_{1,\mu}(x;\alpha)\,X_{5,\gamma}(x;\alpha)\;dx = 0\,. \end{cases} \tag{2.8}$$

Proof. From Proposition 2.1 it follows that the functions $X_{k,\mu}(x;\alpha)$ (2.7) satisfy the differential equation of the boundary value problem, hence, we concentrate our efforts on calculating the one-sided values of $X_{k,\mu}(x;\alpha)$ and $a(x;\alpha)\,X'_{k,\mu}(x;\alpha)$ at the interior degeneracy location. Substituting the known power series [7]

$$\mathtt{Z}_\varrho(s) = \mathtt{J}_{\mp\varrho}(s) = \Big(\frac{s}{2}\Big)^{\mp\varrho} \sum_{\gamma=0}^{\infty} \frac{(-1)^\gamma}{\gamma!\,\Gamma(1+\gamma\mp\varrho)}\,\Big(\frac{s}{2}\Big)^{2\gamma} \tag{2.9}$$

into (2.5) obtains the series representations for the quantities of interest

$$\begin{cases} X_{1,\mu}(x;\alpha) = \Big(\frac{s_{1,\mu}}{2}\Big)^{-\varrho} \displaystyle\sum_{\gamma=0}^{\infty} \frac{(-1)^\gamma\,|x|^{\gamma\theta}}{\gamma!\,\Gamma(1-\varrho+\gamma)}\,\Big(\frac{s_{1,\mu}}{2}\Big)^{2\gamma}\,, \\ X_{5,\mu}(x;\alpha) = \operatorname{sign}(x)\,|x|^\nu\,\Big(\frac{s_{5,\mu}}{2}\Big)^{+\varrho} \displaystyle\sum_{\gamma=0}^{\infty} \frac{(-1)^\gamma\,|x|^{\gamma\theta}}{\gamma!\,\Gamma(1+\varrho+\gamma)}\,\Big(\frac{s_{5,\mu}}{2}\Big)^{2\gamma}\,, \end{cases} \tag{2.10}$$

$$\begin{cases} a(x;\alpha)\,X'_{1,\mu}(x;\alpha) = \Big(\frac{s_{1,\mu}}{2}\Big)^{-\varrho}\,\theta\,x \displaystyle\sum_{\gamma=1}^{\infty} \frac{(-1)^\gamma\gamma\,|x|^{(\gamma-1)\theta}}{\gamma!\,\Gamma(1-\varrho+\gamma)}\,\Big(\frac{s_{1,\mu}}{2}\Big)^{2\gamma}\,, \\ a(x;\alpha)\,X'_{5,\mu}(x;\alpha) = \Big(\frac{s_{5,\mu}}{2}\Big)^{+\varrho} \displaystyle\sum_{\gamma=0}^{\infty} \frac{(-1)^\gamma\,[\nu+\gamma\theta]\,|x|^{\gamma\theta}}{\gamma!\,\Gamma(1+\varrho+\gamma)}\,\Big(\frac{s_{5,\mu}}{2}\Big)^{2\gamma}\,. \end{cases} \tag{2.11}$$

The resulting series (2.10), (2.11) yield to the required values

$$\begin{cases} X_{1,\mu}(0;\alpha) = \Big(\frac{s_{1,\mu}}{2}\Big)^{-\varrho} \dfrac{1}{\Gamma(1-\varrho)}\,, & \alpha \in (0,2)\,, \\ X_{5,\mu}(0;\alpha) = 0\,, & \alpha \in (0,1)\,, \\ \operatorname{sign}(x) \lim\limits_{x\to 0} |x|^{-\nu} X_{5,\mu}(x;\alpha) = \Big(\frac{s_{5,\mu}}{2}\Big)^{+\varrho} \dfrac{1}{\Gamma(1+\varrho)}\,, & \alpha \in [1,2)\,, \end{cases} \tag{2.12}$$

$$\begin{cases} \big[a(x;\alpha)\, X'_{1,\mu}(x;\alpha)\big]\big|_{x=0} = 0\,, \\ \big[a(x;\alpha)\, X'_{5,\mu}(x;\alpha)\big]\big|_{x=0} = \Big(\frac{s_{5,\mu}}{2}\Big)^{\varrho} \dfrac{\nu}{\Gamma(1+\varrho)} \neq 0\,, \end{cases} \qquad \alpha \in (0,2)\,, \tag{2.13}$$

and this completes the proof of the first part of the proposition.

Orthogonality of the eigenfunctions of each kind directly follows from Proposition 2.1, therefore, our concern is orthogonality of the eigenfunctions of the different kinds, that can be quite easily proved, indeed,

$$\begin{aligned} &\int_{-1}^{+1} X_{1,\mu}(x;\alpha)\, X_{5,\gamma}(x;\alpha)\; dx \\ =\ &\int_{-1}^{0} X_{1,\mu}(x;\alpha)\, X_{5,\gamma}(x;\alpha)\; dx + \int_{0}^{+1} X_{1,\mu}(x;\alpha)\, X_{5,\gamma}(x;\alpha)\; dx \\ =\ &-\int_{-1}^{0} Z_{1,\mu}(x;\alpha)\; Z_{5,\gamma}(x;\alpha)\; dx + \int_{0}^{+1} Z_{1,\mu}(x;\alpha)\; Z_{5,\gamma}(x;\alpha)\; dx \\ =\ &-\int_{0}^{+1} Z_{1,\mu}(x;\alpha)\; Z_{5,\gamma}(x;\alpha)\; dx + \int_{0}^{+1} Z_{1,\mu}(x;\alpha)\; Z_{5,\gamma}(x;\alpha)\; dx = 0\,. \end{aligned}$$

This completes the proof of the second part of the proposition. □

Before implementing the method of SV, we make some notes.

First, to build the eigenfunctions $Z_{5,\mu}(x;\alpha)$, we use the Bessel functions of the first kind and order $+\varrho$, rather than the proper Neumann functions [7], to simplify our analysis of the IBVP. It means that the integer values of order $-\varrho$

$$-\varrho = -\frac{1-\alpha}{2-\alpha} = m \in \mathbb{Z} \qquad \Leftrightarrow \qquad \alpha = \frac{2m+1}{m+1}$$

can not be considered, i. e., the values of $\alpha = 1, \frac{3}{2}, \frac{5}{3}, \frac{7}{4}$, etc., produced by the values of $m = 0, 1, 2, 3$, etc.

Second, to guarantee uniform convergency of the expansions in series of the eigen-functions $Z_{1,\mu}(x;\alpha)$, $X_{k,\mu}(x;\alpha)$, based on the Bessel functions $\mathtt{J}_{\mp\varrho}(s)$, we have to impose the following restriction [6, 7] on the values of ϱ

$$-\frac{1}{2} \leqslant \varrho = \frac{1-\alpha}{2-\alpha} \leqslant +\frac{1}{2}\,.$$

Third, to solve the IBVP (1.1) in the case of weak degeneracy, we apply the bounded eigenfunctions of Prop. 2.2.

Fourth, in the case of weak degeneracy we reduce solving the IBVP (1.1) to the following two-step procedure: 1) solving the derived initial boundary value problems

$$\begin{cases} \dfrac{\partial^2 u_1(t,x;\alpha)}{\partial t^2} = \dfrac{\partial}{\partial x}\left(a(x;\alpha)\,\dfrac{\partial u_1(t,x;\alpha)}{\partial x}\right), & (t,x)\in(0,T]\times(0,+1)\,, \\ u_1(t,+1;\alpha) = h_1(t)\,, & t\in[0,T]\,, \\ \left.\begin{aligned} \dfrac{\partial u_1(0,x;\alpha)}{\partial t} &= \overset{**}{u}(x) \\ u_1(0,x;\alpha) &= \overset{*}{u}(x) \end{aligned}\right\}, & x\in[0,+1]\,, \end{cases} \tag{2.14}$$

$$\begin{cases} \dfrac{\partial^2 u_2(t,x;\alpha)}{\partial t^2} = \dfrac{\partial}{\partial x}\left(a(x;\alpha)\,\dfrac{\partial u_2(t,x;\alpha)}{\partial x}\right), & (t,x)\in(0,T]\times(-1,0)\,, \\ u_2(t,-1;\alpha) = h_2(t)\,, & t\in[0,T]\,, \\ \left.\begin{aligned} \dfrac{\partial u_2(0,x;\alpha)}{\partial t} &= \overset{**}{u}(x) \\ u_2(0,x;\alpha) &= \overset{*}{u}(x) \end{aligned}\right\}, & x\in[-1,0]\,, \end{cases} \tag{2.15}$$

posed in the 'right' $[0,T]\times[0,+1]$ and the 'left' $[0,T]\times[-1,0]$ space-time rectangles and referred to as the IBVP_1 and the IBVP_2 respectively; 2) matching the solutions $u_1(t,x;\alpha)$ and $u_2(t,x;\alpha)$ to the above initial boundary value problems

$$u(t,x;\alpha) = \begin{cases} u_2(t,x;\alpha)\,, & (t,x)\in[0,T]\times[-1,0]\,, \\ u_1(t,x;\alpha)\,, & (t,x)\in[0,T]\times[0,+1]\,, \end{cases} \tag{2.16}$$

by imposing the condition of continuity at the degeneracy segment $[0,T]\times\{0\}$

$$u_2(t,0;\alpha) = u_1(t,0;\alpha)\,, \qquad t\in[0,T]\,. \tag{2.17}$$

When applying the above procedure, we drop the subscript k, indicating the first kind of the solutions (1.3), the only one bounded in the case of strong degeneracy, therefore, the only remaining subscript is j.

2.2. Implementing SV to the IBVP

In the current section our concern is the bounded solution to the IBVP in the case of weak degeneracy. The required solution is assumed to have the following representation

$$u(t,x;\alpha) = v(t,x;\alpha) + w(t,x;\alpha)\,, \tag{2.18}$$

where: a) the function $v(t,x;\alpha)$ is also required; b) the function $w(t,x;\alpha)$ is given as follows

$$w(t,x;\alpha) = \phi_{j=2}(x;\alpha)\, h_{j=2}(t;\alpha) + \phi_{j=1}(x;\alpha)\, h_{j=1}(t;\alpha)\,, \tag{2.19}$$

c) the smooth blending functions $\phi_1(x;\alpha)$, $\phi_2(x;\alpha)$ satisfy the following boundary and regularity conditions, respectively

$$\begin{cases} \phi_1(+1;\alpha) = 1\,, & \phi_1(-1;\alpha) = 0\,, \\ \phi_2(+1;\alpha) = 0\,, & \phi_2(-1;\alpha) = 1\,; \end{cases} \tag{2.20}$$

$$\begin{cases} \psi_1(x;\alpha) \equiv \varphi_1'(x;\alpha) = \big[a(x;\alpha)\, \phi_1'(x;\alpha)\big]' \in \mathscr{C}[-1,+1]\,, \\ \psi_2(x;\alpha) \equiv \varphi_2'(x;\alpha) = \big[a(x;\alpha)\, \phi_2'(x;\alpha)\big]' \in \mathscr{C}[-1,+1]\,. \end{cases} \tag{2.21}$$

Combining (2.18) – (2.20) yields to: a) the initial conditions for the required function $v(t,x;\alpha)$

$$\begin{cases} v(0,x;\alpha) = u(0,x;\alpha) - w(0,x;\alpha) \equiv \overset{*}{v}(x;\alpha)\,, \\ \dfrac{\partial v(0,x;\alpha)}{\partial t} = \dfrac{\partial u(0,x;\alpha)}{\partial t} - \dfrac{\partial w(0,x;\alpha)}{\partial t} \equiv \overset{**}{v}(x;\alpha)\,, \end{cases} \tag{2.22}$$

and b) reformulation of the IBVP into the following one with respect to $v(t,x;\alpha)$

$$\begin{cases} \dfrac{\partial^2 v}{\partial t^2} - \dfrac{\partial}{\partial x}\left(a\, \dfrac{\partial v}{\partial x}\right) = g\,, & (t,x) \in (0,T]\times(-1,+1)\,, \\ \left.\begin{array}{l} v(t,-1;\alpha) = 0 \\ v(t,+1;\alpha) = 0 \end{array}\right\}, & t \in [0,T]\,, \\ \left.\begin{array}{l} \dfrac{\partial v(0,x;\alpha)}{\partial t} = \overset{**}{v}(x;\alpha) \\ v(0,x;\alpha) = \overset{*}{v}(x;\alpha) \end{array}\right\}, & x \in [-1,+1]\,, \end{cases} \tag{2.23}$$

where the right-hand side of the above degenerate wave equation reads

$$g(t,x;\alpha) = -\frac{\partial^2 w(t,x;\alpha)}{\partial t^2} + \frac{\partial}{\partial x}\left(a(x;\alpha)\, \frac{\partial w(t,x;\alpha)}{\partial x}\right). \tag{2.24}$$

Then the initial functions (2.22) and the right-hand side (2.24) are expanded into the series

$$\begin{cases} \overset{*}{v}(x;\alpha) = \displaystyle\sum_{\mu=1}^{\infty} \overset{*}{v}_{1,\mu}(\alpha)\, X_{1,\mu}(x;\alpha) + \sum_{\mu=1}^{\infty} \overset{*}{v}_{5,\mu}(\alpha)\, X_{5,\mu}(x;\alpha)\,, \\ \overset{**}{v}(x;\alpha) = \displaystyle\sum_{\mu=1}^{\infty} \overset{**}{v}_{1,\mu}(\alpha)\, X_{1,\mu}(x;\alpha) + \sum_{\mu=1}^{\infty} \overset{**}{v}_{5,\mu}(\alpha)\, X_{5,\mu}(x;\alpha)\,, \end{cases} \tag{2.25}$$

$$g(t,x;\alpha) = \sum_{\mu=1}^{\infty} g_{1,\mu}(t;\alpha)\, X_{1,\mu}(x;\alpha) + \sum_{\mu=1}^{\infty} g_{5,\mu}(t;\alpha)\, X_{5,\mu}(x;\alpha)\,, \tag{2.26}$$

where the functions $X_{k,\mu}(x;\alpha)$ are defined in Prop. 2.2 and the coefficients are calculated directly by integration

$$\begin{cases} \overset{*}{v}_{k,\mu}(\alpha) = \dfrac{1}{\|X_{k,\mu}\|^2} \displaystyle\int_{-1}^{+1} \overset{*}{v}(x;\alpha)\, X_{k,\mu}(x;\alpha)\; dx\,, \\ \overset{**}{v}_{k,\mu}(\alpha) = \dfrac{1}{\|X_{k,\mu}\|^2} \displaystyle\int_{-1}^{+1} \overset{**}{v}(x;\alpha)\, X_{k,\mu}(x;\alpha)\; dx\,, \\ g_{k,\mu}(t;\alpha) = \dfrac{1}{\|X_{k,\mu}\|^2} \displaystyle\int_{-1}^{+1} g(t,x;\alpha)\, X_{k,\mu}(x;\alpha)\; dx\,. \end{cases} \tag{2.27}$$

Assuming that the ansatz for the required solution to the initial boundary value problem (2.23) to be as follows

$$v(t,x;\alpha) = \sum_{\mu=1}^{\infty} O_{1,\mu}(t;\alpha)\, X_{1,\mu}(x;\alpha) + \sum_{\mu=1}^{\infty} O_{5,\mu}(t;\alpha)\, X_{5,\mu}(x;\alpha)\,, \tag{2.28}$$

we obtain the Cauchy problems with respect to the desired coefficient functions of the ansatz

$$\begin{cases} O''_{k,\mu}(t;\alpha) + \sigma^2_{k,\mu} O_{k,\mu}(t;\alpha) = g_{k,\mu}(t;\alpha)\,, \qquad t \in (0,T]\,, \\ \left.\begin{aligned} O'_{k,\mu}(0;\alpha) = \overset{**}{v}_{k,\mu}(\alpha) \\ O_{k,\mu}(0;\alpha) = \overset{*}{v}_{k,\mu}(\alpha) \end{aligned}\right\}. \end{cases} \tag{2.29}$$

The resulting expressions for the coefficients, after applying some trivial trigonometric manipulations, can be presented in the convolution form as follows

$$\begin{aligned} O_{k,\mu}(t;\alpha) &= \overset{*}{v}_{k,\mu}(\alpha)\, \cos\big(\sigma_{k,\mu} t\big) + \sigma^{-1}_{k,\mu}\, \overset{**}{v}_{k,\mu}(\alpha)\, \sin\big(\sigma_{k,\mu} t\big) \\ &\quad + \sigma^{-1}_{k,\mu} \int_0^t g_{k,\mu}(z;\alpha)\, \sin\big[\sigma_{k,\mu}(t-z)\big]\, \mathrm{d}z\,, \end{aligned}$$

or, shortly, as

$$\begin{cases} O_{k,\mu}(t;\alpha) = \overset{*}{v}_{k,\mu}(\alpha)\, \cos\big(\sigma_{k,\mu} t\big) + \sigma^{-1}_{k,\mu}\, \overset{**}{v}_{k,\mu}(\alpha)\, \sin\big(\sigma_{k,\mu} t\big) \\ \qquad\qquad + \sigma^{-1}_{k,\mu}\, g_{k,\mu}(t;\alpha)\, \sin\big(\sigma_{k,\mu} t\big). \end{cases} \tag{2.30}$$

Finally, the representation (2.18) yields to the required unique bounded solution to the IBVP

$$\begin{cases} u(t,x;\alpha) = \displaystyle\sum_{\mu=1}^{\infty} O_{1,\mu}(t;\alpha)\, X_{1,\mu}(x;\alpha) \\ \qquad\qquad\quad + \displaystyle\sum_{\mu=1}^{\infty} O_{5,\mu}(t;\alpha)\, X_{5,\mu}(x;\alpha) \\ \qquad\qquad\quad + \phi_2(x;\alpha)\, h_2(t;\alpha) + \phi_1(x;\alpha)\, h_1(t;\alpha)\,. \end{cases} \tag{2.31}$$

The above procedure can be readily interpreted in terms of decomposition of the functions $v(t,x;\alpha)$, $\overset{*}{v}(x;\alpha)$, $\overset{**}{v}(x;\alpha)$, $w(t,x;\alpha)$, and $g(t,x;\alpha)$ into their even and odd parts, for example

$$v(t,x;\alpha) = v_e(t,x;\alpha) + v_o(t,x;\alpha)\,, \qquad x \in [-1,+1]\,, \tag{2.32}$$

where both parts are defined as follows

$$\begin{cases} 2\, v_e(t,x;\alpha) = v(t,+x;\alpha) + v(t,-x;\alpha)\,, \\ 2\, v_o(t,x;\alpha) = v(t,+x;\alpha) - v(t,-x;\alpha)\,, \end{cases}$$

leading to decomposition of the initial boundary value problem (2.23) into the derived problems

$$\begin{cases} \dfrac{\partial^2 v_e}{\partial t^2} - \dfrac{\partial}{\partial x}\left(a\, \dfrac{\partial v_e}{\partial x}\right) = g_e\,, & (t,x) \in (0,T]\times(-1,+1)\,, \\ \left.\begin{array}{l} v_e(t,-1;\alpha) = 0 \\ v_e(t,+1;\alpha) = 0 \end{array}\right\}, & t \in [0,T]\,, \\ \left.\begin{array}{r} \dfrac{\partial v_e(0,x;\alpha)}{\partial t} = \overset{**}{v}_e(x;\alpha) \\ v_e(0,x;\alpha) = \overset{*}{v}_e(x;\alpha) \end{array}\right\}, & x \in [-1,+1]\,, \end{cases}$$

$$\begin{cases} \dfrac{\partial^2 v_o}{\partial t^2} - \dfrac{\partial}{\partial x}\left(a\, \dfrac{\partial v_o}{\partial x}\right) = g_o\,, & (t,x) \in (0,T]\times(-1,+1)\,, \\ \left.\begin{array}{l} v_o(t,-1;\alpha) = 0 \\ v_o(t,+1;\alpha) = 0 \end{array}\right\}, & t \in [0,T]\,, \\ \left.\begin{array}{r} \dfrac{\partial v_o(0,x;\alpha)}{\partial t} = \overset{**}{v}_o(x;\alpha) \\ v_o(0,x;\alpha) = \overset{*}{v}_o(x;\alpha) \end{array}\right\}, & x \in [-1,+1]\,. \end{cases}$$

Applying SV to the above problems yields to the bounded solutions in the form of the following series

$$\begin{cases} v_e(t,x;\alpha) = \sum\limits_{\mu=1}^{\infty} O_{e,\mu}(t;\alpha)\, X_{1,\mu}(x;\alpha)\,, \\[2ex] v_o(t,x;\alpha) = \sum\limits_{\mu=1}^{\infty} O_{o,\mu}(t;\alpha)\, X_{5,\mu}(x;\alpha)\,, \end{cases} \tag{2.33}$$

where the coefficient functions $O_{e,\mu}(t;\alpha)$ and $O_{o,\mu}(t;\alpha)$ are evidently the solutions to respectively the same Cauchy problems (2.29). And eventually, using the representations (2.33), (2.32) and (2.18), the same unique bounded solution to the IBVP can be found again.

Calculating the flux of the obtained solution to the IBVP

$$\begin{cases} -f(t,x;\alpha) = \sum\limits_{\mu=1}^{\infty} O_{1,\mu}(t;\alpha)\, \big[a(x;\alpha)\, X'_{1,\mu}(x;\alpha)\big] \\[2ex] \qquad\qquad\quad + \sum\limits_{\mu=1}^{\infty} O_{5,\mu}(t;\alpha)\, \big[a(x;\alpha)\, X'_{5,\mu}(x;\alpha)\big] \\[2ex] \qquad\qquad\quad + \psi_2(x;\alpha)\, h_2(t;\alpha) + \psi_1(x;\alpha)\, h_1(t;\alpha) \end{cases} \tag{2.34}$$

proves that the following condition holds

$$f(t,0-0;\alpha) = f(t,0+0;\alpha)\,, \qquad t \in [0,T]\,, \tag{2.35}$$

due to: a) Prop. 2.2 and b) the regularity conditions (2.21) imposed on the blending functions $\phi_1(x;\alpha)$ and $\phi_2(x;\alpha)$ (or, shortly, due to continuous differentiability of the function $w(t,x;\alpha)$ (2.19)).

2.3. Implementing SV to the IBVP$_1$ and the IBVP$_2$

The required solutions to the IBVP$_j$ in the case of strong degeneracy are assumed to have the following representation

$$u_j(t,x;\alpha) = v_j(t,x;\alpha) + w_j(t,x;\alpha)\,, \tag{2.36}$$

where: a) the functions $v_j(t,x;\alpha)$ are required; b) the functions $w_j(t,x;\alpha)$ are given as follows

$$w_j(t,x;\alpha) = \phi_j(x;\alpha)\, h_j(t;\alpha) + \phi_{j+2}(x;\alpha)\, h_{j+2}(t;\alpha)\,, \tag{2.37}$$

c) the smooth blending functions $\phi_j(x;\alpha)$, $\phi_{j+2}(x;\alpha)$ satisfy the following boundary and regularity conditions, respectively:

$$\begin{cases} \phi_1(+1;\alpha) = 1\,, \qquad \phi_1(0;\alpha) = 0\,, \\[1ex] \phi_3(+1;\alpha) = 0\,, \qquad \phi_3(0;\alpha) = 1\,, \end{cases} \tag{2.38}$$

$$\begin{cases} \phi_2(-1;\alpha) = 1\,, & \phi_2(0;\alpha) = 0\,, \\ \phi_4(-1;\alpha) = 0\,, & \phi_4(0;\alpha) = 1\,, \end{cases} \tag{2.39}$$

$$\left.\begin{cases} \psi_1(x;\alpha) \equiv \varphi_1'(x;\alpha) = \big[a(x;\alpha)\,\phi_1'(x;\alpha)\big]' \\ \psi_3(x;\alpha) \equiv \varphi_3'(x;\alpha) = \big[a(x;\alpha)\,\phi_3'(x;\alpha)\big]' \end{cases}\right. \in \mathscr{C}[0,+1]\,, \tag{2.40}$$

$$\left.\begin{cases} \psi_2(x;\alpha) \equiv \varphi_2'(x;\alpha) = \big[a(x;\alpha)\,\phi_2'(x;\alpha)\big]' \\ \psi_4(x;\alpha) \equiv \varphi_4'(x;\alpha) = \big[a(x;\alpha)\,\phi_4'(x;\alpha)\big]' \end{cases}\right. \in \mathscr{C}[-1,0]\,; \tag{2.41}$$

d) $h_{j+2}(t;\alpha)$ are the required corrections to $v_j(t,x;\alpha)$ at the degeneracy segment.

Assuming that $h_{j+2}(0;\alpha) = \overset{*}{v}(0,x;\alpha)$, $h_{j+2}'(0;\alpha) = \overset{**}{v}(0,x;\alpha)$ and combining (2.36) – (2.39) yields to: *a*) the initial conditions for $v_j(t,x;\alpha)$

$$\begin{cases} v_j(0,x;\alpha) \;=\; u_j(0,x;\alpha) \;-\; w_j(0,x;\alpha) \equiv \overset{*}{v}_j(x;\alpha)\,, \\ \dfrac{\partial v_j(0,x;\alpha)}{\partial t} = \dfrac{\partial u_j(0,x;\alpha)}{\partial t} - \dfrac{\partial w_j(0,x;\alpha)}{\partial t} \equiv \overset{**}{v}_j(x;\alpha)\,, \end{cases} \tag{2.42}$$

and *b*) reformulation of the IBVP$_j$ into the following auxiliary IBVP$_j^a$ with respect to the functions $v_j(t,x;\alpha)$

$$\begin{cases} \dfrac{\partial^2 v_1}{\partial t^2} - \dfrac{\partial}{\partial x}\left(a\,\dfrac{\partial v_1}{\partial x}\right) = g_1\,, & (t,x) \in (0,T]\times(0,+1)\,, \\ v_1(t,+1;\alpha) = 0\,, & t \in [0,T]\,, \\ \left.\begin{array}{r} \dfrac{\partial v_1(0,x;\alpha)}{\partial t} = \overset{**}{v}_1(x;\alpha) \\ v_1(0,x;\alpha) \;= \overset{*}{v}_1(x;\alpha) \end{array}\right\}, & x \in [0,+1]\,, \end{cases} \tag{2.43}$$

$$\begin{cases} \dfrac{\partial^2 v_2}{\partial t^2} - \dfrac{\partial}{\partial x}\left(a\,\dfrac{\partial v_2}{\partial x}\right) = g_2\,, & (t,x) \in (0,T]\times(-1,0)\,, \\ v_2(t,-1;\alpha) = 0\,, & t \in [0,T]\,, \\ \left.\begin{array}{r} \dfrac{\partial v_2(0,x;\alpha)}{\partial t} = \overset{**}{v}_2(x;\alpha) \\ v_2(0,x;\alpha) \;= \overset{*}{v}_2(x;\alpha) \end{array}\right\}, & x \in [-1,0]\,, \end{cases} \tag{2.44}$$

where the right-hand sides of the above degenerate wave equations

$$g_j(t,x;\alpha) = -\frac{\partial^2 w_j(t,x;\alpha)}{\partial t^2} + \frac{\partial}{\partial x}\left(a(x;\alpha)\,\frac{\partial w_j(t,x;\alpha)}{\partial x}\right),$$

being expanded due to (2.37), read as follows

$$\begin{cases} g_j(t,x;\alpha) = -\,\phi_j(x;\alpha)\,h_2''(t;\alpha) - \phi_{j+2}(x;\alpha)\,h_{j+2}''(t;\alpha) \\ \qquad\qquad\qquad + \psi_j(x;\alpha)\,h_2(t;\alpha) + \psi_{j+2}(x;\alpha)\,h_{j+2}(t;\alpha)\,. \end{cases} \tag{2.45}$$

Then the initial functions (2.42) and the right-hand sides (2.45) are expanded into the series

$$\begin{cases} \overset{*}{v}_j(x;\alpha) = \sum_{\mu=1}^{\infty} \overset{*}{v}_{j,\mu}(\alpha)\, Z_{1,\mu}(x;\alpha)\,, \\ \overset{**}{v}_j(x;\alpha) = \sum_{\mu=1}^{\infty} \overset{**}{v}_{j,\mu}(\alpha)\, Z_{1,\mu}(x;\alpha)\,, \end{cases} \tag{2.46}$$

$$g_j(t,x;\alpha) = \sum_{\mu=1}^{\infty} g_{j,\mu}(t;\alpha)\, Z_{1,\mu}(x;\alpha)\,, \tag{2.47}$$

where the coefficients are determined straightforwardly by integration. The expanded forms of the coefficients in (2.47) are

$$\begin{aligned} g_{j,\mu}(t;\alpha) &= a_{j,\mu}(\alpha)\, h_j''(t;\alpha) + c_{j,\mu}(\alpha)\, h_{j+2}''(t;\alpha) \\ &\quad + b_{j,\mu}(\alpha)\, h_j(t;\alpha) + d_{j,\mu}(\alpha)\, h_{j+2}(t;\alpha)\,, \end{aligned} \tag{2.48}$$

where

$$\begin{cases} a_{1,\mu}(\alpha) = -\dfrac{1}{\|Z_{1,\mu}\|^2} \displaystyle\int_0^{+1} \phi_1(x;\alpha)\, Z_{1,\mu}(x;\alpha)\; dx\,, \\ b_{1,\mu}(\alpha) = +\dfrac{1}{\|Z_{1,\mu}\|^2} \displaystyle\int_0^{+1} \psi_1(x;\alpha)\, Z_{1,\mu}(x;\alpha)\; dx\,, \\ c_{1,\mu}(\alpha) = -\dfrac{1}{\|Z_{1,\mu}\|^2} \displaystyle\int_0^{+1} \phi_3(x;\alpha)\, Z_{1,\mu}(x;\alpha)\; dx\,, \\ d_{1,\mu}(\alpha) = +\dfrac{1}{\|Z_{1,\mu}\|^2} \displaystyle\int_0^{+1} \psi_3(x;\alpha)\, Z_{1,\mu}(x;\alpha)\; dx\,, \end{cases} \tag{2.49}$$

$$\begin{cases} a_{2,\mu}(\alpha) = -\dfrac{1}{\|Z_{1,\mu}\|^2} \displaystyle\int_{-1}^{0} \phi_2(x;\alpha)\, Z_{1,\mu}(x;\alpha)\; dx\,, \\ b_{2,\mu}(\alpha) = +\dfrac{1}{\|Z_{1,\mu}\|^2} \displaystyle\int_{-1}^{0} \psi_2(x;\alpha)\, Z_{1,\mu}(x;\alpha)\; dx\,, \\ c_{2,\mu}(\alpha) = -\dfrac{1}{\|Z_{1,\mu}\|^2} \displaystyle\int_{-1}^{0} \phi_4(x;\alpha)\, Z_{1,\mu}(x;\alpha)\; dx\,, \\ d_{2,\mu}(\alpha) = +\dfrac{1}{\|Z_{1,\mu}\|^2} \displaystyle\int_{-1}^{0} \psi_4(x;\alpha)\, Z_{1,\mu}(x;\alpha)\; dx\,. \end{cases} \tag{2.50}$$

And now substituting the ansatz for the solutions

$$v_j(t,x;\alpha) = \sum_{\mu=1}^{\infty} O_{j,\mu}(t;\alpha)\, Z_{1,\mu}(x;\alpha) \tag{2.51}$$

into the IBVP^a_j obtains the Cauchy problems for the coefficient functions

$$\begin{cases} O''_{j,\mu}(t;\alpha) + \sigma^2_{1,\mu} O_{j,\mu}(t;\alpha) = g_{j,\mu}(t;\alpha)\,, \qquad t \in (0,T]\,, \\ \left. \begin{aligned} O'_{j,\mu}(0;\alpha) = \overset{**}{v}_{j,\mu}(\alpha) \\ O_{j,\mu}(0;\alpha) = \overset{*}{v}_{j,\mu}(\alpha) \end{aligned} \right\}. \end{cases} \tag{2.52}$$

The resulting expressions for the coefficients can be readily presented in the convolution form as follows

$$\begin{cases} O_{j,\mu}(t;\alpha) = \overset{*}{v}_{j,\mu}(\alpha)\, \cos\big(\sigma_{1,\mu} t\big) + \sigma^{-1}_{k,\mu}\, \overset{**}{v}_{j,\mu}(\alpha)\, \sin\big(\sigma_{1,\mu} t\big) \\ \qquad\qquad + \sigma^{-1}_{1,\mu}\, g_{j,\mu}(t;\alpha)\, \sin\big(\sigma_{1,\mu} t\big)\,. \end{cases} \tag{2.53}$$

Finally, the representation (2.36) obtains the required solutions to the IBVP$_j$

$$\begin{cases} u_1(t,x;\alpha) = \displaystyle\sum_{\mu=1}^{\infty} O_{1,\mu}(t;\alpha)\, Z_{1,\mu}(x;\alpha) \\ \qquad\qquad + \phi_1(x;\alpha)\, h_1(t;\alpha) + \phi_3(x;\alpha)\, h_3(t;\alpha)\,, \end{cases} \tag{2.54}$$

$$\begin{cases} u_2(t,x;\alpha) = \displaystyle\sum_{\mu=1}^{\infty} O_{2,\mu}(t;\alpha)\, Z_{1,\mu}(x;\alpha) \\ \qquad\qquad + \phi_2(x;\alpha)\, h_2(t;\alpha) + \phi_4(x;\alpha)\, h_4(t;\alpha)\,. \end{cases} \tag{2.55}$$

Calculating the fluxes of the obtained solutions $u_j(t,x;\alpha)$

$$\begin{cases} -f_1(t,x;\alpha) = \displaystyle\sum_{\mu=1}^{\infty} O_{1,\mu}(t;\alpha)\, \big[a(x;\alpha)\, Z'_{1,\mu}(x;\alpha)\big] \\ \qquad\qquad + \psi_1(x;\alpha)\, h_1(t;\alpha) + \psi_3(x;\alpha)\, h_3(t;\alpha)\,, \end{cases} \tag{2.56}$$

$$\begin{cases} -f_2(t,x;\alpha) = \displaystyle\sum_{\mu=1}^{\infty} O_{2,\mu}(t;\alpha)\, \big[a(x;\alpha)\, Z'_{1,\mu}(x;\alpha)\big] \\ \qquad\qquad + \psi_2(x;\alpha)\, h_2(t;\alpha) + \psi_4(x;\alpha)\, h_4(t;\alpha)\,, \end{cases} \tag{2.57}$$

proves that the following condition holds

$$f_2(t,0-0;\alpha) = f_1(t,0+0;\alpha) = 0\,, \qquad t \in [0,T]\,, \tag{2.58}$$

yet before matching the solutions, due to: *a*) Prop. 2.1 and *b*) the regularity conditions (2.40) and (2.41) imposed on the blending functions $\phi_j(x;\alpha)$ and $\phi_{j+2}(x;\alpha)$ (or, shortly, due to continuous differentiability of the functions $w_j(t,x;\alpha)$ (2.37)).

2.4. Matching the Solutions to the IBVP$_1$ and the IBVP$_2$

To implement matching the obtained one-sided solutions $u_1(t, x; \alpha)$ (2.54) and $u_2(t, x; \alpha)$ (2.55), we will follow the procedure:

1) substitute the above solutions into the matching condition (2.17), as follows

$$\sum_{\mu=1}^{\infty} O_{2,\mu}(t; \alpha)\, Z_{1,\mu}(0; \alpha) + \phi_2(0; \alpha)\, h_2(t; \alpha) + \phi_4(0; \alpha)\, h_4(t; \alpha)$$

$$= \sum_{\mu=1}^{\infty} O_{1,\mu}(t; \alpha)\, Z_{1,\mu}(0; \alpha) + \phi_1(0; \alpha)\, h_1(t; \alpha) + \phi_3(0; \alpha)\, h_3(t; \alpha)\,;$$

2) replace the values $Z_{1,\mu}(0; \alpha)$ with the pre-derived formula (2.12)

$$Z_{1,\mu}(0; \alpha) = \Big(\frac{s_{1,\mu}}{2}\Big)^{-\varrho} \frac{1}{\Gamma(1-\varrho)} = \frac{\theta^{+\varrho}\, \sigma_{1,\mu}^{-\varrho}}{\Gamma(1-\varrho)} \equiv C_\varrho\, \sigma_{1,\mu}^{-\varrho}\,;$$

3) account for the boundary conditions (2.38) and (2.39) imposed on the blending functions $\phi_j(x; \alpha)$ and $\phi_{j+2}(x; \alpha)$, to obtain the following linear integro-differential equation of convolution type with respect to $h_3(t; \alpha)$ and $h_4(t; \alpha)$

$$C_\varrho \sum_{\mu=1}^{\infty} \sigma_{1,\mu}^{-\varrho}\, O_{2,\mu}(t; \alpha) + h_4(t; \alpha) = C_\varrho \sum_{\mu=1}^{\infty} \sigma_{1,\mu}^{-\varrho}\, O_{1,\mu}(t; \alpha) + h_3(t; \alpha)\,.$$

The above representation of the matching condition (2.17) can be rewritten in the expanded form

$$\begin{cases} \quad a_2(t; \alpha) * h_2''(t; \alpha) + b_2(t; \alpha) * h_2(t; \alpha) \,+\, \overset{*}{\underset{\smile}{v}}_2(t; \alpha) + \overset{**}{\underset{\smile}{v}}_2(t; \alpha) \\ + \, c_2(t; \alpha) * h_4''(t; \alpha) \,+\, d_2(t; \alpha) * h_4(t; \alpha) + h_4(t; \alpha) \\ = a_1(t; \alpha) * h_1''(t; \alpha) + b_1(t; \alpha) * h_1(t; \alpha) \,+\, \overset{*}{\underset{\smile}{v}}_1(t; \alpha) + \overset{**}{\underset{\smile}{v}}_1(t; \alpha) \\ + \, c_1(t; \alpha) * h_3''(t; \alpha) \,+\, d_1(t; \alpha) * h_3(t; \alpha) + h_3(t; \alpha) \end{cases} \tag{2.59}$$

where the coefficient functions are defined by the following series

$$\begin{cases} \overset{*}{\underset{\smile}{v}}_j(t; \alpha) = C_\varrho \displaystyle\sum_{\mu=1}^{\infty} \sigma_{1,\mu}^{-\varrho} \quad \overset{*}{v}_{j,\mu}(\alpha)\, \cos\big(\sigma_{1,\mu} t\big), \\ y_j(t; \alpha) = C_\varrho \displaystyle\sum_{\mu=1}^{\infty} \sigma_{1,\mu}^{-\varrho-1}\, y_{j,\mu}(\alpha)\, \sin\big(\sigma_{1,\mu} t\big), \end{cases} \tag{2.60}$$

and one should substitute symbols ‘$\overset{**}{\underset{\smile}{v}}$’, ‘$a$’, ‘$b$’, ‘$c$’, and ‘$d$’ instead of ‘$y$’ in (2.60).

3. The Laplace Transformation

3.1. Finding the Images

To solve the integro-differential equation (2.59) of convolution type, we apply the Laplace transformation [3], producing for a function $f(t)$, $t \in [0,\infty)$, its transform as follows

$$F(\tau) = \mathfrak{L}\,[f(t)] := \int_0^{\infty} f(t)\, \mathrm{e}^{-\tau t}\, dt\,, \qquad \tau = \xi + i\eta \in \mathbb{C}\,, \tag{3.1}$$

provided the original function $f(t)$ satisfies the known sufficient conditions for the image function $F(\tau)$ to exist.

When applying the Laplace transformation we use:

1) the convolution theorem

$$\mathfrak{L}\,[p(t) * q(t)] = \mathfrak{L}\,[p(t)] \cdot \mathfrak{L}\,[q(t)] = P(\tau) \cdot Q(\tau)\,, \tag{3.2}$$

where the symbol 'middle dot' between the two images is used, where it is needed, for reminding about the origin of their multiplication;

2) the transforms of the control functions $h_j(t;\alpha)$ and their second derivatives, accounting for the given initial conditions

$$\begin{aligned} \mathfrak{L}\big[h_j(t;\alpha)\big] &= H_j(\tau;\alpha)\,, \\ \mathfrak{L}\big[h''_j(t;\alpha)\big] &= H_j(\tau;\alpha)\,\tau^2 - h_j(0;\alpha)\,\tau - h'_j(0;\alpha)\,, \end{aligned}$$

3) the transforms of the required functions $h_3(t;\alpha)$, $h_4(t;\alpha)$ and their second derivatives, accounting for the prescribed initial conditions

$$\begin{aligned} \mathfrak{L}\big[h_{j+2}(t;\alpha)\big] &= H_{j+2}(\tau;\alpha)\,, \\ \mathfrak{L}\big[h''_{j+2}(t;\alpha)\big] &= H_{j+2}(\tau;\alpha)\,\tau^2 - h_{j+2}(0;\alpha)\,\tau - h'_{j+2}(0;\alpha)\,, \end{aligned}$$

4) the transforms of the trigonometric sine and cosine functions

$$\begin{cases} \mathfrak{L}\left[\sin\left(\sigma_{1,\mu} t\right)\right] = \dfrac{\sigma_{1,\mu}}{\tau^2 + \sigma_{1,\mu}^2} \equiv S_\mu(\tau;\alpha)\,, \\[2ex] \mathfrak{L}\left[\cos\left(\sigma_{1,\mu} t\right)\right] = \dfrac{\tau}{\tau^2 + \sigma_{1,\mu}^2} \equiv C_\mu(\tau;\alpha)\,, \end{cases} \tag{3.3}$$

Then, the Laplace transformation applied to the equation (2.59) yields evidently to its image as follows

$$\begin{cases} \quad \big[1 + Q_2(\tau;\alpha)\big] \cdot H_4(\tau;\alpha) + R_2(\tau;\alpha) \\ = \big[1 + Q_1(\tau;\alpha)\big] \cdot H_3(\tau;\alpha) + R_1(\tau;\alpha)\,, \end{cases} \tag{3.4}$$

where

$$R_j(\tau;\alpha) = P_j(\tau;\alpha)\cdot H_j(\tau;\alpha) + V_j(\tau;\alpha) - K_j(\tau;\alpha) - N_j(\tau;\alpha)\,, \tag{3.5}$$

$$\begin{cases} P_j(\tau;\alpha) = A_j(\tau;\alpha)\,\tau^2 + B_j(\tau;\alpha) \\ \qquad\qquad = C_\varrho \displaystyle\sum_{\mu=1}^{\infty} \sigma_{\varrho,\mu}^{-\varrho}\, \frac{a_{j,\mu}(\alpha)\,\tau^2 + b_{j,\mu}(\alpha)}{\tau^2 + \sigma_{1,\mu}^2}\,, \end{cases}$$

$$\begin{cases} Q_j(\tau;\alpha) = C_j(\tau;\alpha)\,\tau^2 + D_j(\tau;\alpha) \\ \qquad\qquad = C_\varrho \displaystyle\sum_{\mu=1}^{\infty} \sigma_{\varrho,\mu}^{-\varrho}\, \frac{c_{j,\mu}(\alpha)\,\tau^2 + d_{j,\mu}(\alpha)}{\tau^2 + \sigma_{1,\mu}^2}\,, \end{cases}$$

$$\begin{cases} V_j(\tau;\alpha) = \overset{*}{V}_j(\tau;\alpha) + \overset{**}{V}_j(\tau;\alpha) \\ \qquad\qquad = C_\varrho \displaystyle\sum_{\mu=1}^{\infty} \sigma_{\varrho,\mu}^{-\varrho}\, \frac{\overset{*}{v}_{j,\mu}(\alpha)\,\tau + \overset{**}{v}_{j,\mu}(\alpha)}{\tau^2 + \sigma_{1,\mu}^2}\,, \end{cases}$$

$$\begin{cases} K_j(\tau;\alpha) = \overset{*}{K}_j(\tau;\alpha)\,h_j(0;\alpha) + \overset{**}{K}_j(\tau;\alpha)\,h_j'(0;\alpha) \\ \qquad\qquad = C_\varrho \displaystyle\sum_{\mu=1}^{\infty} \sigma_{\varrho,\mu}^{-\varrho}\, a_{j,\mu}(\alpha)\, \frac{h_j(0;\alpha)\,\tau + h_j'(0;\alpha)}{\tau^2 + \sigma_{1,\mu}^2}\,, \end{cases}$$

$$\begin{cases} N_j(\tau;\alpha) = \overset{*}{N}_j(\tau;\alpha)\,h_{j+2}(0;\alpha) + \overset{**}{N}_j(\tau;\alpha)\,h_{j+2}'(0;\alpha) \\ \qquad\qquad = C_\varrho \displaystyle\sum_{\mu=1}^{\infty} \sigma_{\varrho,\mu}^{-\varrho}\, c_{j,\mu}(\alpha)\, \frac{h_{j+2}(0;\alpha)\,\tau + h_{j+2}'(0;\alpha)}{\tau^2 + \sigma_{1,\mu}^2}\,, \end{cases}$$

the functions $A_j(\tau;\alpha)$, $B_j(\tau;\alpha)$, $C_j(\tau;\alpha)$, $D_j(\tau;\alpha)$, $\overset{*}{V}_j(\tau;\alpha)$, and $\overset{**}{V}_j(\tau;\alpha)$ being the images of the functions $a_j(t;\alpha)$, $b_j(t;\alpha)$, $c_j(t;\alpha)$, $d_j(t;\alpha)$, $\overset{*}{v}_j(t;\alpha)$, and $\overset{**}{v}_j(t;\alpha)$.

Assuming that $\phi_{1,4}(x;\alpha) = \phi_{1,3}(-x;\alpha)$ (see Section 2 at p. 24), we easily conclude that: 1) the equality $Q_1(\tau;\alpha) = Q_2(\tau;\alpha)$ holds; 2) the image (3.4) of the matching condition (2.59) reduces to

$$\big[1 + Q_1(\tau;\alpha)\big]\cdot \Delta H(\tau;\alpha) = R_2(\tau;\alpha) - R_1(\tau;\alpha)\,, \tag{3.6}$$

where $\Delta H(\tau;\alpha) \equiv H_3(\tau;\alpha) - H_4(\tau;\alpha)$, or after dividing both sides of (3.6) by $[1 + Q_1(\tau;\alpha)]$, to the formula

$$\Delta H(\tau;\alpha) = \frac{R_2(\tau;\alpha) - R_1(\tau;\alpha)}{1 + Q_1(\tau;\alpha)}\,. \tag{3.7}$$

3.2. Finding the Original Functions

We start from estimating applicability of some known approaches to invert the formula (3.7) and find the original function $h(t;\alpha) = h_3(t;\alpha) - h_4(t;\alpha)$.

a) We could expect that rewriting the formula (3.7) as follows

$$\Delta H(\tau;\alpha) = \Big[1 + Q_1(\tau;\alpha)\Big]^{-1} \cdot \Big[R_2(\tau;\alpha) - R_1(\tau;\alpha)\Big] \tag{3.8}$$

makes it possible to invoke the convolution theorem (3.2) and find the function $h(t;\alpha)$ provided both multipliers in (3.8) are the images.

To estimate this approach to be useful, we take into account that for any original function $f(t)$ its transform $F(\tau)$ is necessarily [3]: 1) analytic in the right half of the τ-plane: $\Re\,\tau > \xi^* > 0$, where ξ^* is some proper real value; 2) vanishing when $\Re\,\tau \to +\infty$.

Proposition 3.1. *The functions* $R_1(\tau;\alpha)$, $R_2(\tau;\alpha)$ (3.5) *are transforms, whereas the function* $[1 + Q_1(\tau;\alpha)]^{-1}$ *is not a transform.*

Proof. Let's turn to the expressions (3.5). The functions $P_j(\tau;\alpha)$ are analytic in the whole τ-plane except for the simple poles $\tau^{\mp}_{\mu} = \mp\, i\sigma_{1,\mu}$ [5] and both do not vanish when $\Re\,\tau \to +\infty$. Nevertheless, both products $P_j(\tau;\alpha)\cdot H_j(\tau;\alpha)$ vanish when $\Re\,\tau \to +\infty$, since both multipliers $H_j(\tau;\alpha)$ are the transforms of the control functions $h_j(t;\alpha)$. From this we conclude that the above products are transforms as well. Then, we notice that the functions $\overset{*}{V}_j(\tau;\alpha)$ and $\overset{**}{V}_j(\tau;\alpha)$, $\overset{*}{K}_j(\tau;\alpha)$ and $\overset{**}{K}_j(\tau;\alpha)$, $\overset{*}{N}_j(\tau;\alpha)$ and $\overset{**}{N}_j(\tau;\alpha)$ are themselves the transforms, and this completes the proof of the first part of the proposition.

The function $Q_1(\tau;\alpha)$ has the same properties as both functions $P_j(\tau;\alpha)$ have, therefore the function $[1 + Q_1(\tau;\alpha)]^{-1}$ is not a transform, and this completes the proof of the second part of the proposition. □

Although the first approach turnes out to be unsuccessful, nevertheless it follows from Proposition 3.1 that the right-hand side of the formula (3.7) is indeed the transform of the required function $h(t;\alpha)$.

b) The next approach is to invert the right-hand side of the formula (3.7) directly. Indeed, let the Laplace transform $F(\tau)$ for an original function $f(t)$ be given, then applying the inverse Laplace transformation [3], known also as the Bromwich integral, yields to the required original function

$$f(t) = \mathfrak{L}^{-1}\left[F(\tau)\right] = \frac{1}{2\pi i}\int_{\xi^* - i\infty}^{\xi^* + i\infty} F(\tau)\,\mathsf{e}^{+t\tau}\,d\tau\,, \tag{3.9}$$

where $\Re\,\tau = \xi^*$ is a vertical straight line lying to the right of all the singularities of $F(\tau)$ (see Fig. 3.1, *a*).

Practically, calculating the Bromwich integral is performed using the Cauchy residue theorem [5], but this approach implies that the singularities of the integrand

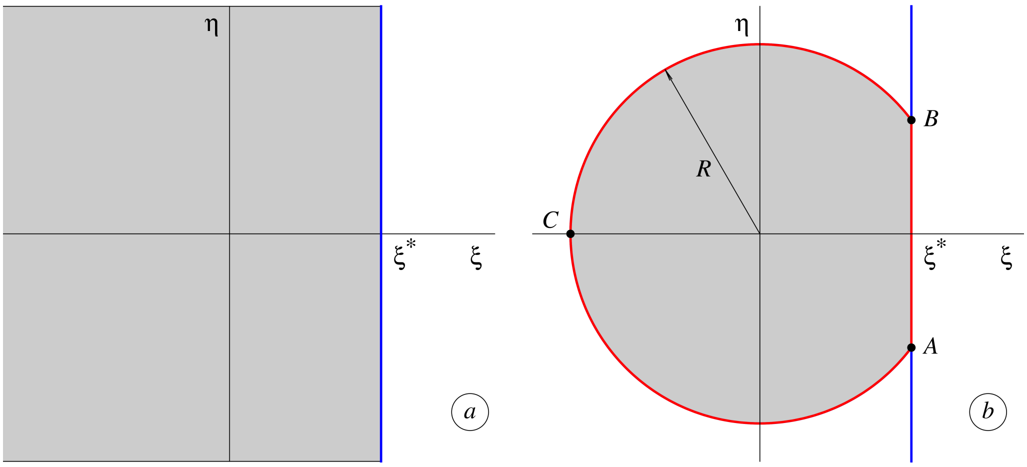

Fig. 3.1. All the singularities of the integrand of the Bromwich integral (3.9) lie in the half-plane (*gray color*) to the right of the path of integration $\tau = \xi^* + i\eta$, $\xi^* = \mathtt{const}, \eta \in (-\infty, +\infty)$ (*dark blue*), or the Bromwich line (a); the oriented Bromwich countour $ABCA$ (*light red*), consists of the segment AB of the Bromwich line and the arc BCA of the circle of radius R centered at the origin; to apply the Cauchy residue theorem, the integrand must vanish at BCA when $R \to \infty$ and all the singularities of the integrand must lie inside $ABCA$ (b)

are isolated and known (see Fig. 3.1, b). The functions $P_j(\tau;\alpha)$ and $Q_1(\tau;\alpha)$ have the same poles being removable singularities of the integrand and having no impact on calculating the integral; whereas finding all zeros of the function $[1 + Q_1(\tau;\alpha)]$ generally implies some proper approximation [4] of the latter and results in a huge bulk of the computational work. Therefore, we do not reject calculating the Bromwich integral at all, but postpone applying this approach for a while.

c) To implement the third approach, we:

1) recombine the terms in the series (3.5)

$$\left\{\begin{aligned} K_j(\tau;\alpha) &= C_\varrho \left(\sum_{\mu=1}^{\infty} \sigma_{1,\mu}^{-\varrho} \quad a_{j,\mu}(\alpha)\, C_\mu(\tau;\alpha) \right) h_j(0;\alpha) \\ &\quad + C_\varrho \left(\sum_{\mu=1}^{\infty} \sigma_{1,\mu}^{-\varrho-1} a_{j,\mu}(\alpha)\, S_\mu(\tau;\alpha) \right) h_j'(0;\alpha)\,, \end{aligned}\right.$$

$$\left\{\begin{aligned} N_j(\tau;\alpha) &= C_\varrho \left(\sum_{\mu=1}^{\infty} \sigma_{1,\mu}^{-\varrho} \quad c_{j,\mu}(\alpha)\, C_\mu(\tau;\alpha) \right) h_{j+2}(0;\alpha) \\ &\quad + C_\varrho \left(\sum_{\mu=1}^{\infty} \sigma_{1,\mu}^{-\varrho-1} c_{j,\mu}(\alpha)\, S_\mu(\tau;\alpha) \right) h_{j+2}'(0;\alpha)\,, \end{aligned}\right.$$

$$\begin{cases} P_j(\tau;\alpha) - \overbrace{C_\varrho \sum_{\mu=1}^{\infty} \sigma_{1,\mu}^{-\varrho} a_{j,\mu}(\alpha)}^{\Psi_j(\alpha)} = -C_\varrho \sum_{\mu=1}^{\infty} \sigma_{1,\mu}^{-\varrho+1} a_{j,\mu}(\alpha) S_\mu(\tau;\alpha) \\ \qquad\qquad\qquad\qquad\qquad\qquad +C_\varrho \sum_{\mu=1}^{\infty} \sigma_{1,\mu}^{-\varrho-1} b_{j,\mu}(\alpha) S_\mu(\tau;\alpha)\,, \end{cases}$$

$$\begin{cases} \overbrace{C_\varrho \sum_{\mu=1}^{\infty} \sigma_{1,\mu}^{-\varrho} c_{j,\mu}(\alpha)}^{\Omega_1(\alpha)} - Q_1(\tau;\alpha) = +C_\varrho \sum_{\mu=1}^{\infty} \sigma_{1,\mu}^{-\varrho+1} c_{j,\mu}(\alpha) S_\mu(\tau;\alpha) \\ \qquad\qquad\qquad\qquad\qquad\qquad -C_\varrho \sum_{\mu=1}^{\infty} \sigma_{1,\mu}^{-\varrho-1} d_{j,\mu}(\alpha) S_\mu(\tau;\alpha) \equiv \hat{Q}_1(\tau;\alpha)\,, \end{cases}$$

and easily find the respective original functions

$$\begin{cases} p_j(t;\alpha) = -C_\varrho \sum_{\mu=1}^{\infty} \sigma_{1,\mu}^{-\varrho+1} a_{j,\mu}(\alpha) \sin\big(\sigma_{1,\mu} t\big) \\ \qquad\qquad +C_\varrho \sum_{\mu=1}^{\infty} \sigma_{1,\mu}^{-\varrho-1} b_{j,\mu}(\alpha) \sin\big(\sigma_{1,\mu} t\big) + \Psi_j(\alpha)\,\delta(t)\,, \end{cases} \tag{3.10}$$

$$\begin{cases} \hat{q}_1(t;\alpha) = +C_\varrho \sum_{\mu=1}^{\infty} \sigma_{1,\mu}^{-\varrho+1} c_{j,\mu}(\alpha) \sin\big(\sigma_{1,\mu} t\big) \\ \qquad\qquad -C_\varrho \sum_{\mu=1}^{\infty} \sigma_{1,\mu}^{-\varrho-1} d_{j,\mu}(\alpha) \sin\big(\sigma_{1,\mu} t\big), \end{cases} \tag{3.11}$$

$$\begin{cases} \overset{*}{k}_j(t;\alpha) = C_\varrho \sum_{\mu=1}^{\infty} \sigma_{1,\mu}^{-\varrho} \quad a_{j,\mu}(\alpha) \cos\big(\sigma_{1,\mu} t\big), \\ \overset{**}{k}_j(t;\alpha) = C_\varrho \sum_{\mu=1}^{\infty} \sigma_{1,\mu}^{-\varrho-1} a_{j,\mu}(\alpha) \sin\big(\sigma_{1,\mu} t\big), \end{cases} \tag{3.12}$$

$$\begin{cases} \overset{*}{n}_j(t;\alpha) = C_\varrho \sum_{\mu=1}^{\infty} \sigma_{1,\mu}^{-\varrho} \quad c_{j,\mu}(\alpha) \cos\big(\sigma_{1,\mu} t\big), \\ \overset{**}{n}_j(t;\alpha) = C_\varrho \sum_{\mu=1}^{\infty} \sigma_{1,\mu}^{-\varrho-1} c_{j,\mu}(\alpha) \sin\big(\sigma_{1,\mu} t\big), \end{cases} \tag{3.13}$$

where $\delta(t)$ is the Dirac delta function;

2) represent the denominator of the formula (3.7) as follows

$$1 + Q_1(\tau;\alpha) = 1 + \Omega_1(\alpha) - \hat{Q}_1(\tau;\alpha) \equiv C_\alpha - \hat{Q}_1(\tau;\alpha)$$
$$= C_\alpha\Big(1 - C_\alpha^{-1}\,\hat{Q}_1(\tau;\alpha)\Big) \equiv C_\alpha\Big(1 - \bar{Q}_1(\tau;\alpha)\Big);$$

3) rewrite the formula (3.7) as is usually done when solving integral equations of convolution type

$$\Delta H(\tau;\alpha) = C_\alpha^{-1}\left(1 + \frac{\bar{Q}_1(\tau;\alpha)}{1 - \bar{Q}_1(\tau;\alpha)}\right) \cdot \Big[R_2(\tau;\alpha) - R_1(\tau;\alpha)\Big]\,; \tag{3.14}$$

4) expand the 'fractional' term in (3.14) in the following power series

$$\frac{\bar{Q}_1(\tau;\alpha)}{1 - \bar{Q}_1(\tau;\alpha)} = \bar{Q}_1(\tau;\alpha) + \sum_{\gamma=2}^{\infty}\big[\bar{Q}_1(\tau;\alpha)\big]^{\cdot\gamma}, \tag{3.15}$$

provided that $|\bar{Q}_1(\tau;\alpha)| < 1$ in a proper right half-plane of the τ-plane [3];

5) invert the above power series in the form of the Neumann series [3]

$$\mathfrak{L}^{-1}\left[\frac{\bar{Q}_1(\tau;\alpha)}{1 - \bar{Q}_1(\tau;\alpha)}\right] = \bar{q}_1(t;\alpha) + \sum_{\gamma=2}^{\infty}\big[\bar{q}_1(t;\alpha)\big]^{*\gamma} \equiv \Phi(t;\alpha)\,, \tag{3.16}$$

or the sum of iterated kernels, where $\bar{q}_1(t;\alpha) = C_\alpha^{-1}\,\hat{q}_1(t;\alpha)$ (3.11);

6) invert the terms in the brackets in (3.14)

$$\begin{cases} r_j(t;\alpha) = p_j(t;\alpha) * h_j(t) + \overset{*}{v}_j(t;\alpha) + \overset{**}{v}_j(t;\alpha) \\ \qquad\qquad - \overset{*}{k}_j(t;\alpha)\,h_j(0;\alpha) - \overset{*}{n}_j(t;\alpha)\,h_{j+2}(0;\alpha) \\ \qquad\qquad - \overset{**}{k}_j(t;\alpha)\,h_j'(0;\alpha) - \overset{**}{n}_j(t;\alpha)\,h_{j+2}'(0;\alpha)\,; \end{cases} \tag{3.17}$$

7) finally, invert the formula (3.7) by invoking the convolution theorem (3.2)

$$\begin{cases} C_\alpha\,(h_3(t;\alpha) - h_4(t;\alpha)) = \qquad [r_2(t;\alpha) - r_1(t;\alpha)] \\ \qquad\qquad + \Phi(t;\alpha) * [r_2(t;\alpha) - r_1(t;\alpha)]\,. \end{cases} \tag{3.18}$$

4. Conclusions

1. In the current study we have applied the previously obtained [2] one-sided solutions $u_{1,j}(t,x;\alpha)$, $u_{5,j}(t,x;\alpha)$ (1.3), (1.4) to the degenerate wave equation as the building blocks of procedures for finding bounded solutions to the IBVP (1.1), posed in the space-time rectangle $[0,T]\times[-1,+1]$, in the cases of weak ($\alpha \in (0,1)$) and strong ($\alpha \in (1,2)$) degeneracy.

2. In the case of weak degeneracy the bounded unique solution (2.31) to the IBVP

$$
\begin{cases}
u(t,x;\alpha) = \displaystyle\sum_{\mu=1}^{\infty} O_{1,\mu}(t;\alpha)\, X_{1,\mu}(x;\alpha) \\
\qquad\qquad + \displaystyle\sum_{\mu=1}^{\infty} O_{5,\mu}(t;\alpha)\, X_{5,\mu}(x;\alpha) \\
\qquad\qquad + \phi_2(x;\alpha)\, h_2(t;\alpha) + \phi_1(x;\alpha)\, h_1(t;\alpha)
\end{cases}
\tag{4.1}
$$

has been obtained in the space-time rectangle $[0,T]\times[-1,+1]$, using the method of SV based on the eigenfunctions $X_{1,\mu}(x;\alpha)$ and $X_{5,\mu}(x;\alpha)$, defined in Prop. 2.2 at p. 6. The solution (4.1) satisfies the following two continuity conditions

$$
\begin{cases}
u(t,0-0;\alpha) = u(t,0+0;\alpha)\,, \\
f(t,0-0;\alpha) = f(t,0+0;\alpha)\,,
\end{cases}
\qquad t \in [0,T]\,,
\tag{4.2}
$$

at the degeneracy segment, where $f(t,x;\alpha)$ is the flux of the solution.

3. In the case of strong degeneracy a family of bounded non-unique solutions to the IBVP have been obtained in the space-time rectangle $[0,T]\times[-1,+1]$, applying the following procedure:

a) two families of bounded solutions (2.54), (2.55)

$$
\begin{cases}
u_1(t,x;\alpha) = \displaystyle\sum_{\mu=1}^{\infty} O_{1,\mu}(t;\alpha)\, Z_{1,\mu}(x;\alpha) \\
\qquad\qquad + \phi_1(x;\alpha)\, h_1(t;\alpha) + \phi_3(x;\alpha)\, h_3(t;\alpha)\,,
\end{cases}
\tag{4.3}
$$

$$
\begin{cases}
u_2(t,x;\alpha) = \displaystyle\sum_{\mu=1}^{\infty} O_{2,\mu}(t;\alpha)\, Z_{1,\mu}(x;\alpha) \\
\qquad\qquad + \phi_2(x;\alpha)\, h_2(t;\alpha) + \phi_4(x;\alpha)\, h_4(t;\alpha)\,.
\end{cases}
\tag{4.4}
$$

to the derived IBVP_1 (2.14) and IBVP_2 (2.15), posed in the 'right' $[0,T]\times[0,+1]$ and the 'left' $[0,T]\times[-1,0]$ space-time rectangles, are obtained, using the method of SV based on the eigenfunctions $Z_{1,\mu}(x;\alpha)$, defined in Prop. 2.1 at p. 4;

b) the solutions of both families, depending on undetermined functions $h_3(t;\alpha)$ and $h_4(t;\alpha)$ and satisfying the only continuity condition for their fluxes

$$
f_2(t,0-0;\alpha) = f_1(t,0+0;\alpha)\,, \qquad t \in [0,T]\,,
\tag{4.5}
$$

are then matched to implement the other continuity condition

$$
u_2(t,0-0;\alpha) = u_1(t,0+0;\alpha)\,, \qquad t \in [0,T]\,,
\tag{4.6}
$$

nevertheless, the resulting matched family still retains one undetermined function.

Appendix. Calculating the Coefficients $\boldsymbol{a}, \boldsymbol{b}, \boldsymbol{c}$, and $\boldsymbol{d}$

In this section the method of calculating the coefficients (2.49), (2.50) is presented. We take for $\phi_{k,j}(x;\alpha)$ and $\phi_{k,j+2}(x;\alpha)$ the following power functions

$$\begin{cases} \phi_j(x;\alpha) = |x|^{\omega_j}, \\ \phi_{j+2}(x;\alpha) = 1 - |x|^{\omega_{j+2}}, \end{cases} \tag{4.7}$$

where the undetermined exponents $\omega_{k,j}$ and $\omega_{k,j+2}$ should be adjusted to the parameter α in a special way. To impose the proper constraint on the exponents, we calculate the derived functions: 1) the 'fluxes' $\varphi(x;\alpha) = a(x;\alpha)\phi'(x;\alpha)$

$$\begin{cases} \varphi_j(x;\alpha) = \ + \operatorname{sign}(x)\ \omega_j\ |x|^{\omega_j - 1 + \alpha}, \\ \varphi_{j+2}(x;\alpha) = \ - \operatorname{sign}(x)\ \omega_{j+2}\ |x|^{\omega_{j+2} - 1 + \alpha}, \end{cases} \tag{4.8}$$

and 2) their derivatives $\psi(x;\alpha) = \varphi'(x;\alpha) = \big[a(x;\alpha)\phi'(x;\alpha)\big]'$

$$\begin{cases} \psi_j(x;\alpha) = +\omega_j\ \big[\omega_j - \theta + 1\big]\ |x|^{\omega_j - \theta}, \\ \psi_{j+2}(x;\alpha) = -\omega_{j+2}\ \big[\omega_{j+2} - \theta + 1\big]\ |x|^{\omega_{j+2} - \theta}, \end{cases} \tag{4.9}$$

and assume that they vanish at $x = 0$ smoothly, i. e., $\psi_j(0;\alpha) = \psi_{j+2}(0;\alpha) = 0$ and $\psi_j'(0;\alpha) = \psi_{j+2}'(0;\alpha) = 0$, whence we immediately deduce that $\omega_j - \theta = 1 + \epsilon_j$, $\omega_{j+2} - \theta = 1 + \epsilon_{j+2}$, where $\epsilon_j, \epsilon_{j+2} > 0$.

Taking $\omega_j = \omega_{j+2} = \omega$ and substituting the functions $\phi_j(x;\alpha)$, $\phi_{j+2}(x;\alpha)$ (4.7) in the coefficients (2.49), (2.50) yields to

$$\begin{cases} a_\mu(\alpha) = -\dfrac{1}{\|Z_{1,\mu}\|^2}\, I_2(\alpha,\omega)\,, \\[2ex] b_\mu(\alpha) = +\dfrac{\vartheta}{\|Z_{1,\mu}\|^2}\, I_1(\alpha,\omega)\,, \\[2ex] c_\mu(\alpha) = -\dfrac{1}{\|Z_{1,\mu}\|^2}\, I_0(\alpha) + \dfrac{1}{\|Z_{1,\mu}\|^2}\, I_2(\alpha,\omega)\,, \\[2ex] d_\mu(\alpha) = -\dfrac{\vartheta}{\|Z_{1,\mu}\|^2}\, I_1(\alpha,\omega)\,. \end{cases} \tag{4.10}$$

The definite integrals $I_0(\alpha), I_1(\alpha,\omega), I_2(\alpha,\omega)$ in (4.10) can be calculated analytically, applying the variable transformation $s = \mathring{s}\, x^{\frac{\theta}{2}}$ as follows

$$
\begin{cases}
I_0(\alpha) &= \displaystyle\int_0^1 Z_{1,\mu}(x;\alpha)\ dx = \\
&= \displaystyle\frac{2}{\theta}\left(\frac{1}{\mathring{s}}\right)^{o+1}\int_0^{\mathring{s}} s^{o}\, \mathtt{Z}_{\varrho}(s)\ ds \equiv \frac{2}{\theta}\left(\frac{1}{\mathring{s}}\right)^{o+1} I_0^*(\alpha)\,, \\
I_1(\alpha,\omega) &= \displaystyle\int_0^1 x^{\omega-\theta}\, Z_{1,\mu}(x;\alpha)\ dx = \int_0^1 x^{\epsilon+1}\, x^{\frac{\nu}{2}}\, \mathtt{Z}_{\varrho}(s)\ dx \\
&= \displaystyle\frac{2}{\theta}\left(\frac{1}{\mathring{s}}\right)^{\upsilon+1}\int_0^{\mathring{s}} s^{\upsilon}\, \mathtt{Z}_{\varrho}(s)\ ds \equiv \frac{2}{\theta}\left(\frac{1}{\mathring{s}}\right)^{\upsilon+1} I_1^*(\alpha,\epsilon)\,, \\
I_2(\alpha,\omega) &= \displaystyle\int_0^1 x^{\omega} Z_{1,\mu}(x;\alpha)\,\mathrm{d}x = \int_0^1 x^{\theta+\epsilon+1}\, x^{\frac{\nu}{2}}\, \mathtt{Z}_{\varrho}(s)\ dx \\
&= \displaystyle\frac{2}{\theta}\left(\frac{1}{\mathring{s}}\right)^{\upsilon+3}\int_0^{\mathring{s}} s^{\upsilon+2}\, \mathtt{Z}_{\varrho}(s)\ ds \equiv \frac{2}{\theta}\left(\frac{1}{\mathring{s}}\right)^{\upsilon+3} I_2^*(\alpha,\epsilon)\,,
\end{cases}
\tag{4.11}
$$

where

$$
o = \frac{1}{\theta}\,, \qquad \upsilon = \frac{2\epsilon+3}{\theta}\,, \tag{4.12}
$$

and to avoid confusion with zero, small letter ‘o’ is used only for the exponents, and the notation $\mathring{s} = s_{1,\mu}$ is used hereinafter to present calculations of the transformed integrals $I_0^*(\alpha)$, $I_1^*(\alpha)$ and $I_2^*(\alpha,\epsilon)$ in a compact form.

We chose the analytical approach to calculate the integrals in (4.11), hence, our concern is calculating the transformed integrals

$$
\begin{cases}
I_0^*(\alpha) &= \displaystyle\int_0^{\mathring{s}} s^{o}\, \mathtt{Z}_{\varrho}(s)\ ds\,, \\
I_1^*(\alpha,\epsilon) &= \displaystyle\int_0^{\mathring{s}} s^{\upsilon}\, \mathtt{Z}_{\varrho}(s)\ ds\,, \\
I_2^*(\alpha,\epsilon) &= \displaystyle\int_0^{\mathring{s}} s^{\upsilon+2}\, \mathtt{Z}_{\varrho}(s)\ ds\,,
\end{cases}
\tag{4.13}
$$

using the following recurrence formula [7]

$$
s^{\varrho+1}\mathtt{Z}_{\varrho}(s) = \left[s^{\varrho+1}\mathtt{Z}_{\varrho+1}(s)\right]'. \tag{4.14}
$$

The integral $I_0^*(\alpha)$ is easily shown to be calculated exactly for any α. Indeed, keeping in mind (4.14), we obtain that

$$
\begin{cases}
I_0^*(\alpha) = \displaystyle\int_0^{\mathring{s}} s^{o}\, \mathtt{Z}_{\varrho}(s)\ ds = \int_0^{\mathring{s}} s^{\varrho+1}\, \mathtt{Z}_{\varrho}(s)\ ds \\
\qquad\quad = \displaystyle\int_0^{\mathring{s}} \left[s^{\varrho+1}\, \mathtt{Z}_{\varrho+1}(s)\right]'\ ds = \mathring{s}^{\varrho+1}\, \mathtt{Z}_{\varrho+1}(\mathring{s})\,.
\end{cases}
\tag{4.15}
$$

To calculate the transformed integrals $I_1^*(\alpha;\epsilon), I_2^*(\alpha;\epsilon)$ (4.13), we introduce the following

Definition 4.1. The values of the parameter $\epsilon > 0$ in the exponents $\omega = \theta + 1 + \epsilon$ (4.7), (4.9), allowing for: 1) the function (4.9) to be continuously differentiable and 2) the transformed integrals $I_1^*(\alpha,\epsilon)$, $I_2^*(\alpha,\epsilon)$ (4.13) to be calculated by parts (this is referred to as *integrability*), are called *proper.*

Proposition 4.1. *The proper values of the parameter ϵ are the positive values produced by the formula*

$$\epsilon = -1 + k\,\theta = -1 + k\,(2-\alpha)\,, \tag{4.16}$$

where $k \in \mathbb{N}$.

Proof. First, we find the values of the exponent υ leading to integration by parts using the following formula (4.14). Presenting the exponent of the integrand of I_2^* as $\upsilon = \upsilon - \varrho - 1 + (\varrho + 1) = \upsilon' + (\varrho + 1)$ makes it clear that: 1) it is the term $\upsilon' \geqslant 0$ that is responsible for integrability; 2) $\upsilon' \equiv 0 \pmod 2$ is the integrability condition. Indeed, let:

a) $\upsilon' = 0$, then the integral I_2^* reads

$$I_2^*(\alpha,\epsilon) = \int_0^{\mathring{s}} s^{\upsilon'}\left[s^{\varrho+1}\mathrm{Z}_\varrho(s)\right]\,ds = \int_0^{\mathring{s}} \left[s^{\varrho+1}\mathrm{Z}_{\varrho+1}(s)\right]'\,ds = \mathring{s}^{\varrho+1}\mathrm{Z}_{\varrho+1}(\mathring{s})\,;$$

b) $\upsilon' = 2$, then integration by parts is performed successfully as well

$$\begin{aligned}I_2^*(\alpha,\epsilon) &= \int_0^{\mathring{s}} s^{\upsilon'}\left[s^{\varrho+1}\mathrm{Z}_\varrho(s)\right]\,ds = \int_0^{\mathring{s}} s^2\left[s^{\varrho+1}\mathrm{Z}_{\varrho+1}(s)\right]'\,ds\\ &= \mathring{s}^{\varrho+3}\mathrm{Z}_{\varrho+1}(\mathring{s}) - 2\int_0^{\mathring{s}} s^{\varrho+2}\mathrm{Z}_{\varrho+1}(s)\,ds\\ &= \mathring{s}^{\varrho+3}\mathrm{Z}_{\varrho+1}(\mathring{s}) - 2\int_0^{\mathring{s}} \left[s^{\varrho+2}\mathrm{Z}_{\varrho+2}(s)\right]'\,ds = \mathring{s}^{\varrho+3}\mathrm{Z}_{\varrho+1}(\mathring{s}) - 2\,\mathring{s}^{\varrho+2}\mathrm{J}_{\varrho+2}(\mathring{s})\,;\end{aligned}$$

c) $\upsilon' = 4$, then integration is reduced to the previous case

$$\begin{aligned}I_2^*(\alpha,\epsilon) &= \int_0^{\mathring{s}} s^4\left[s^{\varrho+1}\mathrm{Z}_{\varrho+1}(s)\right]'\,ds = \mathring{s}^{\varrho+5}\mathrm{Z}_{\varrho+1}(\mathring{s}) - 4\int_0^{\mathring{s}} s^2\left[s^{\varrho+3}\mathrm{Z}_{\varrho+1}(s)\right]\,ds\\ &= \mathring{s}^{\varrho+5}\mathrm{Z}_{\varrho+1}(\mathring{s}) - 4\int_0^{\mathring{s}} s^2\left[s^{\varrho+3}\mathrm{Z}_{\varrho+3}(s)\right]'\,ds\,,\end{aligned}$$

..., etc. It is evident that no value of the exponent leading to integrability other than those indicated above exists.

Second, considering the integral I_1^* is performed exactly in the same way as the integral I_2^*.

Third, we gather our observations on integrability as the following condition imposed on υ': $\upsilon' = 2k$, $k \in \mathbb{Z}_+$, or reformulated for υ as follows

$$\upsilon - \varrho - 1 = 2\,k\,, \qquad k \in \mathbb{Z}_+,$$

and substituting the expressions for υ (4.12) and ϱ (2.3) in the above condition we obtain

$$\frac{2\epsilon + 3}{2-\alpha} + \frac{1-\alpha}{2-\alpha} - 1 = 2\,\frac{\epsilon+1}{2-\alpha} = 2\,k\,.$$

Resolving the above condition with respect to ϵ yields to (4.16). It is evident, that zero value of k produces the value $\epsilon = -1$ and must be neglected. Unfortunately, other values of k produce negative values of the parameter ϵ as well, indeed: *a*) for $k=1$ we obtain $\epsilon = 1-\alpha$; *b*) for $k=2$ it yields to $\epsilon = 3-2\alpha$, etc., therefore (4.16) needs to be adjusted as the proposition says. $\square$

The 1-parameter family (4.2) of the admissible values of ϵ is shown in Fig. 4.2.

We show below, how the transformed integrals I_1^* and I_2^* (4.13) can be calculated exactly for non-unique proper values of the parameter ϵ, choosing the following values of the parameter α: 1) $\frac{1}{2}$, 2) 1, and 3) $\frac{3}{2}$.

1) Let $\alpha = \frac{1}{2}$, then $\theta = \frac{3}{2}$, $\nu = \frac{1}{2}$, $\varrho = -\frac{1}{3}$, and $\upsilon = \frac{4}{3}\,\epsilon + 2$ (4.12), and applying the property (4.14) yields to

$$\begin{cases} I_1^* = \displaystyle\int_0^{\mathring{s}} s^{\frac{4}{3}\epsilon+2}\,\mathtt{Z}_{-\frac{1}{3}}(s)\;ds = \mathring{s}^{\frac{4}{3}\epsilon+2}\,\mathtt{Z}_{\frac{2}{3}}(\mathring{s}) - \frac{4\epsilon+4}{3}\,\bar{I}_1^*\,, \\ I_2^* = \displaystyle\int_0^{\mathring{s}} s^{\frac{4}{3}\epsilon+4}\,\mathtt{Z}_{-\frac{1}{3}}(s)\;ds = \mathring{s}^{\frac{4}{3}\epsilon+4}\,\mathtt{Z}_{\frac{2}{3}}(\mathring{s}) - \frac{4\epsilon+10}{3}\left\{\mathring{s}^{\frac{4}{3}\epsilon+3}\,\mathtt{Z}_{\frac{5}{3}}(\mathring{s}) - \frac{4\epsilon+4}{3}\,\bar{I}_2^*\right\}, \end{cases}$$

where the integrals $\bar{I}_1^*$ and $\bar{I}_2^*$ are

$$\begin{cases} \bar{I}_1^* = \displaystyle\int_0^{\mathring{s}} s^{\frac{4}{3}\epsilon-\frac{2}{3}}\,s^{\frac{5}{3}}\mathtt{Z}_{\frac{2}{3}}(s)\;ds\,, \\ \bar{I}_2^* = \displaystyle\int_0^{\mathring{s}} s^{\frac{4}{3}\epsilon-\frac{2}{3}}\,s^{\frac{8}{3}}\mathtt{Z}_{\frac{5}{3}}(s)\;ds\,. \end{cases}$$

Assuming that $\epsilon = \frac{1}{2}$, we easily find that

$$\begin{cases} \bar{I}_1^* = \displaystyle\int_0^{\mathring{s}} s^{\frac{5}{3}}\mathtt{Z}_{\frac{2}{3}}(s)\;ds = \mathring{s}^{\frac{5}{3}}\mathtt{Z}_{\frac{5}{3}}(\mathring{s})\,, \\ \bar{I}_2^* = \displaystyle\int_0^{\mathring{s}} s^{\frac{8}{3}}\mathtt{Z}_{\frac{5}{3}}(s)\;ds = \mathring{s}^{\frac{8}{3}}\mathtt{Z}_{\frac{8}{3}}(\mathring{s})\,, \end{cases}$$

and complete the calculating of the integrals I_1^* and I_2^* as follows

$$\begin{cases} I_1^* = \mathring{s}^{\frac{8}{3}}\;\mathtt{Z}_{\frac{2}{3}}(\mathring{s}) - 2\,\mathring{s}^{\frac{5}{3}}\;\mathtt{Z}_{\frac{5}{3}}(\mathring{s})\,, \\ I_2^* = \mathring{s}^{\frac{14}{3}}\mathtt{Z}_{\frac{2}{3}}(\mathring{s}) - 4\,\mathring{s}^{\frac{11}{3}}\mathtt{Z}_{\frac{5}{3}}(\mathring{s}) + 8\,\mathring{s}^{\frac{8}{3}}\mathtt{Z}_{\frac{8}{3}}(\mathring{s})\,, \end{cases}$$

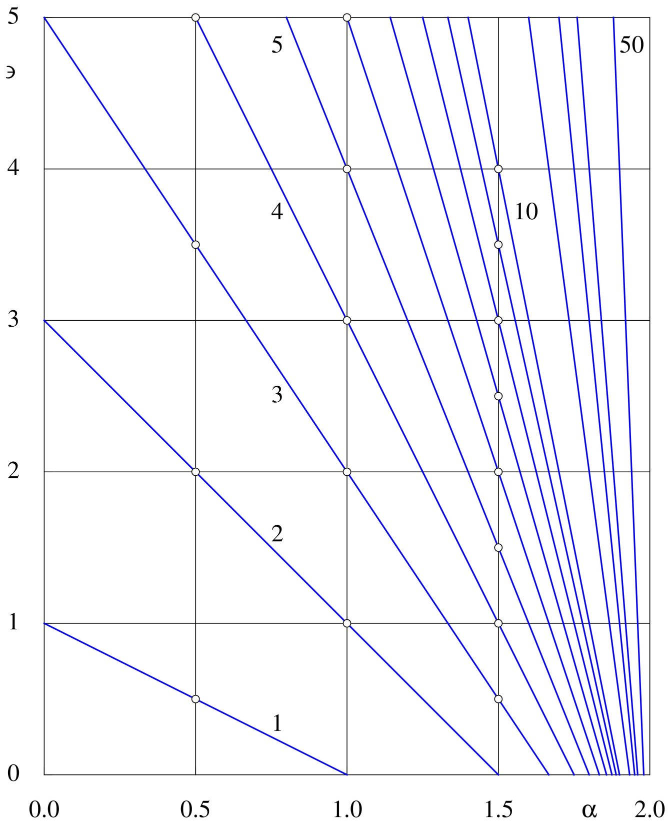

Fig. 4.2. The proper values of ϵ vs α (4.16) for various values of the parameter k: $k = 1(1)10; 15, 20, 25, 50$. Multiple proper values of ϵ for $\alpha = 0.5, 1.0, 1.5$ are marked with the white disks. The upper side of the 1-parameter family (4.16) is cut off along the straight line $\epsilon = 5$

then, assuming that $\epsilon = 2$

$$\begin{cases} \bar{I}_1^* = \displaystyle\int_0^{\mathring{s}} s^2 s^{\frac{5}{3}} \mathtt{Z}_{\frac{2}{3}}(s)\ ds = \mathring{s}^{\frac{11}{3}} \mathtt{Z}_{\frac{5}{3}}(\mathring{s}) - 2\,\mathring{s}^{\frac{8}{3}}\ \mathtt{Z}_{\frac{8}{3}}\ (\mathring{s})\,, \\ \bar{I}_2^* = \displaystyle\int_0^{\mathring{s}} s^2 s^{\frac{8}{3}} \mathtt{Z}_{\frac{5}{3}}(s)\ ds = \mathring{s}^{\frac{14}{3}} \mathtt{Z}_{\frac{8}{3}}(\mathring{s}) - 2\,\mathring{s}^{\frac{11}{3}} \mathtt{J}_{\frac{11}{3}}(\mathring{s})\,, \end{cases}$$

and complete the calculation of the integrals I_1^* and I_2^* as follows

$$\begin{cases} I_1^* = \mathring{s}^{\frac{8}{3}}\ \mathtt{J}_{\frac{2}{3}}(\mathring{s}) - 2\,\mathring{s}^{\frac{5}{3}}\ \mathtt{Z}_{\frac{5}{3}}(\mathring{s})\,, \\ I_2^* = \mathring{s}^{\frac{14}{3}} \mathtt{Z}_{\frac{2}{3}}(\mathring{s}) - 4\,\mathring{s}^{\frac{11}{3}} \mathtt{J}_{\frac{5}{3}}(\mathring{s}) + 8\,\mathring{s}^{\frac{8}{3}} \mathtt{Z}_{\frac{8}{3}}(\mathring{s})\,. \end{cases}$$

2) Let $\alpha = 1$, then $\theta = 1$, $\nu = 0$, $\varrho = 0$, and $\upsilon = 2\epsilon + 3$ (4.12), and applying

the property (4.14) yields to

$$\begin{cases} I_1^* = \displaystyle\int_0^{\mathring{s}} s^{2\epsilon+2}\left[s\,\mathtt{Z}_0(s)\right]\,ds = \mathring{s}^{2\epsilon+3}\,\mathtt{Z}_0(\mathring{s}) - (2\epsilon+2)\,\bar{I}_1^*\,, \\ I_2^* = \displaystyle\int_0^{\mathring{s}} s^{2\epsilon+4}\left[s\,\mathtt{Z}_0(s)\right]\,ds = \mathring{s}^{2\epsilon+5}\,\mathtt{Z}_0(\mathring{s}) - (2\epsilon+4)\left\{\mathring{s}^{2\epsilon+4}\,\mathtt{Z}_2(\mathring{s}) - (2\epsilon+2)\,\bar{I}_2^*\right\}, \end{cases}$$

where the integrals $\bar{I}_1^*$ and $\bar{I}_2^*$ are

$$\begin{cases} \bar{I}_1^* = \displaystyle\int_0^{\mathring{s}} s^{2\epsilon}\left[s^2\mathtt{Z}_2(s)\right]'\,ds\,, \\ \bar{I}_2^* = \displaystyle\int_0^{\mathring{s}} s^{2\epsilon}\left[s^3\mathtt{Z}_3(s)\right]'\,ds\,. \end{cases}$$

Assuming that $\epsilon=1$, we easily calculate both integrals $\bar{I}_{1,2}^*$

$$\begin{cases} \bar{I}_1^* = \displaystyle\int_0^{\mathring{s}} s^2\left[s^2\mathtt{Z}_2(s)\right]'\,ds = \mathring{s}^4\mathtt{Z}_2(\mathring{s}) - 2\int_0^{\mathring{s}}\left[s^3\mathtt{Z}_3(s)\right]'\,ds = \mathring{s}^4\mathtt{Z}_2(\mathring{s}) - 2\,\mathring{s}^3\mathtt{Z}_3(\mathring{s})\,, \\ \bar{I}_2^* = \displaystyle\int_0^{\mathring{s}} s^2\left[s^3\mathtt{J}_3(s)\right]'\,ds = \mathring{s}^5\mathtt{Z}_3(\mathring{s}) - 2\int_0^{\mathring{s}}\left[s^4\mathtt{Z}_4(s)\right]'\,ds = \mathring{s}^5\mathtt{Z}_3(\mathring{s}) - 2\,\mathring{s}^4\mathtt{Z}_4(\mathring{s})\,, \end{cases}$$

and eventually find

$$\begin{cases} I_1^* = \mathring{s}^5\mathtt{Z}_0(\mathring{s}) - 4\,\mathring{s}^4\mathtt{Z}_2(\mathring{s}) + \ \ 8\,\mathring{s}^3\mathtt{Z}_3(\mathring{s})\,, \\ I_2^* = \mathring{s}^7\mathtt{Z}_0(\mathring{s}) - 6\,\mathring{s}^6\mathtt{Z}_2(\mathring{s}) + 24\,\mathring{s}^5\mathtt{Z}_3(\mathring{s}) - 48\,\mathring{s}^4\mathtt{Z}_4(\mathring{s})\,, \end{cases} \tag{4.17}$$

whereas assuming that $\epsilon=2$, we find both integrals $\bar{I}_{1,2}^*$ to equal

$$\begin{cases} \bar{I}_1^* = \displaystyle\int_0^{\mathring{s}} s^4\left[s^2\mathtt{Z}_2(s)\right]'\,ds = \mathring{s}^6\mathtt{Z}_2(\mathring{s}) - 4\,\mathring{s}^5\mathtt{Z}_3(\mathring{s}) + 8\,\mathring{s}^4\,\mathtt{J}_4(\mathring{s})\,, \\ \bar{I}_2^* = \displaystyle\int_0^{\mathring{s}} s^4\left[s^3\mathtt{Z}_3(s)\right]'\,ds = \mathring{s}^7\mathtt{Z}_3(\mathring{s}) - 4\,\mathring{s}^6\mathtt{Z}_4(\mathring{s}) + 8\,\mathring{s}^5\mathtt{Z}_5(\mathring{s})\,, \end{cases}$$

yielding to

$$\begin{cases} I_1^* = \mathring{s}^7\mathtt{Z}_1(\mathring{s}) - 6\,\mathring{s}^6\mathtt{Z}_2(\mathring{s}) + 24\,\mathring{s}^5\mathtt{Z}_3(\mathring{s}) - \ \ 48\,\mathring{s}^4\mathtt{Z}_4(\mathring{s})\,, \\ I_2^* = \mathring{s}^9\mathtt{Z}_1(\mathring{s}) - 8\,\mathring{s}^8\mathtt{Z}_2(\mathring{s}) + 48\,\mathring{s}^7\mathtt{Z}_3(\mathring{s}) - 192\,\mathring{s}^6\mathtt{Z}_4(\mathring{s}) + 384\,\mathring{s}^5\mathtt{Z}_5(\mathring{s})\,. \end{cases} \tag{4.18}$$

3) Let $\alpha=\frac{3}{2}$, then $\theta=\frac{1}{2}$, $\nu=-\frac{1}{2}$, $\varrho=1$, and $\upsilon=4\epsilon+6$ (4.12), and applying the property (4.14) yields to

$$\begin{cases} I_1^* = \displaystyle\int_0^{\mathring{s}} s^{4\epsilon+4}\left[s^2\mathtt{Z}_1(s)\right]\,ds = \mathring{s}^{4\epsilon+6}\,\mathtt{Z}_2(\mathring{s}) - (4\epsilon+4)\left\{\mathring{s}^{4\epsilon+5}\,\mathtt{Z}_3(\mathring{s}) - (4\epsilon+2)\,\bar{I}_1^*\right\}, \\ I_2^* = \displaystyle\int_0^{\mathring{s}} s^{4\epsilon+6}\left[s^2\mathtt{Z}_1(s)\right]\,ds \\ \quad = \mathring{s}^{4\epsilon+8}\,\mathtt{Z}_2(\mathring{s}) - (4\epsilon+6)\left\{\mathring{s}^{4\epsilon+7}\,\mathtt{Z}_3(\mathring{s}) - (4\epsilon+4)\left[\mathring{s}^{4\epsilon+6}\,\mathtt{Z}_4(\mathring{s}) - (4\epsilon+2)\,\bar{I}_2^*\right]\right\}, \end{cases}$$

where the integrals $\bar{I}_1^*$ and $\bar{I}_2^*$ are

$$\begin{cases} \bar{I}_1^* = \displaystyle\int_0^{\mathring{s}} s^{4\epsilon} \left[s^4 \mathtt{Z}_4(s)\right]' \, ds \,, \\ \bar{I}_2^* = \displaystyle\int_0^{\mathring{s}} s^{4\epsilon} \left[s^5 \mathtt{Z}_5(s)\right]' \, ds \,. \end{cases}$$

Assumption $\epsilon = \frac{1}{2}$ gives

$$\begin{cases} \bar{I}_1^* = \displaystyle\int_0^{\mathring{s}} s^2 \left[s^4 \mathtt{Z}_4(s)\right]' \, ds = \mathring{s}^6 \mathtt{Z}_4(\mathring{s}) - 2\,\mathring{s}^5 \mathtt{Z}_5(\mathring{s}) \,, \\ \bar{I}_2^* = \displaystyle\int_0^{\mathring{s}} s^2 \left[s^5 \mathtt{Z}_5(s)\right]' \, \mathrm{d}s = \mathring{s}^7 \mathtt{Z}_5(\mathring{s}) - 2\,\mathring{s}^6 \mathtt{Z}_6(\mathring{s}) \,, , \end{cases}$$

that yields to

$$\begin{cases} I_1^* = \mathring{s}^8 \; \mathtt{Z}_2(\mathring{s}) - 6\,\mathring{s}^7 \mathtt{Z}_3(\mathring{s}) + 24\,\mathring{s}^6 \mathtt{Z}_4(\mathring{s}) - \;\; 48\,\mathring{s}^5 \mathtt{Z}_5(\mathring{s}) \,, \\ I_2^* = \mathring{s}^{10} \mathtt{Z}_2(\mathring{s}) - 8\,\mathring{s}^9 \mathtt{Z}_3(\mathring{s}) + 48\,\mathring{s}^8 \mathtt{Z}_4(\mathring{s}) - 192\,\mathring{s}^7 \mathtt{Z}_5(\mathring{s}) + 384\,\mathring{s}^6 \mathtt{Z}_6(\mathring{s}) \,, \end{cases}$$

whereas assumption $\epsilon = 1$ leads to

$$\begin{cases} \bar{I}_1^* = \displaystyle\int_0^{\mathring{s}} s^4 \left[s^4 \mathtt{J}_4(s)\right]' \, ds = \mathring{s}^8 \mathtt{J}_4(\mathring{s}) - 4\,\mathring{s}^7 \mathtt{J}_5(\mathring{s}) + 8\,\mathring{s}^6 \mathtt{J}_6(\mathring{s}) \,, \\ \bar{I}_2^* = \displaystyle\int_0^{\mathring{s}} s^4 \left[s^5 \mathtt{J}_5(s)\right]' \, ds = \mathring{s}^9 \mathtt{J}_5(\mathring{s}) - 4\,\mathring{s}^8 \mathtt{J}_6(\mathring{s}) + 8\,\mathring{s}^7 \mathtt{J}_7(\mathring{s}) \,, \end{cases}$$

and eventually to

$$\begin{cases} I_1^* = \mathring{s}^5 \mathtt{Z}_0(\mathring{s}) - 4\,\mathring{s}^4 \mathtt{Z}_2(\mathring{s}) + 8\,\mathring{s}^3 \mathtt{Z}_3(\mathring{s}) \,, \\ I_2^* = \mathring{s}^{10} \mathtt{Z}_2(\mathring{s}) - 6\,\mathring{s}^6 \mathtt{Z}_2(\mathring{s}) + 24\,\mathring{s}^5 \mathtt{Z}_3(\mathring{s}) - 48\,\mathring{s}^4 \mathtt{Z}_4(\mathring{s}) \,. \end{cases}$$

As an example, we choose the values $\alpha = 1$ ($\varrho = 0,\ \theta = 1$) and $\epsilon = 1$, then substitute the formula (4.15) and the values (4.17) of I_1^*, I_2^* into the expressions (4.11) to obtain

$$\begin{cases} I_0 = \dfrac{2}{\mathring{s}^2} \left[\mathring{s}\, \mathtt{Z}_1(\mathring{s})\right] , \\ I_1 = \dfrac{2}{\mathring{s}^6} \left[\mathring{s}^5 \mathtt{Z}_1(\mathring{s}) - 4\,\mathring{s}^4 \mathtt{Z}_2(\mathring{s}) + \;\; 8\,\mathring{s}^3 \mathtt{Z}_3(\mathring{s})\right] , \\ I_2 = \dfrac{2}{\mathring{s}^8} \left[\mathring{s}^7 \mathtt{Z}_1(\mathring{s}) - 6\,\mathring{s}^6 \mathtt{Z}_2(\mathring{s}) + 24\,\mathring{s}^5 \mathtt{Z}_3(\mathring{s}) - 48\,\mathring{s}^4 \mathtt{Z}_4(\mathring{s})\right] , \end{cases}$$

and eventually find the required coefficients (4.10)

$$
\begin{cases}
a_\mu = -\dfrac{2}{\mathring{s}^4 \mathtt{J}_1^2(\mathring{s})} \left[\mathring{s}^3 \mathtt{J}_1(\mathring{s}) - 6\,\mathring{s}^2 \mathtt{J}_2(\mathring{s}) + 24\,\mathring{s} \mathtt{J}_3(\mathring{s}) - 48\,\mathtt{J}_4(\mathring{s})\right], \\
b_\mu = +\dfrac{18}{\mathring{s}^4 \mathtt{J}_1^2(\mathring{s})} \left[\mathring{s}^3 \mathtt{J}_1(\mathring{s}) - 4\,\mathring{s}^2 \mathtt{J}_2(\mathring{s}) + 8\,\mathring{s} \mathtt{J}_3(\mathring{s})\right], \\
c_\mu = -\dfrac{2}{\mathring{s}^4 \mathtt{J}_1^2(\mathring{s})} \left[\mathring{s}^3 \mathtt{J}_1(\mathring{s})\right] \\
\qquad + \dfrac{2}{\mathring{s}^4 \mathtt{J}_1^2(\mathring{s})} \left[\mathring{s}^3 \mathtt{J}_1(\mathring{s}) - 6\,\mathring{s}^2 \mathtt{J}_2(\mathring{s}) + 24\,\mathring{s} \mathtt{J}_3(\mathring{s}) - 48\,\mathtt{J}_4(\mathring{s})\right], \\
d_\mu = -\dfrac{18}{\mathring{s}^4 \mathtt{J}_1^2(\mathring{s})} \left[\mathring{s}^3 \mathtt{J}_1(\mathring{s}) - 4\,\mathring{s}^2 \mathtt{J}_2(\mathring{s}) + 8\,\mathring{s} \mathtt{J}_3(\mathring{s})\right].
\end{cases}
$$

References

1. V. L. Borsch, *On initial boundary value problems for the degenerate 1D wave equation*, Journal of Optimization, Differential Equations, and their Applications (JODEA), **27**(2) (2019), 27–44.
2. V. L. Borsch, P. I. Kogut, G. Leugering, *On an initial boundary-value problem for 1D hyperbolic equation with interior degeneracy: series solutions with the continuously differentiable fluxes*, Journal of Optimization, Differential Equations, and their Applications (JODEA), **28**(1) (2020), 1 – 42.
3. G. Doetsch, *Introduction to the Theory and Application of the Laplace Transformation*, Springer, NY, 1974.
4. A. M. Kohen, *Numerical Methods for Laplace Transform Inversion*, Springer Science+Business Media, LLC, NY, 2007.
5. Yu. V. Sidorov, M. V. Fedoryuk, M. I. Shabunin, *Lectures on the Theory of Functions of a Complex Variable*, Mir Publishers, Moscow, 1985.
6. G. P. Tolstov, *Fourier Series*, Dover, NY, 1962.
7. G. N. Watson, *A Treatise on the Theory of Bessel Functions*, Cambridge University Press, Cambridge, 1922.

Received 30.04.2021

JOURNAL OF OPTIMIZATION, DIFFERENTIAL EQUATIONS AND THEIR APPLICATIONS (JODEA)
Volume **29**, Issue **1**, June **2021**, pp. 32–41, DOI 10.15421/142102

ISSN (print) 2617–0108
ISSN (on-line) 2663–6824

MATHEMATICAL MODEL AND CONTROL DESIGN OF A FUNCTIONALLY STABLE TECHNOLOGICAL PROCESS

Volodymyr V. Pichkur[*], Valentyn V. Sobchuk[†]

Communicated by Prof. A.V. Plotnikov

Abstract. The paper suggests an approach to modeling of industrial enterprises providing production according to the set standard with admissible tolerances and requirements. The mathematical model has the form of a discrete control system. We use the properties of generalized inverse matrices to design the control. We present an algorithm of the control of a production process providing release of production. This approach allows to simulate the technological processes (including metallurgical, chemical, energy, etc.) and gives the operating conditions under the constant influence of internal and external destabilizing factors.

Key words: Functional stability, mathematical model of technological process, control design, generalized invertion.

2010 Mathematics Subject Classification: 93C55, 93C95, 03C45, 03H10.

1. Introduction

Nowadays the problem of improving the efficiency of the production enterprise management is of constant interest to the researchers. The problem is related to the improvement of the operations management and production planning system at the enterprise level. The main purpose of organization of the planning processes is to ensure thorough fulfillment of the production tasks together with maximal utilization of the production resources. This allows timely fulfillment of the obligations to produce outputs by the time they are required at the next production line, guarantees the optimal duration of the production cycle, and leads to the reduction of work in progress and to the minimization of shortages.

It is advisable to use the methods of mathematical modeling and simulation to create a technology of planning in production. Approaches to the mathematical modeling of production processes in an enterprise as a whole and in its individual production centers are underdeveloped. Therefore, it is necessary to create the techniques which allow describing the production processes in the strict mathematical terms. The authors suggest an approach which can be practically integrated into wide classes of the information platforms for manufacturing enterprises: MRP

[*]Department of Complex Systems Modeling, Faculty of Computer Science and Cybernetics, Taras Shevchenko National University of Kyiv, Acad. Glushkov Ave, 4d, Kyiv, Ukraine, 03680, v.pichkur@gmail.com

[†]Department of Higher Mathematics, State University of Telecommunications, 7, Solomianska str., 03110 Kyiv, Ukraine v.v.sobchuk@gmail.com

II (Manufacturing Resource Planning), ERP (Enterprise Resource Planning), APS (Advanced Planning & Scheduling Systems) and MES (Manufacturing Execution Systems). Given the high level of the automation of production, the introduction of effective tools in the form of production planning system class APS (Advanced Planning & Scheduling Systems) in combination with MES - systems (Manufacturing Execution Systems) provides high-precision production process planning in real time [1, 2].

2. Mathematical Model of the Production Process Management System of an Industrial Enterprise

Considering the problem of designing the control which ensures the execution of the production process in accordance with the established standards the authors have reviewed the mathematical model of the production control system of an industrial enterprise. Having analyzed the problems of the automation of the enterprise management systems the authors intend to suggest an algorithm for the automation of the production process using the technique of genelized inversion [2].

The production process of a modern enterprise consists of a set of measures to produce finished, semi-finished or other products. One of the main tasks of industrial development is the introduction of the new products, machine and equipment designs, automation tools, the latest technologies, etc. Each product industry has its own specifics depending on the type of production, purpose, size and accuracy of the machines, level of production and technical equipment. In general case, automation of the production is a stage of machine production, characterized by the release of the human factor from the direct performance of the management functions in the production processes and the delegation of these functions to the information and computing systems [3]. Control is a purposeful action on the object to ensure its operation in the optimal or specified mode within acceptable tolerances.

Automation of the production processes does not exclude a person completely from the value chain. Automation rather means the most rational distribution of computing and production load at each production center. The proportions of such distribution depends on the specific enterprise and the goals of automation. The enterprise automation processes are subject to certain requirements, without which they become inefficient and difficult to implement.

Firstly, a process management model is a must. At present, significant number of the enterprises operate on the basis of a system-functional approach, which preceded the process approach. The complexity of the transition to the process management model depends on the scale and specifics of an enterprise.

Secondly, compliance of the current model of the enterprise processes with the technical criteria used in their automation is a very important requirement.

Nowadays at modern enterprises it is impossible to organize a serial production of the quality products without automation of the process of control over the parameters of production processes. We suggest a mathematical model for solving the similar problems of the manufacturing plants, to ensure the stability of production processes with real-time control of key production parameters. This model can be integrated into an automated enterprise management system. The property of functional stability of complex technical systems must be realized. It means that the technological process must perform its main technological tasks as intended under the influence of external and internal destabilizing factors [4].

The automation stage allows re-engineering of the processes. The purpose of reengineering is to find and overcome the bottlenecks in the enterprise. It is necessary to monitor the production potential, to identify the opportunities for expansion of the production system of the enterprise, the resources that are not used rationally, and so on. It is important to prepare the companies for the re-engineering process. It is necessary to bring the structures of its processes in the most efficient configuration and in the most efficient form. It is necessary to ensure strict compliance with the requirements for the technological process at each production center in accordance with the standards, with the deviations only within the permissible tolerance standards.

In practice, the principal characteristics of integrated automated enterprise management systems are widely implemented for this purpose. These systems automate a wide range of the management functions, including the tasks of strategic, production and financial planning, operational management of supply, procurement, and inventory. In addition, they automate the tasks of design, technological and technical preparation of production, etc.

Automation of the modern technological processes leads to the creation of the complex dynamic models. The behavior of such models has a fractal structure [5]. Many processes are described by nonlinear dynamical systems of complex structure that have global attractors [6–8]. At the same time problems of control arise in such systems [9–13].

Producing usually consists of a number of stages, at each of which there are certain requirements for the parameters and characteristics of the raw materials, semifinished and finished products. Denote by $x(i)$ the vector of parameters at i -th stage, $i = 1, 2, \dots N$ (2.1). At each stage there is an external influence $u(i)$ on the production process to obtain the desired parameters (work effect, energy effect, chemical or other technological influences at each stage). It is clear that the final quality of the product, as well as the intermediate quantity at each stage, depends on the strict adherence to the technology and ensuring the endurance of the necessary parameters at each previous step. We assume that this requirement holds.

Also we denote by $A(i)$ a matrix of dependence of product quality indicators at $i+1$-st stage on the indicators at i-th stage, and by $C(i)$ a matrix that determines the structure of influence on the production process $u(i)$. Then the mathematical model of the technological process can be written as follows

$$x\,(t+1) = A\,(t)\,x\,(t) + C\,(t)\,u\,(t)\,,\ t = 0, 1, \dots, N-1, \tag{2.1}$$

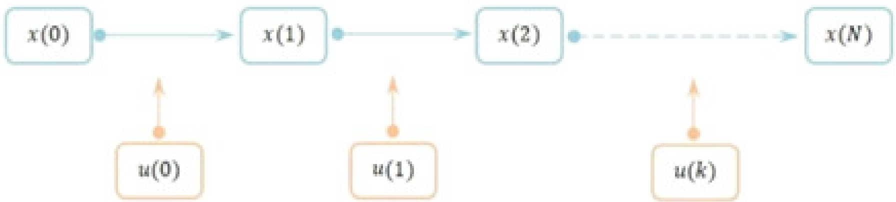

Fig. 2.1. Topology of linear technological production process

$$x(t) \in \mathbb{R}^n,\ A(t) \in \mathbb{R}^{n\times n},\ C(t) \in \mathbb{R}^{n\times m},\ u(t) \in \mathbb{R}^m.$$

Here we denote by $\mathbb{R}^n$ the n-dimensional Euclidean space with the Euclidean norm $\|\cdot\|$ in it, $x = (x_1, x_2, \ldots, x_n)^T$ is a state vector of system (2.1), $u = (u_1, \ldots, u_m)^T$ is a control vector, $A(t)$ is an $n \times n$ matrix, $C(t)$ is an $n \times m$ matrix, $t = 0, 1, \ldots, N-1$. Let $I_N = \{0, 1, \ldots, N\}$, $x(t, x_0, u)$ be a solution of system (2.1), $t \in I_N$ under the control $u(t)$, $t \in I_{N-1}$.

We admit that there is an accurately defined set of certain works and a number of criteria in order to fulfill during realization of process. It means that we know characteristics of the process at the initial stage, requirements for products at the end of the process, and intermediate characteristics of products at control points at stages of this process. At the same time, in the automation of such processes in practice it is necessary to set control tasks describing the design conditions for the control function u providing controlled purposeful execution of the process. In addition, it is advisable to provide conditions for practical stability for these processes [13–18].

3. Control Design

The main problem we analyze consists of finding the control function providing execution of the process, so that the result of the process ensures ultimately in $x(N)$ products that meet all the quality characteristics required by current standards for it.

The purpose of designing a control function u is to ensure that the process is performed in such a way that we end up with a product that meets all the characteristics required by the standards. If at the end of the process the product has deviations from the specified standard parameters, then such deviations are guaranteed to fall into the set of permissible tolerances, which are defined by current standards for such products [2]. This means that there is a desired final state $x_N \in \mathbb{R}^n$ and a positive parameter $\varepsilon > 0$ such that

$$\|x(N) - x_N\| < \varepsilon.$$

Let us define a set of admissible controls. To do this, we consider space $\ell_2^{(m)}$ of sequences of vectors from $\mathbb{R}^m$ such that if $u \in \ell_2^{(m)}$ then $\sum_{t=0}^{\infty} \| u(t) \|^2 < \infty$,

$u(t) \in \mathbb{R}^m$, $t = 0, 1, 2, \ldots$. $\ell_2^{(m)}$ is a real Hilbert space with inner product

$$\langle u, v \rangle_{\ell_2} = \sum_{t=0}^{\infty} \langle u(t), v(t) \rangle, \ u, v \in \ell_2^{(m)}$$

and norm

$$\| u \|_{\ell_2} = \sqrt{\sum_{t=0}^{\infty} \|u(t)\|^2} < \infty.$$

We assume that a control function u is admissible if $u \in \ell_2^{(m)}$ and $u(t) = 0$, $t = N+1, N+2, \ldots$.

Denote $\Theta(t) = A_{t-1}A_{t-2}\ldots A_1 A_0$, $\Theta(t,s) = A_{t-1}A_{t-2}\ldots A_s$, $\Theta(t,t) = E$, where E is the identity matrix, $t, s \in I_N$. The problem is to find a control that moves the system (2.1) from the initial state $x(0) = x_0$ to the nearest point $x(N)$ to a given state x_N [12]. This way we get the problem of minimization

$$I(u) = \|x(N, x_0, u) - x_N\| \tag{3.1}$$

on the solutions of system (2.1) with the initial condition $x(0) = x_0$. Here $x(N, x_0, u)$ denotes the value of the solution of system (2.1) with the initial condition $x(0) = x_0$ for an admissible control $u \in \ell_2^{(m)}$ at the moment $t = N$. Since

$$x(N, x_0, u) = \Theta(N)\, x_0 + \sum_{k=0}^{N-1} \Theta(N,k)\, C(k)\, u(k),$$

then the substitution of the last equality in (3.1) gives

$$\begin{aligned} I(u) = \|x(N, x_0, u) - x_N\| &= \|\Theta(N)\, x_0 + \sum_{k=0}^{N-1} \Theta(N,k)\, C(k)\, u(k) - x_N\| \\ &= \| \sum_{k=0}^{N-1} W(k)\, u(k) - c\|, \end{aligned} \tag{3.2}$$

where $c = x_N - \Theta(N)x_0$,

$$W(t) = \Theta(N,t)\, C(t), \ W^T(t) = (w_1(t) \ w_2(t) \ \ldots \ w_n(t)),$$

$w_j(t) \in \mathbb{R}^m$, $t \in I_{N-1}$, $j = 1, 2, \ldots, n$ are vectors describing the matrix $W(t)$ rows, $t \in I_{N-1}$. At the same time, one can observe that

$$H = \{w_1(\cdot), w_2(\cdot), \ldots, w_n(\cdot)\} \subset \ell_2^{(m)}$$

and $w_j(t) = 0$, $t = N, N+1, \ldots$, $j = 1, 2, \ldots, n$.

We define a linear manifold $L = Lin\ H$. Since $\ell_2^{(m)}$ is Hilbert space then $\ell_2^{(m)}$ decomposes into a direct sum

$$\ell_2^{(m)} = L \oplus L^{\perp},$$

where $L^{\perp}$ is an orthogonal complement to L. Any control $u \in \ell_2^{(m)}$ can be represented as follows

$$u(t) = u_0(t) + v(t), \ t{=}\ 0, 1, \ldots. \tag{3.3}$$

Here $u_0 \in L$, $v \in L^{\perp}$. Therefore

$$\langle u_0, v \rangle_{\ell_2} = 0$$

for $u_0 \in L$. Since $u_0 \in Lin\ H$ there exists a vector $\lambda = (\lambda_1, \lambda_2, \ldots, \lambda_n)^T$ such that

$$u_0(t) = \lambda_1 w_1(t) + \lambda_2 w_2(t) + \lambda_n w_n(t) = W^T(t)\lambda \in Im(W^T(t)).$$

Here $Im(\cdot)$ denotes an image of a linear operator. From (3.3) we have

$$u(t) = W^T(t)\,\lambda + v(t), \quad t{=}\ 0, 1, \ldots. \tag{3.4}$$

Observe that $\sum_{k=0}^{N-1} W(k)\,v(k) = 0$ since $v \in L^{\perp}$. Substituting (3.4) in (3.2) transforms problem (3.1) into

$$J(\lambda) = \| \sum_{k=0}^{N-1} W(k)\,W^T(k)\,\lambda - c\| \to \min_{\lambda \in \mathbb{R}^n}, \tag{3.5}$$

$c = x_N - \Theta(N)x_0$. We see that $v \in L^{\perp}$ does not affect the solution (3.1), it plays the role of an invariant and it can be considered zero. Using the properties of generalized inversion [19] we obtain the solution of problem (3.5)

$$\widehat{\lambda} = \Phi^{+}(N)c + z, \tag{3.6}$$

where $\Phi(N) = \sum_{k=0}^{N-1} W(k)\,W^T(k)$, $\Phi^{+}(N)$ is a generalized inverse matrix to the matrix $\Phi(N)$, $z \in Ker(\Phi(N))$ is an arbitrary vector [19].

Since $Ker(\Phi(N)) = Z_N\mathbb{R}^n$, $Z_N = Z(\Phi(N)) = E - \Phi^{+}(N)\Phi(N)$ is the projection operator onto $Ker(\Phi(N))$, then (3.6) has the following representation

$$\widehat{\lambda} = \Phi^{+}(N)c + Z_N p, \tag{3.7}$$

where $p \in \mathbb{R}^n$, $c = x_N - \Theta(N)x_0$ [19]. Formula (3.7) describes the set of all solutions of problem (3.4). Note that among the vectors that solve the problem (3.5), the vector

$$\widehat{\lambda} = \Phi^{+}(N)c$$

has the smallest norm. This follows from the properties of generalized inverse matrices. Substituting (3.7) in (3.4) at $v(t) = 0$, $t \in I_{N-1}$ gives

$$u(t) = W^T(t)\,\Phi^{+}(N)\,(x_N - \Theta(N)x_0) + W^T(t)\,Z_N p. \tag{3.8}$$

$p \in \mathbb{R}^n$, $t \in I_{N-1}$. Formula (3.8) solves problem (3.1). If $p = 0$ then

$$u(t) = W^T(t)\,\Phi^{+}(N)\,(x_N - \Theta(N)x_0), \ t \in I_{N-1}.$$

Substituting (3.8) in (3.5) we obtain

$$I(u) = J(\widehat{\lambda}) = \|\Phi(N)\widehat{\lambda} - c\| = \|\Phi(N)\Phi^{+}(N)c + \Phi(N)Z_N p - c\|.$$

Since $Z_N p \in Ker(\Phi(N)$ then $\Phi(N)Z_N p = 0$. Therefore

$$I(u) = \|\Phi(N)\Phi^{+}(N)c - c\| = \|(I - \Phi(N)\Phi^{+}(N))c\|.$$

Since $Y(\Phi(N)) = \Phi(N)\Phi^{+}(N)$ is a projector onto the image $Im(\Phi(N))$ of the matrix $\Phi(N)$, $Z(\Phi^T(N)) = E - \Phi(N)\Phi^{+}(N)$ is a projector onto the kernel $Ker\left(\Phi^T(N)\right)$ of the matrix $\Phi^T(N)$ [19], then

$$I(u) = \|Y(\Phi(N))c - c\| = \|Z(\Phi^T(N))c\|. \tag{3.9}$$

Formula (3.9) shows how accurately we can move system (2.1) from the point $x(0) = x_0$ to the state $x(N) = x_N$. From (3.9) it follows, that $I(u) = 0$ if and only if $(\Phi(N))c = c$ or $Z(\Phi^T(N)) = 0$. Thus the following statement is true.

Theorem 3.1. *The control function*

$$u(t) = W^T(t)\,\Phi^{+}(N)\,(x_N - \Theta(N)x_0) + W^T(t)\,Z_N p \tag{3.10}$$

moves system (2.1) *from the initial state $x(0) = x_0$ to the nearest point $x(N)$ to a given state x_N. Here $p \in \mathbb{R}^n$, $t \in I_{N-1}$, $Z_N = Z(\Phi(N)) = E - \Phi^{+}(N)\,\Phi(N)$. Moreover*

$$\|x(N) - x_N\| = \|Y(\Phi(N))c - c\| = \|Z(\Phi^T(N))c\|$$

describes Euclidean distance from $x(N)$ to x_N, where $c = x_N - \Theta(N)x_0$. If $Y(\Phi(N))c = c$ so that $c = x_N - \Theta(N)x_0$ belongs to the image $Im(\Phi(N))$ of the matrix $\Phi(N)$, then (3.10) *moves system* (2.1) *from $x(0) = x_0$ to the point $x(N) = x_N$.*

Note that control function (3.10) solves the problem for arbitrary x_0, x_N if and only if $Z(\Phi^T(N)) = 0$ or in equivalent form $\Phi(N)\Phi^{+}(N) = E$. Since the matrix $\Phi(N)$ is symmetric of $n \times n$, this means that $\Phi^{+}(N) = \Phi^{-1}(N)$.

Theorem 3.2. *Among the control functions that moves system* (2.1) *from $x(0) = x_0$ to the nearest state $x(N)$ to the point x_N, the function*

$$u_*(t) = W^T(t)\,\Phi^{+}(N)\,(x_N - \Theta(N)x_0)\,,\ t \in I_{N-1} \tag{3.11}$$

has the smallest norm in $\ell_2^{(m)}$.

Proof. From the proof of theorem (3.1) it follows that the admissible control u moving system (2.1) from $x(0) = x_0$ to the nearest point to x_N $x(N)$ satisfies (3.3), where $u_0 = u_* + z_0 \in L$, u_* is determined by (3.11), $z_0(t) = W^T(t)\,Z_N p$, $p \in \mathbb{R}^n$, $t \in I_{N-1}$, $v \in L^{\perp}$. Then

$$\begin{aligned}
\|u\|_{\ell_2}^2 &= \langle u, u\rangle_{\ell_2} = \langle u_0 + v_0, u_0 + v_0\rangle_{\ell_2} \\
&= \langle u_0, u_0\rangle_{\ell_2} + \langle v_0, v_0\rangle_{\ell_2} + 2\langle u_0, v_0\rangle_{\ell_2} = \langle u_0, u_0\rangle_{\ell_2} + \langle v_0, v_0\rangle_{\ell_2} \\
&\geqslant \langle u_0, u_0\rangle_{\ell_2} = \langle u_* + z_0, u_* + z_0\rangle_{\ell_2} = \langle u_*, u_*\rangle_{\ell_2} + \langle z_0, z_0\rangle_{\ell_2} + 2\langle u_*, z_0\rangle_{\ell_2}.
\end{aligned}$$

Since $Z_N p \in Ker\Phi(N)$ we have $\Phi(N)Z_N p = 0$ and

$$\begin{aligned}\langle u_*, z_0\rangle_{\ell_2} &= \sum_{t=0}^{N-1} \left\langle W^T(t)\,\Phi^+(N)\,(x_N - \Theta(N)x_0)\,, W^T(t)\,Z_N p\right\rangle \\ &= \left\langle \Phi^+(N)\,(x_N - \Theta(N)x_0)\,, \sum_{t=0}^{N-1} W(t)\,W^T(t)\,Z_N p\right\rangle \\ &= \left\langle \Phi^+(N)\,(x_N - \Theta(N)x_0)\,, \Phi(N)Z_N p\right\rangle = 0.\end{aligned}$$

Finally, we obtain

$$\|u\|^2_{\ell_2} \geqslant \langle u_*, u_*\rangle_{\ell_2} + \langle z_0, z_0\rangle_{\ell_2} \geqslant \langle u_*, u_*\rangle_{\ell_2} = \|u_*\|^2_{\ell_2}.$$

The last inequality proves the theorem. □

4. Algorithm of Control of Production Process

We offer an algorithm of control design of the production process, which ensures the production according to a standard in compliance with the permissible standards of tolerances at a production plant.

Step 1. Given the initial state $x(0) = x_0$ and the final state $x(N) = x_N$, the parameter $\varepsilon > 0$ determining the set of possible deviations (tolerances) for the product from the requirements of the standard, the matrices $A(t)$, $C(t)$, $t = 0, 1, \ldots N-1$.

Step 2. Find the matrices

$$\Theta(N) = A_{N-1}A_{N-2}\ldots A_1A_0,\ \ \Theta(N,t) = A_{N-1}A_{N-2}\ldots A_t,$$
$$W(t) = \Theta(N,t)\,C(t),\ \ t = 0, 1, \ldots N-1.$$

Step 3. Find the matrix $\Phi(N) = \sum_{k=0}^{N-1} W(k)\,W^T(k)$.

Step 4. Find the generalized inverse matrix $\Phi^+(N)$.

Step 5. Find the control function

$$u(t) = K(t)\,(x_N - \Theta(N)x_0)\,,$$

where $K(t) = W^T(t)\,\Phi^+(N)$ for all $t = 0, 1, \ldots N-1$.

Step 6. Find the matrix $Z_N = E - \Phi^+(N)\Phi(N)$. If the condition

$$\|Z_N\,(x_N - \Theta(N)x_0)\| < \varepsilon$$

is true then the control $u(t)$ solves the problem with specified tolerances

$$\|x(N) - x_N\| < \varepsilon.$$

Otherwise the control $u(t)$ ensuring the producing of products with given tolerances does not exist. End of the algorithm description.

5. Conclusion

In this paper we have analyzed the modern approaches to the automation of production process management in the industrial enterprises, we have solved the problem of designing of a control function that ensures the implementation of the production process. As a result of the process, we get a finished product that meets all the characteristics required by the current standards. We propose an algorithm for automating the atomic process of production.

The research results are important for the design, modernization and integration of the enterprise information systems into one generalized enterprise information system. This will ensure their high efficiency in operation. The lack of such solutions in our country and abroad makes research results a priority.

We see the prospects for further research in the design and improvement of the models and methods for constructing functionally stable technological processes that are integrated into the information system of the enterprise. This approach ensures the efficiency of the information infrastructure during the time required to perform the technological processes and sustainable operation of the enterprise as a whole. In doing so, we will take into account the specific needs of the enterprises operating in the sectors with continuous production cycle, such as metallurgy, energy, chemical industry and so on.

References

1. Zagidullin, R.R., *Management of machine-building production by means of MES, APS, ERP systems*, *TNT*, Stary Oskol, 2011 (in Russian).
2. Sobchuk, V., Pichkur, V., Barabash, O., Laptiev, O., Kovalchuk, I., Zidan, A., *Algorithm of control of functionally stable manufacturing processes of enterprises*, *2020 2nd IEEE International Conference on Advanced Trends in Information Theory*, (2020), 206-210 doi:10.1109/ATIT50783.2020.9349332.
3. Barabash, H. Tverdenko, V. Sobchuk, A. Musienko and N. Lukova-Chuiko, *The Assessment of the Quality of Functional Stability of the Automated Control System with Hierarchic Structure*, *2020 IEEE 2nd International Conference on System Analysis & Intelligent Computing (SAIC), Kyiv, Ukraine*, (2020), 158 – 161, doi: 10.1109/SAIC51296.2020.9239122.
4. Maksymuk, O., Sobchuk, V., Salanda, I., Sachuk, Yu., *A system of indicators and criteria for evaluation of the level of functional stability of information heterogenic networks*, *Mathematical Modeling and Computing*, **7** (2) (2020), 285 – 292, DOI 10.23939/mmc2020.02.285.
5. Oleg Barabash, Oleg Kopiika, Iryna Zamrii, Valentyn Sobchuk, Andrey Musienko, *Fraktal and Differential Properties of the Inversor of Digits of Q_s-Representation of Real Number*, *Modern Mathematics and Mechanics: Fundamentals, Problems and Challenges*, *Springer*, 2019, 79–95.
6. Kapustyan, A.V., *Global attractors of a nonautonomous reaction-diffusion equation*, *Differential Equations*, **38** (10) (2002), 1467–1471.
7. Kapustyan, O.V., Shkundin, D.V., *Global attractors of one nonlinear parabolic equation*, *Ukrainian Mathematical Journal*, **55** (4) (2003), 446–455.
8. Pichkur, V.V., Kapustyan, O.V., Sobchuk, V.V., *Theory of dynamical systems. Lutsk*, *Vezha*, 2020 (in Ukrainian).

9. Garashchenko, F.G., Pichkur, V.V., *Structural optimization of dynamic systems by use of generalized Bellman's principle*, Journal of Automation and Information Sciences, **32** (3) (2000), 1–6.
10. Peter I. Kogut, Olha P. Kupenko, Guenter Leugering, Yue Wang, *A note on weighted sobolev spaces related to weakly and strongly degenerate differential operators*, Journal Of Optimization, Differential Equations and their Applications, **29** (1) (2021), 1–22, DOI 10.15421/141905.
11. Kirichenko, N.F., Matvienko, V.T., *General solution of terminal control and observation problems*, Cybernetics and Systems Analysis, **36** (2) (2000), 219 – 228.
12. Matvienko, V.T., *Control of trajectories set by linear dynamic systems with discrete argument*, Journal of Automation and Information Sciences, **39** (11) (2007), 4–10.
13. Pichkur, V.V., Sasonkina, M.S., *Practical stabilization of discrete control systems*, International Journal of Pure and Applied Mathematics, **81** (6) (2012), 877–884.
14. Bashnyakov, A.N., Pichkur, V.V., Hitko, I.V., *On Maximal Initial Data Set in Problems of Practical Stability of Discrete System*, Journal of Automation and Information Sciences, **43** (3) (2001), 1–8.
15. Garashchenko, F. G., Pichkur, V. V., *Properties of optimal sets of practical stability of differential inclusions. part I. part II*, Journal of Automation and Information Sciences, **38** (3) (2006), 1–11.
16. Pichkur, V., *On practical stability of differential inclusions using Lyapunov functions*, Discrete and Continuous Dynamical Systems - Series B, **22** (5) (2017), 1977-1986.
17. Pichkur, V.V., *Maximum sets of initial conditions in practical stability and stabilization of differential inclusions*, In: Sadovnichiy, V.A., Zgurovsky, M. (eds.) Modern Mathematics and Mechanics. Fundamentals, Problems and Challenges. Understanding Complex Systems, *Springer*, Berlin, 2019, 397-410.
18. Pichkur, V.V., Linder, Y.M., *Practical Stability of Discrete Systems: Maximum Sets of Initial Conditions Concept*, In: Sadovnichiy, V.A., Zgurovsky, M. (eds.) Contemporary Approaches and Methods in Fundamental Mathematics and Mechanics. Understanding Complex Systems, *Springer*, Berlin, 2021, 381-394.
19. Albert, Arthur, *Regression and the Moore-Penrose pseudoinverse. Burlington, Elsevier*, MA, 1972.

Received 06.05.2021

JOURNAL OF OPTIMIZATION, DIFFERENTIAL EQUATIONS AND THEIR APPLICATIONS (JODEA)
Volume **29**, Issue **1**, June **2021**, pp. 42–53, DOI 10.15421/142103

ISSN (print) 2617–0108
ISSN (on-line) 2663–6824

COMPUTER SIMULATION OF THE STRESS-STRAIN STATE OF THE PLATE WITH CIRCULAR HOLE AND FUNCTIONALLY GRADED INCLUSION

Eteri L. Hart*, Bohdan I. Terokhin†

Communicated by Prof. V.O. Kapustyan

Abstract. Computer simulation of the behavior of a thin elastic rectangular plate with a circular hole and an annular inclusion made of functionally graded material has been carried out. Using the finite element method, the influence of the geometric and mechanical parameters of the inclusion on the concentration of stresses around the hole is investigated and various laws of the change in the modulus of elasticity of a functionally graded material are specified. A comparative analysis of the results has been carried out. The recommendations for reducing stress concentration are given.

Key words: Elastic plate, circular hole, inclusion, functionally graded material, stress concentration factor, finite element method.

2010 Mathematics Subject Classification: 35J50, 35J57, 39B42,74G70,74K20, 74S05.

1. Introduction

Plates and shells with holes are quite often used in various fields of technology, power engineering, construction, etc. The presence of holes leads to the appearance of local (additional) stresses, which can be several times higher than the basic stresses in an element that is not weakened by a concentrator. Under certain conditions, this initiates destruction processes. That is why, in order to increase the strength of the structure, it is necessary to look for ways to influence the distribution of stresses in the body, in particular, on the value of the stress concentration factor (SCF). One of these methods is the use of inclusions around the holes, of various geometric shapes and mechanical properties [5, 6, 11].

Recently, in the manufacture of plate-shell structural elements of new technology, in particular, aerospace, functionally graded materials (FGM) [16, 17] are used, which are classified as materials with unique mechanical, technological and special properties. A specific feature of FGM is a smooth change in mechanical properties and chemical composition in a certain direction. The gradient structure of materials provides an increase in the level of service properties of parts and structural elements, taking into account the respective operating conditions. FGMs have

*Department of Theoretical and Computer Mechanics, Oles Honchar Dnipro National University, 72, Gagarin av., Dnipro, 49010, Ukraine, hart@ua.fm
†Department of Theoretical and Computer Mechanics, Oles Honchar Dnipro National University, 72, Gagarin av., Dnipro, 49010, Ukraine, bogdan.teryokhin@gmail.com

high strength and a set of properties when working for impact, wear, fatigue, they can withstand increased cyclic and alternating loads, etc.

Taking into account the presence of this kind of material inhomogeneity leads to an increase in the complexity of the mathematical model of the problem. Finding the exact solution of the obtained boundary value problem in an analytical form is possible only in some individual cases of the load of bodies and under certain conditions of their fixation [3, 12, 13, 19–23]. Therefore, when studying the stress-strain state (SSS) of structures made of FGM and with various inhomogeneities (holes, inclusions, etc.), it is advisable to use numerical methods of mechanics, which, unlike analytical ones, are quite universal and effective for solving a wide class of problems. [2, 4, 6–11]. The most effective are grid methods: the finite element method [27], the finite difference method, the method of local variations and their projection-iterative implementation schemes [6–8], which accelerate the convergence of the process of obtaining a solution to the problem and significantly reduce the cost of computer computation time.

FGM mechanics has attracted great interest in the last two decades, and many works have appeared on theoretical, numerical and experimental studies of FGM. Thus, in [1], analytical solutions of mixed axisymmetric problems for functionally graded media were obtained. In [25, 26], using an analytical method, the stress distribution in a plate with an FGM with a circular hole was investigated. In [15], the stress concentration in multi-wedge systems with functionally graded wedges was estimated. In [14], using various isoparametrical finite elements, the SCF was determined in the vicinity of a circular cut in an inhomogeneous plate under uniaxial tension, in [18] the SCF was determined around a circular cut in an FGM plate under biaxial tension and shear.

In this work, using the finite element method (FEM), a computer simulation of the behavior of a thin elastic rectangular plate with a circular hole and an annular inclusion under the action of a uniaxial tensile load was carried out for various properties of the inclusion material and its dimensions.

2. Statement of the Problem

A thin elastic homogeneous isotropic plate is given with dimensions a×b and thickness t with a centrally located circular hole of radius R and an annular inclusion of radius R_1 (Fig. 2.1). A uniform uniaxial tensile load $p = \text{const}$ acts on the plate, which does not lead to the appearance of plastic deformations.

It is believed that the inclusion is modeled by an insert, which is in the plane of the plate and has the same thickness as it; conditions of rigid adhesion are specified at the boundary of the inclusion with the plate.

FGM inclusions with arbitrary radial elastic properties are considered. In the numerical examples, six model materials were selected with the same Poisson's ratio $\nu_0 = 0.25$, but with different inclusion elastic modulus $E_i(r)$ $(i = \overline{1,6})$. The first three materials have the following laws of change in the modulus of elasticity $E_i(r)$ $(i = \overline{1,3})$:

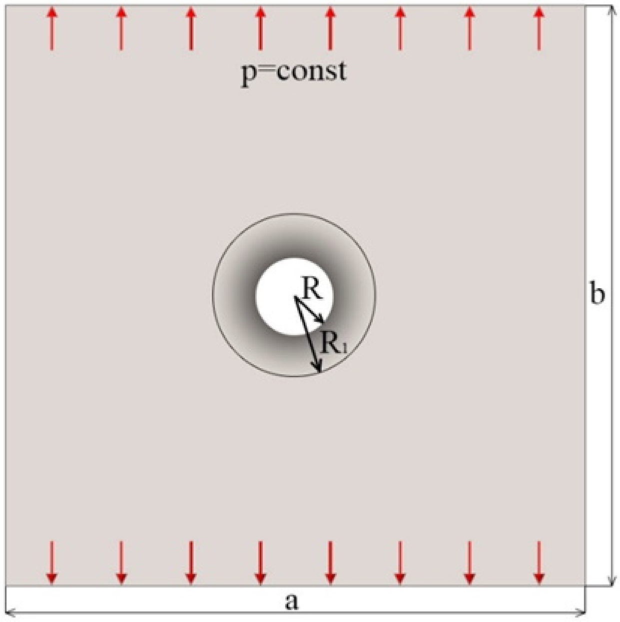

Fig. 2.1. Plate geometry and loading diagram

$$E_1(r) = \begin{cases} E_0(1+l), l \in [0;0,5] \\ E_0(2-l), l \in [0,5;1] \end{cases} ; \tag{2.1}$$

$$E_2(r) = \begin{cases} E_0(1+\frac{5}{4}l), l \in [0;0,4] \\ 1,5E_0, l \in [0,4;0,6] \\ E_0(2\frac{1}{4}-\frac{5}{4}l), l \in [0,6;1] \end{cases} ; \tag{2.2}$$

$$E_3(r) = \begin{cases} E_0(1+\frac{5}{3}l), l \in [0;0,3] \\ 1,5E_0, l \in [0,3;0,7] \\ E_0(2\frac{2}{3}-\frac{5}{3}l), l \in [0,7;1] \end{cases} , \tag{2.3}$$

where $E_0 = 100\,GPa$ is the modulus of elasticity of the plate; $0 \leqslant l \leqslant 1$ is the normalized parametric distance in the radial direction from the center of the hole along the width of the inclusion $h = R_1 - R : l = (r - R)/(R_1 - R)$, r is the distance from the center of the hole to an arbitrary point of inclusion; R and R_1 are the radii of the hole and the annular inclusion, respectively.

Note that for the given materials of inclusions (2.1)–(2.3), the values of the elastic modulus are in the range from 100 to 150 GPa. For three other model materials, the laws of change in the modulus of elasticity $E_i(r)$ $(i = \overline{4,6})$ are similar, but the values of the modulus of elasticity vary in the range from 100 to 200 GPa.

In Fig. 2.2 we show a graphical representation of the laws of change in the elastic modulus of an FGM inclusion. Lines 1-3 correspond to dependencies (2.1)–(2.3).

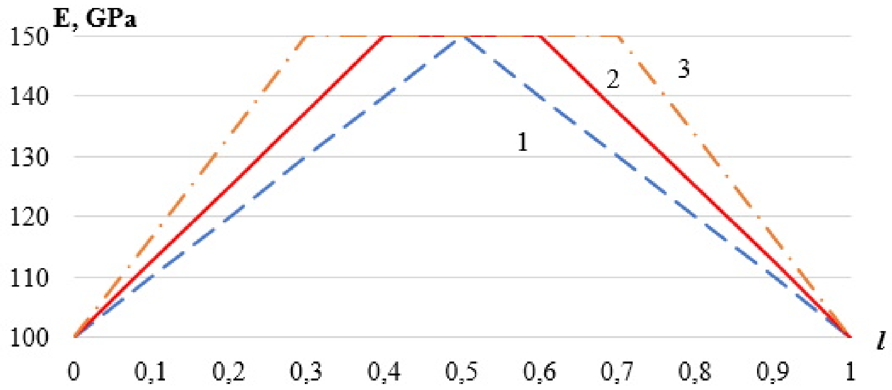

Fig. 2.2. The laws of change in the elastic modulus of FGM inclusions

It is necessary to determine the SSS of a given plate for each of the specified variants of inclusions to study the effect of the size and nature of the change in the modulus of elasticity of the inclusion on the SSS of the plate in the zones of local stress concentration and the effect on the value of the SCF; to carry out a comparative analysis of the results for a plate without an inclusion with a plate in the presence of an FGM-inclusion (Fig. 2.2).

3. Mathematical Model of the Problem

The relationship of the theory of elasticity for the region of a plane-stressed plate has the form [23, 24]:

— equilibrium equations:

$$\left\{ \begin{array}{l} \dfrac{\partial \sigma_{11}}{\partial x} + \dfrac{\partial \sigma_{12}}{\partial y} + R_1 = 0, \\ \dfrac{\partial \sigma_{21}}{\partial x} + \dfrac{\partial \sigma_{22}}{\partial y} + R_2 = 0, \end{array} \right. ; \tag{3.1}$$

or in matrix form

$$[\partial]^T \{\sigma\} + \{R\} = 0,$$

where $\left\{ \begin{array}{c} R_1 \\ R_2 \end{array} \right\}$ is a vector of volumetric forces, $[\partial] = \left[\begin{array}{ll} \partial/\partial x & 0 \\ 0 & \partial/\partial y \\ \partial/\partial y & \partial/\partial x \end{array} \right]$ is the differentiation matrix, $\{\sigma\} = \left\{ \begin{array}{c} \sigma_{11} \\ \sigma_{22} \\ \sigma_{12} \end{array} \right\}$ is the stress vector$(\sigma_{12} = \sigma_{21})$;

— geometric equations (in Cauchy form):

$$\varepsilon_{11} = \frac{\partial u_1}{\partial x}, \quad \varepsilon_{22} = \frac{\partial u_2}{\partial y}, \quad \gamma_{12} = \frac{\partial u_1}{\partial y} + \frac{\partial u_2}{\partial x} \tag{3.2}$$

or in matrix form

$$\{\varepsilon\} = [\partial]\,\{u\}\,,$$

where $\{u\} = \left\{ \begin{array}{c} u_1(x,\, y) \\ u_2(x,\, y) \end{array} \right\}$ is the displacement vector, $\{\varepsilon\} = \left\{ \begin{array}{c} \varepsilon_{11} \\ \varepsilon_{22} \\ \gamma_{12} \end{array} \right\}$ is the deformation vector;

— physical equations:

$$\varepsilon_{11} = \frac{\partial u_1}{\partial x}, \quad \varepsilon_{22} = \frac{\partial u_2}{\partial y}, \quad \gamma_{12} = \frac{\partial u_1}{\partial y} + \frac{\partial u_2}{\partial x} \tag{3.3}$$

which with respect to stresses have the form:

$$\begin{cases} \sigma_{11} = \dfrac{E}{1-\nu^2}\varepsilon_{11} + \dfrac{E\nu}{1-\nu^2}\varepsilon_{22}, \quad \sigma_{12} = \gamma_{12}\dfrac{E}{2(1+\nu)}, \\ \sigma_{22} = \dfrac{E\nu}{1-\nu^2}\varepsilon_{11} + \dfrac{E}{1-\nu^2}\varepsilon_{22}, \end{cases} \tag{3.4}$$

in the matrix form $\{\sigma\} = [E]\,\{\varepsilon\}$, where $[E]$ is the elastic matrix, ν is the Poisson's ratio,

$$[E] = \begin{bmatrix} \frac{E}{1-\nu^2} & \frac{E\nu}{1-\nu^2} & 0 \\ \frac{E\nu}{1-\nu^2} & \frac{E}{1-\nu^2} & 0 \\ 0 & 0 & \frac{E}{2(1-\nu)} \end{bmatrix}, \quad \{\varepsilon\} = \left\{ \begin{array}{c} \frac{\partial u_1}{\partial x} \\ \frac{\partial u_2}{\partial y} \\ \frac{\partial u_1}{\partial y} + \frac{\partial u_2}{\partial x} \end{array} \right\} \tag{3.5}$$

The work of internal forces on possible displacements:

$$\delta U = \frac{1}{2}\int_\Omega (\sigma_{11}\delta\varepsilon_{11} + \sigma_{22}\delta\varepsilon_{22} + \sigma_{12}\delta\gamma_{12})\, d\Omega = \frac{1}{2}\int_\Omega \{\delta\varepsilon\}^T\, \{\sigma\}\, d\Omega.$$

The work of external forces on possible displacements:

$$\delta A = \int_L \{P\}^T\, \{\delta u\}\, dL,$$

where $\{P\} = \left\{ \begin{array}{c} p_x(x,\, y) \\ p_y(x,\, y) \end{array} \right\}$ is the external load vector.

In the case of a uniform uniaxial tensile load $p_x(x,\, y) = p = \text{const}$; $p_y(x,\, y) = 0$.

For FGM in formulas (3.3)–(3.5), we set $E = E(x, y)$.

The functional of the total potential energy of deformation of a plate, which is loaded in its plane, has the form:

$$\prod = \frac{1}{2} \int_{\Omega} \{\delta\varepsilon\}^T \{\sigma\} \, d\Omega - \int_{L} \{P\}^T \{\delta u\} \, dL. \tag{3.6}$$

4. Solution Method

The solution of the obtained variational problem was carried out using the FEM [27]. The main idea of this method when analyzing the behavior of a structure is as follows: a continuous medium (the structure as a whole) is modeled by dividing it into subdomains (finite elements), in each of which the behavior of the medium is described using a separate set of selected, so-called basis functions representing stresses and move in the specified area. Within each finite element, the selected continuous function is approximated by a polynomial of some degree. As a result, the original variational problem is replaced by a discrete model, a system of linear or nonlinear algebraic equations with unknown values of the sought function at the nodes of the finite element mesh.

The calculations were carried out using triangular (six-node) Lagrangian finite elements of the second degree (Fig. 4.3, a), while the unknown displacement functions inside each finite element are approximated by a quadratic polynomial. In the areas of stress concentration, an adaptive mesh with a refinement factor of 10 was used (Fig. 4.3, b).

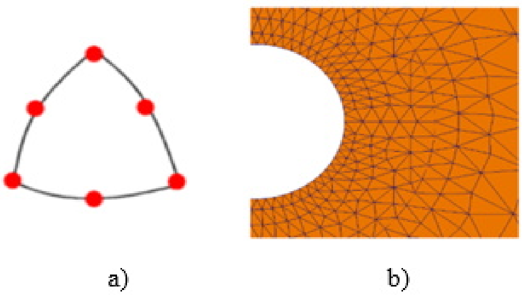

Fig. 4.3. Breakdown of an area into finite elements: a) the type of the final element; b) a fragment of an adaptive finite element mesh

5. Numerical Analysis

The calculations were carried out on a PC ARTLINE Gaming X75 (X75v16), with an Intel Core i7-10700F processor with a clock rate of 2.9–4.8GHz, 32 GB of RAM, an nVidia GeForce RTX 2060 SUPER video card, system bit width x64. The number of finite elements is 1871, the number of nodes is 3885 The calculation time on average is 4s.

Numerical studies were carried out for square plates of thickness $t = 0.01$m, with sides $a = b = 0.2$m. The radius of the circular hole is $R = a/20$, the tensile load is $p = 10$MPa.

For the purpose of comparative analysis, a calculation was carried out for a homogeneous plate with a circular hole without inclusion. Received $SCF = 3.05$; the maximum values of the intensity of deformations in this case, which is in good agreement with the results from [19].

As a result of the computational experiments using the FEM, the distribution of the stress and strain intensities in the plate was obtained, the SCF was calculated for uniaxial tension of the plate with inclusions from the FGM with the inclusion width R and $2R$.

When using FGM-inclusions 1, 2, 3 with the width of the inclusion $h = R$, the SCF almost does not change. Calculations for these inclusions at $h = 2R$ are given in Table 1. Here, δ_1 and δ_2 are the deviation of SCF and the maximum

Problem	SCF	δ_1, %	$\varepsilon_i^{\max}$, 10^{-4}	δ_2, %
FGM inclusion 1	2,84	-6,9	1,93	-9,4
FGM inclusion 2	2,81	-7,9	1,89	-11,3
FGM inclusion 3	2,79	-8,5	1,85	-13,1

Table 1. Stress concentration factor and corresponding deformations in a plate with FGM-inclusion at $h = 2R$

value of the intensity of deformation $\varepsilon_i^{\max}$ from the corresponding value for the plate without inclusion.

From Table. 1 it can be seen that in the case of an annular inclusion of width $2R$ from an FGM, the maximum deformations and SCF in a plate with a hole are less than in a plate without inclusions. The smallest SCFs and strains were obtained in the case of FGM inclusion 3.

In the presence of inclusions from FGM of width 2R, a redistribution of stresses occurs along the section AB from the edge of the inclusion to its middle part. Thus, the maximum stresses decrease, but the stresses increase along the width of the inclusion in the section AB in the interval $l \in [0,1;\ 0,7]$. The nature of the stress distribution is close to the parabolic pattern (Fig. 5.4).

The SCF and deformations under uniaxial tension of a plate with FGM inclusions 4, 5, 6 with the width of the inclusion R and $2R$ are shown in Table 2 and Table 3 respectively.

In the case with the inclusion width $h = R$ for all three variants of inclusions, the SCF decreased by about 8%, and the maximum deformations by 13-17% compared to the plate without inclusions. FGM-inclusion 6 turned out to be the best from the point of view of reducing the concentration of SSS parameters (Fig. 5.5).

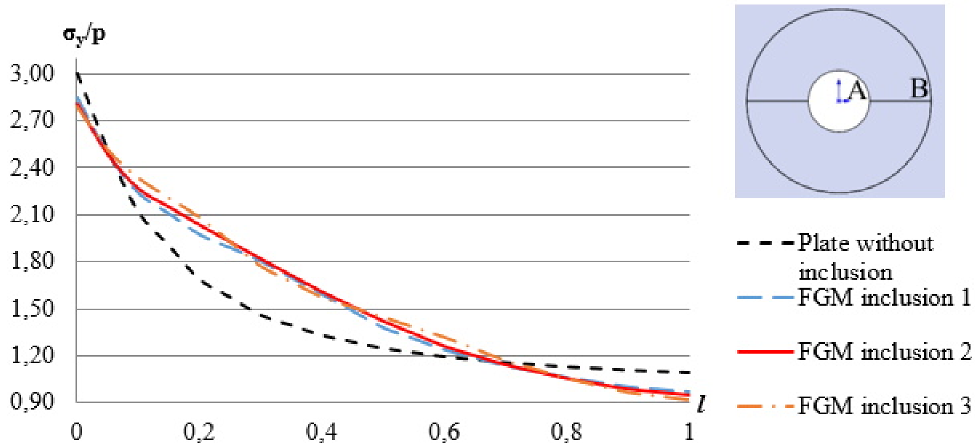

Fig. 5.4. Distribution of relative stresses σ_y/p in a plate with an FGM-inclusion over the width of the inclusion in the section AB at $h = 2R$

Problem	SCF	δ_1, %	$\varepsilon_i^{\max}$, 10^{-4}	δ_2, %
FGM inclusion 1	2,82	-7,5	1,85	-13,1
FGM inclusion 2	2,79	-7,5	1,80	-15,5
FGM inclusion 3	2,79	-8,5	1,76	-17,4

Table 2. Stress concentration factor and corresponding deformations in a plate with FGM-inclusion at $h = R$

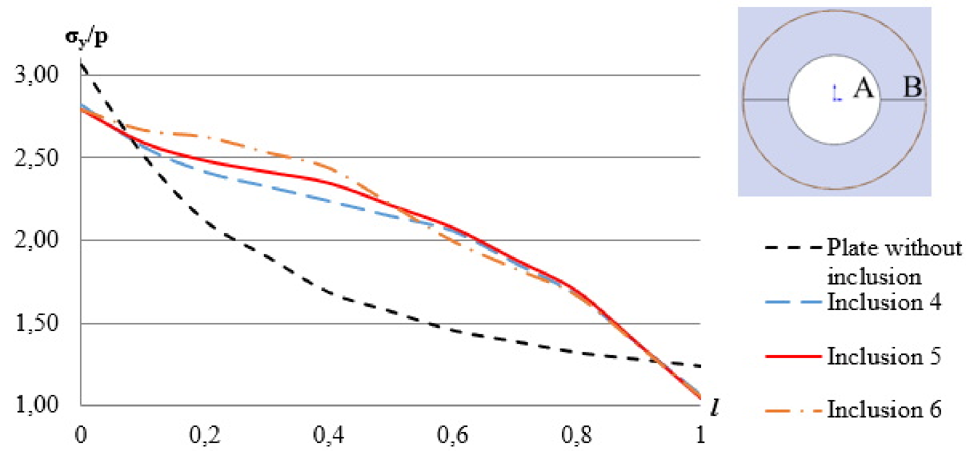

Fig. 5.5. Distribution of relative stresses σ_y/p in a plate with an FGM-inclusion over the width of the inclusion in the section AB at $h = R$

Analogical calculations were carried out for a plate with an inclusion width equal to $2R$. The results are shown in Table 3.

Problem	SCF	δ_1, %	$\varepsilon_i^{\max}$, 10^{-4}	δ_2, %
FGM inclusion 1	2,67	-12,8	1,76	-17,4
FGM inclusion 2	2,62	-14,4	1,70	-20,2
FGM inclusion 3	2,59	-15,4	1,64	-23,0

Table 3. Stress concentration factor and corresponding deformations in a plate with FGM inclusion at $h = 2R$

Here, the SCF and the maximum deformations in the plate in the presence of FGM inclusions also turn out to be less than in the case of a plate without inclusions, and the stress across the width of the inclusion in the section AB increases in the interval $l \in [0,1;\ 0,7]$ (Fig. 5.6). The nature of stress distribution in section AB for all three inclusions is similar. The best turns out to be FGM-inclusion 6, which makes it possible to reduce the stress concentration by $\sim 15\%$, and deformations by $\sim 23\%$.

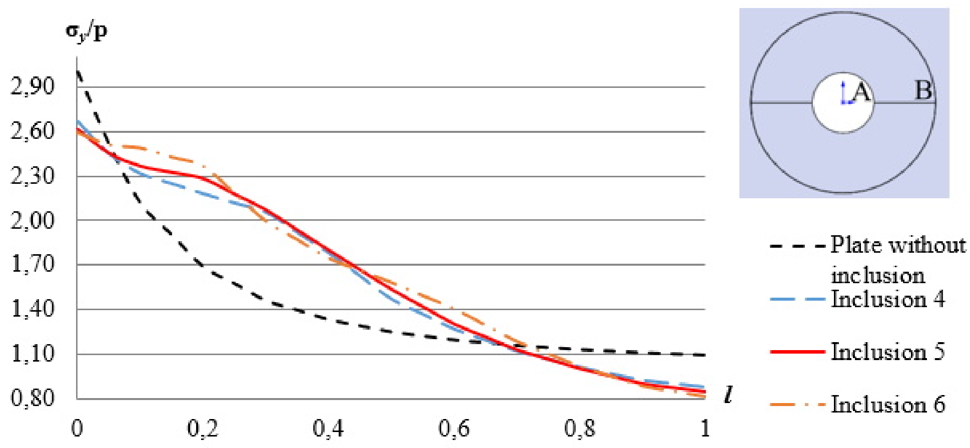

Fig. 5.6. Distribution of relative stresses σ_y/p in a plate with an FGM-inclusion over the width of the inclusion in the section AB at $h = 2R$

As an example (see Fig. 5.7), we show the distribution patterns of stress and strain intensities in a plate with FGM-inclusion 1.

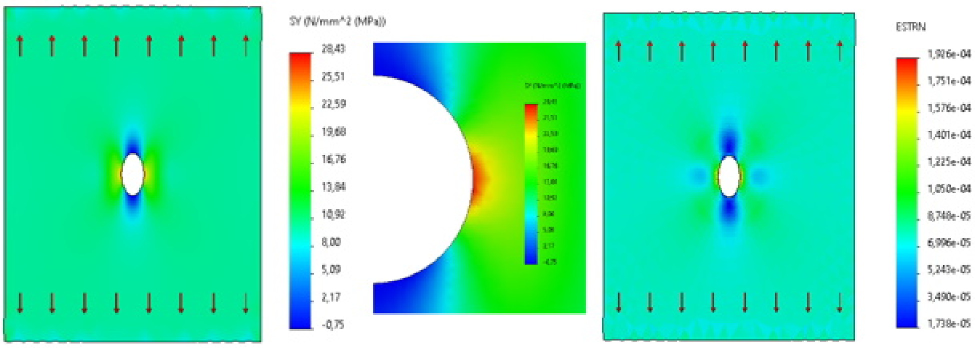

a) b) c)

Fig. 5.7. SSS components in a plate with FGM-inclusion 1 at $h = 2R$:
a) stress intensity; b) the intensity of stresses in the vicinity of the hole; c) the intensity of deformations

6. Conclusions

As a result of the computer simulation and numerical study of the effect of a change in the elastic modulus of an inclusion in the radial direction on the distribution of stress and strain intensities in a thin homogeneous plate near a circular hole, it has been established that in the presence of FGM inclusions with certain mechanical properties, it becomes possible to influence not only the SCF value in plate near local stress concentrators, but also on the stress distribution over the width of the inclusion. In a comparative analysis of the results obtained for a plate with an FGM inclusion and a plate without an inclusion, it was shown that the use of FGM inclusions is effective. This makes it possible to simultaneously reduce the concentration of SSS parameters (stresses and strains) around the hole and increase the strength of the plate as a whole.

The nature of the stress distribution in the plate is influenced by both the width of the FGM inclusion and the law of change in the modulus of elasticity: the larger the width of the inclusion and the larger the region with the maximum value of the elastic modulus of the inclusion, the greater the effect of the inclusion on the value of SCF and the magnitude of maximum deformations. The influence of the range of the change in the value of the elastic modulus is also established: the greater it is, the greater the effect on the value of the SCF in the plate.

References

1. S.M. Aizikovich, V.M. Aleksandrov at al. *Analytical solutions of mixed axisymmetric problems for functionally graded media*, *Fizmatlit*, Moscow, 2011.
2. S.K. Deb Nath, C.H. Wong, S.-G. Kim, *A finite-difference solution of boron/epoxy composite plate with an internal hole subjected to uniform tension/displacements using displacement potential approach*, Intern. J. Mech. Sci., **58** (2012), 1–12.

3. X.Q. Fang, C. Hu, S.Y. Du, *Strain energy density of a circular cavity buried in semi-infinite functionally graded materials subjected to shear waves*, Theoret. Appl. Fracture Mech., **46**(2006), 166–174.
4. V.S. Gudramovich, É.L. Gart, K.A. Strunin, *Modeling of the behavior of plane-deformable elastic media with elongated elliptic and rectangular inclusion*, Materials Science, **52** (6) (2017), 768–774.
5. E.L. Hart, V.S. Hudramovich, *Projection-iterative schemes for implementation of the finite element method in problems of deformation of plates with holes and inclusions*, Mathem. methods and phys.-mech. Fields, **56**(2) (2013), 48–59.
6. E.L. Hart, V.S. Hudramovich, *Projection-iterative schemes for the realization of the finite-element method in problems of deformation of plates with holes and inclusions*, J. Math. Sci., **203** (1) (2014), 55–69.
7. E.L. Hart, V.S. Hudramovich, *Projection-iterative modification of the method of local variations for problems with a quadratic functional*, J. Appl. Math. Mech., **80**(2) (2016), 156–163.
8. E.L. Hart, V.S. Hudramovich, *Projection-iterative schemes for the implementation of variational-grid methods in the problems of elastoplastic deformation of inhomogeneous thin-walled structures*, J. Math. Sci., **254** (1) (2021), 21–38.
9. E. Hart, B. Terokhin, *Influence of inclusion from functional-gradient material on stress concentration factor in a homogeneous plate with a circular hole*, Science and practice: implementation to modern society: Proceedings of the 9th International Scientific and Practical Conference (April 18–19, 2021), Peal Press Ltd, Manchester, Great Britain (2021), 866–872.
10. A. Haque, L. Ahmed, A. Ramasetty, *Stress concentrations and notch sensitivity in woven ceramic matrix composites containing a circular hole – an experimental, analytical, and finite element study*, J. Amer. Ceramic Soc., **88** (8) (2005), 2195–2201.
11. V.S. Hudramovich, E.L. Hart, O.A. Marchenko, *Reinforcing inclusion effect on the stress concentration within the spherical shell having an elliptical opening under uniform internal pressure*, Strength of Materials, **52**(6) (2021), 832–842.
12. M. Jabbari, S. Sohrabpour, M.R. Eslami, *General solutions for mechanical and thermal stresses in a functionally graded hollow cylinder due to nonaxisymmetric steady-state loads*, J. Appl. Mech.-T. ASME, **70** (2003), 111–118.
13. M. Janghorban, A. Zare, *Thermal effect on free vibration analysis of functionally graded arbitrary straight-sided plates with different cutouts*, Latin Amer. J. Solids Structures, **8** (2011), 245–257.
14. D.V. Kubair, B. Bhanu-Chandar, *Stress concentration factor due to a circular hole in functionally graded panels under uniaxial tension*, Intern. J. Mech. Sci., **50** (2008), 732–742.
15. A. Linkov, L. Rybarska-Rusinek, *Evaluation of stress concentration in multi-wedge systems with functionally graded wedges*, Intern. J. Engng Sci., **61** (2012), 87–93.
16. A.J. Markworth, K.S. Ramesh, W.P. Parks, *Modelling studies applied to functionally graded materials*, J. Mater. Sci., **30** (1995), 2183–2193.
17. Y. Miyamoto, W.A. Kaysser, R.H. Rabin, A. Kawasaki, R.G. Ford, *Functionally graded materials: design processing and applications*, Kluwer Academic Publishers, USA, 1999.
18. M. Mohammadi, J.R. Dryden, L. Jiang, *Stress concentration around a hole in a radially inhomogeneous plate*, Intern. J. Solids Structures, **48** (2011), 483–491.

19. G.N. Savin, *Stress distribution around holes*, Naukova dumka, Kiev, 1968.
20. G.N. Savin, V.I. Tulchiy, *Plates reinforced with compound rings and elastic overlays*, Naukova dumka, Kiev, 1971.
21. A. Siasiev, A. Dreus, S. Horbonos, I. Balanenko, S. Dziuba, *The stressed–strained state of a rod at crystallization considering the mutual influence of temperature and mechanical fields*, Eastern-European Journal of Enterprise Technologies, **3/5**(105) (2020), 38–49.
22. A. Syasev, T. Zelenskaya, *Lengthwise movement dynamic boundary-value problem for trailing boundary ropes*, Metallurgical and Mining Industry, **3** (2015), 283–287.
23. S.P. Timoshenko, J.N. Goodier, *Theory of elasticity*, Nauka, Moscow, 1975.
24. K. Washizu, *Variational methods in elasticity and plasticity*, Mir, Moscow, 1987.
25. Q. Yang, C.-F. Gao, W. Chen, *Stress analysis of a functional graded material plate with a circular hole*, Arch. Appl. Mech., **80** (2010), 895–907.
26. Z. Yang, C.B. Kim, C. Cho, H.G. Beom, *The concentration of stress and strain in finite thickness elastic plate containing a circular hole*, Intern. J. Solids Structures, **45** (2008), 713–731.
27. O.C. Zienkiewicz, R.L. Teylor, *The finite element method for solid and structural mechanics*, Elsevier, New York, 2005.

Received 12.05.2021

JOURNAL OF OPTIMIZATION, DIFFERENTIAL EQUATIONS AND THEIR APPLICATIONS (JODEA)
Volume **29**, Issue **1**, June **2021**, pp. 54–78, DOI 10.15421/142104

ISSN (print) 2617–0108
ISSN (on-line) 2663–6824

ON INCREASING OF RESOLUTION OF SATELLITE IMAGES VIA THEIR FUSION WITH IMAGERY AT HIGHER RESOLUTION

Peter I. Kogut[*], Olga P. Kupenko[†‡], Mykola V. Uvarov[§]

Communicated by Prof. P. O. Kasyanov

Abstract. In this paper we propose a new statement of the spatial increasing resolution problem of MODIS-like multi-spectral images via their fusion with Lansat-like imagery at higher resolution. We give a precise definition of the solution to the indicated problem, postulate assumptions that we impose at the initial data, establish existence and uniqueness result, and derive the corresponding necessary optimality conditions. For illustration, we supply the proposed approach by results of numerical simulations with real-life satellite images.

Key words: Satellite data fusion, image interpolation, image processing, variational approach, objective functional with non-standard growth conditions..

2010 Mathematics Subject Classification: 49Q20, 49K10, 49J45, 26B30.

1. Introduction

Following in some aspects the paper [5], we propose a new variational approach to the spatial increasing resolution of multi spectral MODIS-like images via their fusion with Lansat-like imagery at higher resolution. Our approach is based on the variational model in Sobolev-Orlicz space with a non-standard growth condition of the objective functional and on the assumption that, to a large extent, the image topology in the each spectral channel is contained in the topographic map of its spectral energy. We discuss the well foundedness of the above approach, the consistency of the corresponding variational problem, and show that this problem admits a unique solution. We also derive some optimality conditions and supply our approach by results of numerical simulations with the real satellite images.

[*]Department of Differential Equations, Oles Honchar Dnipro National University, 72, Gagarin av., Dnipro, 49010, Ukraine; EOS Data Analytics Ukraine, Gagarin av., 103a, Dnipro, Ukraine `p.kogut@i.ua`, `peter.kogut@eosda.com`

[†]Department of System Analysis and Control, Dnipro University of Technology 'Dnipro Polytechnics', 19, Yavornitskii av., 49005 Dnipro

[‡]Institute Applied System Analysis, National Academy of Sciences and Ministry of Education and Science of Ukraine, 37/35, Peremogy av., IASA, 03056 Kyiv, Ukraine, `kupenko.olga@gmail.com`

[§]EOS Data Analytics Ukraine, Desyatynny lane, 5, 01001 Kyiv, Ukraine, `nikolay.uvarov@eosda.com`

2. Preliminaries

We begin with some notation. Let $\Omega \subset \mathbb{R}^2$ be a bounded open set with a Lipschitz boundary $\partial\Omega$. Let $I : \Omega \to \mathbb{R}^m$, with $m \geqslant 3$, be a multispectral image containing the usual R, G, B channels I_R, I_G, I_B, and arguably some others ones like the infrared channel I_{NIR}, i.e.,

$$I(x) = [I_R(x), I_G(x), I_B(x), \dots]^t \in \mathbb{R}^m, \quad \forall\, x \in \Omega.$$

We say that $Y_I : \Omega \to \mathbb{R}$ is the panchromatic component of the multispectral image $I : \Omega \to \mathbb{R}^m$ (or in other words Y_I is the spectral energy coming from the RGB-channels) if the following representation

$$Y_I(x) = \alpha_R I_R(x) + \alpha_G I_G(x) + \alpha_B I_B(x), \quad \forall\, x \in \Omega$$

holds for some weight coefficients $\alpha_R, \alpha_G, \alpha_B \geqslant 0$. In particular, if

$$\alpha_R = 0.299, \quad \alpha_G = 0.587, \quad \alpha_B = 0.114$$

then Y_I can be interpreted as the luma component of I and it represents the perceptual brightness of the multispectral image $I : \Omega \to \mathbb{R}^m$.

For each $\lambda \in \mathbb{R}$, we define the upper level set of the spectral energy Y_I as follows

$$X_\lambda = \{x \in \Omega : Y_I(x) \geqslant \lambda\}.$$

Then the spectral energy Y_I can be recovered from its level sets by the reconstruction formula

$$Y_I(x) = \sup\{\lambda \ : \ x \in X_\lambda\}, \quad \forall\, x \in \Omega.$$

Hereinafter, we will refer to the family of connected components of the upper level sets of Y_I as the topographic map of Y_I.

Let $S_H \subset \Omega$ and $S_L \subset \Omega$ be two sample grids on Ω such that

$$S_H = \left\{ (x_i, y_j) \;\middle|\; \begin{array}{l} x_1 = x_H,\ x_i = x_1 + \Delta_{H,x}(i-1),\ i = 1, \dots, N_x, \\ y_1 = y_H,\ y_j = y_1 + \Delta_{H,y}(j-1),\ j = 1, \dots, N_y, \end{array} \right\},$$

$$S_L = \left\{ (x_i, y_j) \;\middle|\; \begin{array}{l} x_1 = x_L,\ x_i = x_1 + \Delta_{L,x}(i-1),\ i = 1, \dots, M_x, \\ y_1 = y_L,\ y_j = y_1 + \Delta_{L,y}(j-1),\ j = 1, \dots, M_y, \end{array} \right\},$$

where $N_x >> M_x$ and $N_y >> M_y$.

Let $H : \Omega \to \mathbb{R}^3$ be a given multispectral (Landsat-like) image which is sampled at the grid of high resolution S_H. We suppose that, in practice, this image can be identified with an 3-D array

$$H = \left\{ \begin{bmatrix} H_R(x_i, y_j) \\ H_G(x_i, y_j) \\ H_B(x_i, y_j) \end{bmatrix},\ i = 1, \dots, N_x,\ j = 1, \dots, N_y \right\}.$$

Let $L : \Omega \to \mathbb{R}^4$ be a given multispectral (MODIS-like) image which is sampled at the grid of low resolution S_L, and it has 4 spectral channels R, G, B, and NIR. So, we can indentify this image with an 4-D array

$$L = \left\{ \begin{bmatrix} L_R(x_i, y_j) \\ L_G(x_i, y_j) \\ L_B(x_i, y_j) \\ L_{NIR}(x_i, y_j) \end{bmatrix},\ i = 1, \dots, M_x,\ j = 1, \dots, M_y \right\}.$$

The problem, we are going to consider, can be formally stated as follows: Using only the data $H : S_H \to \mathbb{R}^3$ and $L : S_L \to \mathbb{R}^4$, we have to increase the resolution of the four-band image $L : S_L \to \mathbb{R}^4$ via its fusion with the three-band image $H : S_H \to \mathbb{R}^3$ at higher resolution such that the following properties for the retrieved high resolution multispectral image $I : S_H \to \mathbb{R}^4$ would be satisfied:

(i) The image $I : \Omega \to \mathbb{R}^4$ we are going to retrieve, should be of bounded variation, $I \in BV(\Omega; \mathbb{R}^4)$.

(ii) The topographic maps for each spectral channel at higher resolution must have a similar structure to the topographic map of the spectral energy Y_H coming from the RGB-channels of $H : S_H \to \mathbb{R}^3$.

(iii) The spectral energies Y_I and Y_H should be as close as possible with respect to the $L^2(\Omega)$-norm.

(iv) The sampled values of $I : \Omega \to \mathbb{R}^4$ on the grid of low resolution S_L should be as close as possible in L^2-metric to the multispectral imagery $L : S_L \to \mathbb{R}^4$.

(v) The NIR-channel I_{NIR} for the retrieved high resolution multispectral image $I : \Omega \to \mathbb{R}^4$ should be in the same regression relationship with I_R, I_G, I_B channels as L_{NIR} with L_R, L_G, L_B, that is, if

$$L_{NIR}(x_i, y_j) = \gamma_R L_R(x_i, y_j) + \gamma_G L_G(x_i, y_j) + \gamma_B L_B(x_i, y_j), \quad \forall\, (x_i, y_j) \in S_L$$

is a linear regression model which is fitted using the least squares approach, then

$$I_{NIR}(x_i, y_j) = \gamma_R I_R(x_i, y_j) + \gamma_G I_G(x_i, y_j) + \gamma_B I_B(x_i, y_j), \quad \forall\, (x_i, y_j) \in S_H$$

with the same regression coefficients $\gamma_R, \gamma_G, \gamma_B \in \mathbb{R}$.

3. Auxiliaries

3.1. BV-Space

By $BV(\Omega)$ we denote the space of all functions $u \in L^1(\Omega)$ for which their distributional derivatives are representable by finite Borel measures in Ω, i.e.

$$\int_\Omega u \frac{\partial \phi}{\partial x_i}\, dx = -\int_\Omega \phi\, dD_i u, \quad \forall\, \phi \in C_0^\infty(\Omega),\ i = 1, 2$$

for some $\mathbb{R}^2$-valued measure $Du = (D_1 u, D_2 u) \in \mathcal{M}^2(\Omega)$. It can be shown that $BV(\Omega)$, endowed with the norm

$$\|u\|_{BV(\Omega)} = \|u\|_{L^1(\Omega)} + |Du|(\Omega)$$

is a Banach space, where

$$\begin{aligned} |Du|(\Omega) &:= \int_\Omega d|Du| \\ &= \sup\left\{ \int_\Omega u \operatorname{div} \varphi\, dx \ :\ \varphi \in C_0^1(\Omega; \mathbb{R}^2),\ |\varphi(x)| \leqslant 1 \text{ for } x \in \Omega \right\} \end{aligned} \tag{3.1}$$

stands for the total variation of u in Ω. It is clear that $|Du|(\Omega) = \int_\Omega |\nabla u|\, dx$ if u is continuously differentiable in Ω.

The following embedding results for BV-function plays a crucial role for qualitative analysis of variational problems that we study in this paper.

Proposition 3.1. [4, p.378] Let Ω be an open bounded Lipschitz subset of $\mathbb{R}^2$. Then the embedding $BV(\Omega; \mathbb{R}^M) \hookrightarrow L^2(\Omega; \mathbb{R}^M)$ is continuous and the embeddings $BV(\Omega; \mathbb{R}^M) \hookrightarrow L^p(\Omega; \mathbb{R}^M)$ are compact for all p such that $1 \leqslant p < 2$. Moreover, there exists a constant $C_{em} > 0$ which depends only on Ω and p such that for all u in $BV(\Omega; \mathbb{R}^M)$,

$$\left(\int_\Omega |u|^p\, dx \right)^{1/p} \leqslant C_{em} \|u\|_{BV(\Omega; \mathbb{R}^M)}, \quad \forall\, p \in [1, 2].$$

According to the Radon-Nikodym theorem, if $u \in BV(\Omega)$ then there exists $\nabla u \in L^1(\Omega; \mathbb{R}^2)$ and a measure $D_s u$ singular with respect to the 2-dimensional Lebesgue measure $\mathcal{L}^2 \llcorner \Omega$ restricted to Ω, such that $Du = \nabla u \mathcal{L}^2 \llcorner \Omega + D_s u$.

We recall that if $u \in BV(\Omega)$, then almost all its level sets $\{x \in \Omega : u(x) \geqslant \lambda\}$ are sets of finite perimeter. Hence, at almost all points of almost all level sets of $u \in BV(\Omega)$ we may define a normal vector $\theta(x)$. This vector field of normals $\theta(x)$ can be also defined as the Radon-Nikodym derivative of the measure Du with respect to $|Du|$, i.e., it formally satisfies the following relations

$$(\theta, Du) = |Du| \quad \text{and} \quad |\theta| \leqslant 1 \text{ a.e. in } \Omega.$$

In the sequel, we will refer to the vector field θ as the vector field of unit normals to the topographic map of a function u. Further information on BV-functions and their properties can be found in [1, 4].

Remark 3.1. In practice, at the discrete level, $\theta(x,y)$ can be defined by the rule $\theta(x_i,y_j) = \frac{Du(x_i,y_j)}{|Du(x_i,y_j)|}$ when $Du(x_i,y_j) \neq 0$, and $\theta = 0$ when $Du(x_i,y_j) = 0$. However, as was mentioned in [5], a better choice for $\theta(x,y)$ would be to compute it as $\xi(t) = \frac{DU(t,\cdot)}{|DU(t,\cdot)|}$ for some small value of $t > 0$, where $U(t,x,y)$ is a solution of the following initial-boundary value problem with $1D$-Laplace operator in the right hand side

$$\frac{\partial U}{\partial t} = \operatorname{div}\left(\frac{DU}{|DU|}\right), \quad t \in (0,+\infty),\ (x,y) \in \Omega, \tag{3.2}$$

$$U(0,x,y) = u(x,y), \quad (x,y) \in \Omega, \tag{3.3}$$

$$\frac{\partial U(0,x,y)}{\partial \nu} = 0, \quad t \in (0,+\infty),\ (x,y) \in \partial\Omega. \tag{3.4}$$

As a result, for any $t > 0$, there can be found a vector field

$$\xi \in L^\infty(\Omega;\mathbb{R}^2) \ \text{ with } \ \|\xi(t)\|_{L^\infty(\Omega;\mathbb{R}^2)} \leqslant 1$$

such that

$$(\xi(t), U(t,\cdot)) = |DU(t,\cdot)| \text{ in } \Omega, \quad \xi(t)\cdot\nu = 0 \text{ on } \partial\Omega, \tag{3.5}$$

and $U_t(t,x,y) = \operatorname{div}\xi(t,x,y)$ in the sense of distributions on Ω for a.a. $t > 0$.

We notice that following this procedure, for small value of $t > 0$, we do not distort the geometry of the function $u(x,y)$ in an essential way. Moreover, it can be shown that this regularization of the vector field $\theta(x,y) = \frac{DU(x,y)}{|DU(x,y)|}$ satisfies condition $\operatorname{div}\theta \in L^2(\Omega)$.

3.2. On Orlicz Spaces

Let $p(\cdot)$ be a measurable exponent function on Ω such that

$$1 \leqslant \alpha \leqslant p(x) \leqslant \beta < \infty \quad \text{a.e. in } \Omega, \tag{3.6}$$

where α and β are given constants. Let $p'(\cdot) = \frac{p(\cdot)}{p(\cdot)-1}$ be the corresponding conjugate exponent. It is clear that

$$1 \leqslant \underbrace{\frac{\beta}{\beta-1}}_{\beta'} \leqslant p'(x) \leqslant \underbrace{\frac{\alpha}{\alpha-1}}_{\alpha'} \ \text{a.e. in } \Omega, \tag{3.7}$$

where β' and α' stand for the conjugates of constant exponents. Denote by $L^{p(\cdot)}(\Omega)$ the set of all measurable functions $f(x)$ on Ω such that $\int_\Omega |f(x)|^{p(x)}\,dx < \infty$. Then $L^{p(\cdot)}(\Omega)$ is a reflexive separable Banach space with respect to the Luxemburg norm (see [7,8] for the details)

$$\|f\|_{L^{p(\cdot)}(\Omega)} = \inf\left\{\lambda > 0 \ : \ \rho_p(\lambda^{-1}f) \leqslant 1\right\}, \tag{3.8}$$

where $\rho_p(f) := \int_\Omega |f(x)|^{p(x)}\,dx$.

It is well-known that $L^{p(\cdot)}(\Omega)$ is reflexive provided $\alpha > 1$, and its dual is $L^{p'(\cdot)}(\Omega)$, that is, any continuous functional $F = F(f)$ on $L^{p(\cdot)}(\Omega)$ has the form (see [21, Lemma 13.2])

$$F(f) = \int_\Omega fg\,dx, \quad \text{with} \;\; g \in L^{p'(\cdot)}(\Omega).$$

As for the infimum in (3.8), we have the following result.

Proposition 3.2. The infimum in (3.8) is attained if $\rho_p(f) > 0$. Moreover,

$$\text{if} \;\; \lambda_* := \|f\|_{L^{p(\cdot)}(\Omega)} > 0, \;\; \text{then} \;\; \rho_p(\lambda_*^{-1}f) = 1. \tag{3.9}$$

Taking this result and condition $1 \leqslant \alpha \leqslant p(x) \leqslant \beta$ into account, we see that

$$\begin{gathered}\frac{1}{\lambda_*^\beta}\int_\Omega |f(x)|^{p(x)}\;dx \leqslant \int_\Omega \left|\frac{f(x)}{\lambda_*}\right|^{p(x)}\;dx \leqslant \frac{1}{\lambda_*^\alpha}\int_\Omega |f(x)|^{p(x)}\;dx,\\ \frac{1}{\lambda_*^\beta}\int_\Omega |f(x)|^{p(x)}\;dx \leqslant 1 \leqslant \frac{1}{\lambda_*^\alpha}\int_\Omega |f(x)|^{p(x)}\;dx.\end{gathered}$$

provided $\lambda_* \geqslant 1$. And we arrive at the reverse inequality if $0 < \lambda_* < 1$. Hence, (see [7, 8, 20] for the details)

$$\begin{aligned}\|f\|^\alpha_{L^{p(\cdot)}(\Omega)} \leqslant \int_\Omega |f(x)|^{p(x)}\,dx \leqslant \|f\|^\beta_{L^{p(\cdot)}(\Omega)}, \text{ if } \|f\|_{L^{p(\cdot)}(\Omega)} > 1,\\ \|f\|^\beta_{L^{p(\cdot)}(\Omega)} \leqslant \int_\Omega |f(x)|^{p(x)}\,dx \leqslant \|f\|^\alpha_{L^{p(\cdot)}(\Omega)}, \text{ if } \|f\|_{L^{p(\cdot)}(\Omega)} < 1,\end{aligned} \tag{3.10}$$

and, therefore,

$$\|f\|^\alpha_{L^{p(\cdot)}(\Omega)} - 1 \leqslant \int_\Omega |f(x)|^{p(x)}\,dx \leqslant \|f\|^\beta_{L^{p(\cdot)}(\Omega)} + 1, \quad \forall\, f \in L^{p(\cdot)}(\Omega), \tag{3.11}$$

$$\|f\|_{L^{p(\cdot)}(\Omega)} = \int_\Omega |f(x)|^{p(x)}\,dx, \text{ if } \|f\|_{L^{p(\cdot)}(\Omega)} = 1. \tag{3.12}$$

The following estimates are well-known (see, for instance, [7, 8, 20]): if $f \in L^{p(\cdot)}(\Omega)$ then

$$\|f\|_{L^\alpha(\Omega)} \leqslant (1 + |\Omega|)^{1/\alpha}\,\|f\|_{L^{p(\cdot)}(\Omega)}, \tag{3.13}$$

$$\|f\|_{L^{p(\cdot)}(\Omega)} \leqslant (1 + |\Omega|)^{1/\beta'}\,\|f\|_{L^\beta(\Omega)}, \quad \beta' = \frac{\beta}{\beta - 1}, \quad \forall\, f \in L^\beta(\Omega). \tag{3.14}$$

Let $\left\{f_k \in L^{p(\cdot)}(\Omega)\right\}_{k\in\mathbb{N}}$ be a given sequence, where the exponent $p \in C(\overline{\Omega})$ satisfies property (3.6). We say that the sequence $\left\{f_k \in L^{p(\cdot)}(\Omega)\right\}_{k\in\mathbb{N}}$ is bounded if (see [15, Section 6.2])

$$\limsup_{k\to\infty} \int_\Omega |f_k(x)|^{p(x)}\,dx < +\infty. \tag{3.15}$$

Definition 3.1. A bounded sequence $\left\{f_k \in L^{p(\cdot)}(\Omega)\right\}_{k\in\mathbb{N}}$ is weakly convergent in the Orlicz space $L^{p(\cdot)}(\Omega)$ to a function $f \in L^{p(\cdot)}(\Omega)$, if

$$\lim_{k\to\infty}\int_\Omega f_k\varphi\,dx = \int_\Omega f\varphi\,dx, \quad \forall\,\varphi \in C_0^\infty(\mathbb{R}^2). \tag{3.16}$$

For our further analysis, we make use of the following lower semicontinuity property of the $L^{p(\cdot)}$-norm with respect to the weak convergence in $L^{p(\cdot)}(\Omega)$ (we refer to [21, Lemma 13.3] for details).

Proposition 3.3. If a bounded sequence $\left\{f_k \in L^{p(\cdot)}(\Omega)\right\}_{k\in\mathbb{N}}$ converges weakly in $L^\alpha(\Omega)$ to f, where $\alpha > 1$ is defined in (3.6), then $f \in L^{p(\cdot)}(\Omega)$, $f_k \rightharpoonup f$ in $L^{p(\cdot)}(\Omega)$, and

$$\liminf_{k\to\infty}\int_\Omega |f_k(x)|^{p(x)}\,dx \geqslant \int_\Omega |f(x)|^{p(x)}\,dx. \tag{3.17}$$

Remark 3.2. Arguing in a similar manner as in [21, Lemma 13.3] and using the estimate

$$\liminf_{k\to\infty}\int_\Omega \frac{1}{p_k(x)}|f_k(x)|^{p_k(x)}\,dx \geqslant \int_\Omega f(x)\varphi(x)\,dx - \int_\Omega \frac{1}{p_k'(x)}|\varphi(x)|^{p'(x)}\,dx,$$

which is valid for any smooth function φ, it is easy to show that the lower semicontinuity property (3.17) can be generalized as follows

$$\liminf_{k\to\infty}\int_\Omega \frac{1}{p(x)}|f_k(x)|^{p(x)}\,dx \geqslant \int_\Omega \frac{1}{p(x)}|f(x)|^{p(x)}\,dx. \tag{3.18}$$

We need the following result that leads to the analog of the Hölder inequality in Lebesgue spaces with variable exponents (for the details we refer to [7, 8]).

Proposition 3.4. If $f \in L^{p(\cdot)}(\Omega)^N$ and $g \in L^{p'(\cdot)}(\Omega)^N$, then $(f,g) \in L^1(\Omega)$ and

$$\int_\Omega (f,g)\;dx \leqslant 2\|f\|_{L^{p(\cdot)}(\Omega)^N}\|g\|_{L^{p'(\cdot)}(\Omega)^N}. \tag{3.19}$$

3.3. Sobolev Spaces with Variable Exponent

We recall here the well-known facts concerning the Sobolev spaces with variable exponent. Let $p(\cdot)$ be a measurable exponent function on Ω such that $1 < \alpha \leqslant p(x) \leqslant \beta < \infty$ a.e. in Ω, where α and β are given constants. We associate with it the so-called Sobolev-Orlicz space

$$W^{1,p(\cdot)}(\Omega) := \left\{ y \in W^{1,1}(\Omega)\ :\ \int_\Omega \left[|y(x)|^{p(x)} + |\nabla y(x)|^{p(x)}\right]\,dx < +\infty \right\} \tag{3.20}$$

and equip it with the norm $\|y\|_{W_0^{1,p(\cdot)}(\Omega)} = \|y\|_{L^{p(\cdot)}(\Omega)} + \|\nabla y\|_{L^{p(\cdot)}(\Omega;\mathbb{R}^2)}$.

It is well-known that, in general, unlike classical Sobolev spaces, smooth functions are not necessarily dense in $W = W_0^{1,p(\cdot)}(\Omega)$. Hence, with the given variable exponent $p = p(x)$ $(1 < \alpha \leqslant p \leqslant \beta)$ there can be associated another Sobolev space with variable exponent,

$$H = H^{1,p(\cdot)}(\Omega) \ \text{ as the closure of the set } \ C^\infty(\overline{\Omega}) \ \text{ in } W^{1,p(\cdot)}(\Omega)\text{-norm.}$$

Since the identity $W = H$ is not always valid, it makes sense to say that an exponent $p(x)$ is regular if $C^\infty(\overline{\Omega})$ is dense in $W^{1,p(\cdot)}(\Omega)$.

The following result reveals an important property ensuring the regularity of exponent $p(x)$.

Proposition B.1. *Assume that there exists $\delta \in (0,1]$ such that $p \in C^{0,\delta}(\overline{\Omega})$. Then the set $C^\infty(\overline{\Omega})$ is dense in $W^{1,p(\cdot)}(\Omega)$, and, therefore, $W = H$.*

Proof. Let $p \in C^{0,\delta}(\overline{\Omega})$ be a given exponent. Since

$$\lim_{t\to 0} |t|^\delta \log(|t|) = 0 \qquad \text{with an arbitrary } \delta \in (0,1], \tag{3.21}$$

it follows from the Hölder continuity of $p(\cdot)$ that

$$|p(x) - p(y)| \leqslant C|x-y|^\delta \leqslant \left[\sup_{x,y\in\Omega} \||x-y|^\delta \log(|x-y|^{-1})\right] \omega(|x-y|), \ \forall\, x, y \in \Omega, \tag{3.22}$$

where $\omega(t) = C/\log(|t|^{-1})$, and $C > 0$ is some positive constant.

Then property (3.21) implies that $p(\cdot)$ is a log-Hölder continuous function. So, to deduce the density of $C^\infty(\overline{\Omega})$ in $W^{1,p(\cdot)}(\Omega)$ it is enough to refer to Theorem 13.10 in [21].

4. Main Assumptions

Let $H : S_H \to \mathbb{R}^3$ and $L : S_L \to \mathbb{R}^4$ be given digital images. Hereinafter, we assume that their continuous counterparts $H : \Omega \to \mathbb{R}^3$ and $L : \Omega \to \mathbb{R}^4$ are such that

$$Y_H \in BV(\Omega) \quad \text{and} \quad Y_L \in L^2(\Omega), \tag{4.1}$$

where Y_H and Y_L stand for the spectral energies of the H and L images, respectively.

Before proceed further, we associate with the spectral energy Y_H the so-called texturity characteristic $p : \Omega \to \mathbb{R}$ following the rule

$$p(x) := \mathfrak{F}(Y_H(x)) = 1 + g\left(|\left(\nabla G_\sigma * Y_H\right)(x)|\right), \quad \forall\, x \in \Omega, \tag{4.2}$$

where g:$[0,\infty) \to (0,\infty)$ is the edge-stopping function which we take it in the form of the Cauchy law $g(t) = \frac{1}{1+(t/a)^2}$ with an appropriate $a > 0$, $\left(\nabla G_\sigma * Y_H\right)(x)$ determines the convolution of function Y_H with the two-dimensional Gaussian filter kernel G_σ,

$$G_\sigma(x) = \frac{1}{2\pi\sigma^2} e^{-\frac{|x|^2}{2\sigma^2}}, \quad x \in \mathbb{R}^2, \tag{4.3}$$

$$\left(\nabla G_\sigma * Y_H\right)(x) := \int_\Omega \nabla G_\sigma(x-y) Y_H(y)\, dy, \quad \forall\, x \in \Omega. \tag{4.4}$$

Here, the parameter $\sigma>0$ determines the spatial size of the image details which are removed by this $2D$ filter.

Since the magnitude $g\left(\left|\left(\nabla G_\sigma * Y_H\right)(x)\right|\right)$ is close to one at those points, where the spectral energy Y_H is slowly varying, and this value is close to zero at the edges of Y_H, it follows that the function $p(x)$ can be interpreted as a texturity characteristic of the panchromatic image Y_H.

The following result plays a crucial role in the sequel.

Lemma 4.1. *Let $Y_H \in L^1(\Omega)$ be a given spectral energy. Let*

$$p = 1 + g\left(\left|\left(\nabla G_\sigma * Y_H\right)\right|\right)$$

be the corresponding texturity characteristic. Then

$$p \in C^{0,1}(\overline{\Omega}), \tag{4.5}$$

$$\alpha := 1 + \delta \leqslant p(x) \leqslant \beta := 2, \quad \forall\, x \in \Omega, \tag{4.6}$$

where $\delta = \dfrac{a^2}{a^2 + \|G_\sigma\|^2_{C^1(\overline{\Omega-\Omega})}\|Y_H\|^2_{L^1(\Omega)}}$.

Proof. By smoothness of the Gaussian filter kernel G_σ, we have

$$\left|\left(\nabla G_\sigma * Y_H\right)(x)\right| \leqslant \int_\Omega \left|\nabla G_\sigma(x-y)\right| Y_H(y)\, dy \leqslant \|G_\sigma\|_{C^1(\overline{\Omega-\Omega})}\|Y_H\|_{L^1(\Omega)},$$

$$\begin{aligned} p(x) &= 1 + \frac{a^2}{a^2 + \left(\left|\left(\nabla G_\sigma * Y_H\right)(x)\right|\right)^2} \\ &\geqslant 1 + \frac{a^2}{a^2 + \|G_\sigma\|^2_{C^1(\overline{\Omega-\Omega})}\|Y_H\|^2_{L^1(\Omega)}}, \quad \forall\, x \in \Omega. \end{aligned}$$

From this the existence of a positive value $\delta \in (0,1)$ such that estimate (4.6) holds true follows. Combining this fact with $\max_{x\in\overline{\Omega}} |p(x)| \leqslant \beta := 2$, we arrive at the announced estimate (4.6).

As for the property (4.5), we make use of the estimate

$$\begin{aligned} |p(x) - p(y)| &\leqslant a^2 \left| \frac{\left|\left(\nabla G_\sigma * Y_H\right)(x)\right|^2 - \left|\left(\nabla G_\sigma * Y_H\right)(y)\right|^2}{\left(a^2 + \left|\left(\nabla G_\sigma * Y_H\right)(x)\right|^2\right)\left(a^2 + \left|\left(\nabla G_\sigma * Y_H\right)(y)\right|^2\right)} \right| \\ &\leqslant \frac{2\|G_\sigma\|_{C^1(\overline{\Omega-\Omega})}\|Y_H\|_{L^1(\Omega)}}{a^2} \left|\left|\left(\nabla G_\sigma * Y_H\right)(x)\right| - \left|\left(\nabla G_\sigma * Y_H\right)(y)\right|\right| \\ &\leqslant \frac{2\|G_\sigma\|_{C^1(\overline{\Omega-\Omega})}\gamma_1^2|\Omega|}{a^2} \int_\Omega \left|\nabla G_\sigma(x-z) - \nabla G_\sigma(y-z)\right| dz, \ \forall\, x, y \in \Omega, \end{aligned} \tag{4.7}$$

with $\gamma_1 = \max_{x\in\Omega} |Y_H(x)|$. Then, by smoothness of the function $\nabla G_\sigma(\cdot)$, we deduce: there exists a positive constant $C_G > 0$ such that

$$|p(x) - p(y)| \leqslant \frac{2\|G_\sigma\|_{C^1(\overline{\Omega-\Omega})}\gamma_1^2|\Omega| C_G}{a^2}|x-y|, \ \forall\, x, y \in \Omega.$$

Setting $C := \dfrac{2\|G_\sigma\|_{C^1(\overline{\Omega-\Omega})}\gamma_1^2|\Omega|C_G}{a^2}$, we finally see that

$$p(\cdot) \in \mathfrak{S} = \left\{ h \in C^{0,1}(\Omega) \;\middle|\; \begin{array}{c} |h(x) - h(y)| \leqslant C|x-y|,\ \forall\, x, y, \in \Omega, \\ 1 < \alpha \leqslant h(\cdot) \leqslant \beta \text{ in } \overline{\Omega}. \end{array} \right\} \tag{4.8}$$

□

The algorithm that we propose to realize for the spatial interpolation of MODIS-like multi-band color images to the Landsat-like imagery at high resolution, is essentially grounded on the following key assumptions.

Assumption 1. The MODIS image $L : S_L \to \mathbb{R}^4$ and the Landsat image $H : S_H \to \mathbb{R}^3$ are rigidly co-registered.

This means that there exists an affine transformation $\mathcal{F} : \mathbb{R}^2 \to \mathbb{R}^2$ of the form

$$\mathcal{F}(x) = Bx + a, \quad \forall\, x \in \mathbb{R}^2, \tag{4.9}$$

where

$$a = \begin{bmatrix} a_1 \\ a_2 \end{bmatrix} \quad \text{and} \quad = \begin{bmatrix} b_{11} & b_{12} \\ b_{21} & b_{22} \end{bmatrix}$$

such that the MODIS-like image after the affine transformation $L\left(\mathcal{F}^{-1}(\cdot)\right) : S_L \to \mathbb{R}^4$ and Landsat-like image $H : S_H \to \mathbb{R}^3$, after the bilinear resampling to the grid of low resolution S_L, could be successfully matched.

In practice, the co-registration procedure can be realized using, for instance, the open-source LSReg v2.0.2 software [16, 19] that has been used in a number of recent studies [9, 17], or the rigid co-registration approach that was recently developed by the EOS Company [11, 12]. However, in both cases, in order to find an appropriate affine transformation, we propose to apply the above mentioned procedure not to the original images, but rather to their spectral energies

$$Y_L(x_i, y_j) = \alpha_R L_R(x_i, y_j) + \alpha_G L_G(x_i, y_j) + \alpha_B L_B(x_i, y_j), \quad \forall\, (x_i, y_j) \in S_L$$

and

$$Y_H(x_i, y_j) = \alpha_R H_R(x_i, y_j) + \alpha_G H_G(x_i, y_j) + \alpha_B H_B(x_i, y_j), \quad \forall\, (x_i, y_j) \in S_H, \tag{4.10}$$

where the last one should be previously resampled to the grid of low resolution S_L.

Assumption 2. The low resolution pixels in the image $L : S_L \to \mathbb{R}^4$ are formed from the high resolution pixels of $I : S_H \to \mathbb{R}^4$ by a low pass filtering (the se-called subsampling procedure).

As a consequence of this Assumption, we can suppose that there exists an impulse response K such that

$$L(x_i, y_j) = [\mathcal{K} * I]\,(x_i, y_j), \quad \forall\, i = 1, \dots, M_x,\ \forall\, j = 1, \dots, M_y. \tag{4.11}$$

where $[\mathcal{K} * I]$ stands for the convolution operator. In particular, if $\mathcal{K} = [k_{p,q}]_{p,q=1,\dots,K}$ is a squared matrix, then

$$[\mathcal{K} * I]\,(x_i, y_j) = \sum_{p=1}^{K}\sum_{q=1}^{K} k_{p,q} I(x_{i-p+1}, y_{j-q+1})$$

provided $I(x, y) = 0$ if $(x, y) \notin \Omega$. For practical implementation, we usually set

$$k_{p,q} = \frac{1}{K^2}, \quad \forall\, p, q = 1, \dots, K$$

with an appropriate choice of $K \in \mathbb{N}$.

Assumption 3. The spectral energy Y_I of the retrieved high resolution multispectral image $I : \Omega \to \mathbb{R}^4$ is an element of the Sobolev space with variable exponent $W^{1,p(\cdot)}(\Omega)$, where $p(\cdot)$ is defined in (4.2), and

$$Y_I(x) = \alpha_R I_R(x) + \alpha_G I_G(x) + \alpha_B I_B(x), \quad \forall\, x \in \Omega$$

with $\alpha_R = 0.299$, $\alpha_G = 0.587$, and $\alpha_B = 0.114$.

Assumption 4. The topographic maps for each spectral channels I_R, I_G, I_B, and I_{NIR} of the retrieved image $I : \Omega \to \mathbb{R}^4$ have a similar structure to the topographic map of the spectral energy Y_H of the Landsat image $H : \Omega \to \mathbb{R}^3$.

As follows from this Assumption, all spectral channels of the retrieved image should share the geometry of the panchromatic image Y_H in Ω. It means that, due to the property $Y_H \in BV(\Omega)$, for almost all points of almost all level sets of Y_H we can define a normal vector $\theta(x)$, i.e., it formally satisfies $(\theta, Y_H) = |\nabla Y_H|$ and $|\theta| \leqslant 1$ a.e. in Ω (see Remark 3.1 for the details). So, if $\theta \in L^\infty(\Omega, \mathbb{R}^2)$ is a vector field with indicated properties, it follows that $\theta(x)$ has the direction of the normal to the level lines of Y_H. Therefore, the counterclockwise rotation of angle $\pi/2$, denoted by $\theta^\perp$, represents the tangent vector to the level lines of Y_H. In this case, if the spectral channels of $I : \Omega \to \mathbb{R}^4$ share the geometry of the panchromatic image Y_H, we have

$$\left(\theta^\perp, \nabla I_i\right)_{\mathbb{R}^2} = 0, \quad i \in \{R, G, B, NIR\} \text{ in } \Omega.$$

5. Statement of the Spatial Interpolation Problem

The problem of spatial interpolation of the MODIS-like image $L : S_L \to \mathbb{R}^4$ to the resolution of three-band Landsat-like image $H : S_H \to \mathbb{R}^3$ consists in the restoration of the four-band image $I:\Omega\to\mathbb{R}^4$ such that properties (i)–(v) would be satisfied. To do so, we propose at the first stage to compute the high resolution images $I_R, I_G, I_B : \Omega\to\mathbb{R}$ as a solution of the following constrained minimization problem

$$\inf_{(I_R,I_G,I_B)\in\Xi} \mathcal{J}\left(I_R, I_G, I_B\right), \tag{5.1}$$

where Ξ denotes the set of admissible images, and $\mathcal{J}\left(I_R, I_G, I_B\right)$ stands for the energy functional. Here, we define the set Ξ as follows: $(I_R, I_G, I_B)\in\Xi$ if and only if

(A) $(I_R, I_G, I_B)\in W^{1,p(\cdot)}(\Omega;\mathbb{R}^3)$, where $p(\cdot)$ stands for the texturity characteristic of the spectral energy $Y_H\in BV(\Omega)$;

(B) the following pointwise inequalities

$$0 \leqslant I_R(x,y) \leqslant \max_{(x_i,y_j)\in S_L} L_R(x_i,y_j) \text{ a.e. in } \Omega, \tag{5.2}$$

$$0 \leqslant I_G(x,y) \leqslant \max_{(x_i,y_j)\in S_L} L_G(x_i,y_j) \text{ a.e. in } \Omega, \tag{5.3}$$

$$0 \leqslant I_B(x,y) \leqslant \max_{(x_i,y_j)\in S_L} L_B(x_i,y_j) \text{ a.e. in } \Omega. \tag{5.4}$$

hold true.

As for the energy functional $\mathcal{J}:\Xi\to\mathbb{R}$, we construct it in the form

$$\mathcal{J} = \mathcal{J}_0 + \gamma\mathcal{J}_1 + \lambda\mathcal{J}_2 + \mu\mathcal{J}_3, \tag{5.5}$$

where

$$\begin{aligned}
\mathcal{J}_0\left(I_R, I_G, I_B\right) &= \int_\Omega \frac{1}{p(x)}|\nabla I_R(x)|^{p(x)}\,dx + \int_\Omega \frac{1}{p(x)}|\nabla I_G(x)|^{p(x)}\,dx \\
&\quad + \int_\Omega \frac{1}{p(x)}|\nabla I_B(x)|^{p(x)}\,dx
\end{aligned} \tag{5.6}$$

$$\begin{aligned}
\mathcal{J}_1\left(I_R, I_G, I_B\right) &= \int_\Omega \left|\left(\theta^\perp, \nabla I_R\right)\right|^\alpha dx + \int_\Omega \left|\left(\theta^\perp, \nabla I_G\right)\right|^\alpha dx \\
&\quad + \int_\Omega \left|\left(\theta^\perp, \nabla I_B\right)\right|^\alpha dx,
\end{aligned} \tag{5.7}$$

$$\mathcal{J}_2\left(I_R, I_G, I_B\right) = \int_\Omega \left[\alpha_R I_R + \alpha_G I_G + \alpha_B I_B - Y_H\right]^2\,dx, \tag{5.8}$$

$$\begin{aligned}
\mathcal{J}_3\left(I_R, I_G, I_B\right) &= \sum_{i=1}^{M_x}\sum_{j=1}^{M_y}\left(\left[\mathcal{K}*I_R\right](x_i,y_j) - L_R(x_i,y_j)\right)^2 \\
&\quad + \sum_{i=1}^{M_x}\sum_{j=1}^{M_y}\left(\left[\mathcal{K}*I_G\right](x_i,y_j) - L_G(x_i,y_j)\right)^2 \\
&\quad + \sum_{i=1}^{M_x}\sum_{j=1}^{M_y}\left(\left[\mathcal{K}*I_B\right](x_i,y_j) - L_B(x_i,y_j)\right)^2,
\end{aligned} \tag{5.9}$$

and

$$\theta(x,y) = \frac{DU(t,x,y)}{|DU(t,x,y)|} \text{ for small values of } t > 0. \tag{5.10}$$

Here, the exponent $\alpha > 0$ is defined by (4.6), and $U(t,x,y)$ is the solution of the parabolic problem (3.2)–(3.4) with the initial condition

$$U(0,x,y) = Y_H(x,y) = \alpha_R H_R(x,y) + \alpha_G H_G(x,y) + \alpha_B H_B(x,y), \quad \forall\,(x,y) \in \Omega.$$

The main motivation for such choice of the energy functional is rather clear. As follows from (5.9), each term in $\mathcal{J}_3\,(I_R, I_G, I_B)$ represents an L^2-distortion between a particular spectral channel in the MODIS image $L : S_L \to \mathbb{R}^4$ and the corresponding channel of the retrieved image $I : S_H \to \mathbb{R}^4$ which is resampled to the grid of low resolution S_L. So, the $\mathcal{J}_3$-term should be minimal and it is mainly motivated by Assumption 2.

As for the term $\mathcal{J}_2\,(I_R, I_G, I_B)$, it reflects the fact that the spectral energy $Y_I = \alpha_R I_R + \alpha_G I_G + \alpha_B I_B$ of the retrieved image should be as close as possible to the spectral energy of the Landsat image $H : S_H \to \mathbb{R}^3$. We interpret this closedness in the sense of L^2-norm.

Now about the term $\mathcal{J}_1\,(I_R, I_G, I_B)$. As was mentioned before, the main goal, we are going to follows in the spatial interpolation problem, is to preserve the following property: the geometry of each spectral channels in the retrieved image should be as close as possible to the geometry of the spectral energy of the Landsat image $H : S_H \to \mathbb{R}^3$. Formally, it means that the following relations have to be satisfied

$$\left(\theta^\perp, \nabla I_R\right)_{\mathbb{R}^2} = 0, \quad \left(\theta^\perp, \nabla I_G\right)_{\mathbb{R}^2} = 0, \quad \left(\theta^\perp, \nabla I_B\right)_{\mathbb{R}^2} = 0 \quad \text{a.e. in } \Omega.$$

Hence, the magnitude

$$\int_\Omega \left[\left| \left(\theta^\perp, \nabla I_R\right) \right|^\alpha + \left| \left(\theta^\perp, \nabla I_G\right) \right|^\alpha + \left| \left(\theta^\perp, \nabla I_B\right) \right|^\alpha \right] dx$$

must be small enough, where $\theta = \theta(x,y)$ stands for the vector field of unit normals to the topographic map of the spectral energy $Y_H = \alpha_R H_R + \alpha_G H_G + \alpha_B H_B$.

The first term $\mathcal{J}_0\,(I_R, I_G, I_B)$ is the regularization. Since $p(x) \approx 1$ in places in Ω where edges or discontinuities are present in the spectral energy Y_H of the image H, and $p(x) \approx 2$ in places where $Y_H(x)$ is smooth or contains homogeneous features, the main benefit of the model (5.1) is the manner in which it accommodates the local image information. The places where the gradient is sufficiently large (i.e. likely edges), we deal with the so-called TV-based diffusion [18], whereas the places where the gradient is close to zero (i.e. homogeneous regions), the model becomes isotropic. Specifically, the type of anisotropy at these ambiguous regions varies according to the strength of the gradient. This enables the model to have a much lower dependence on the approximation schemes for the variable exponent $p(x)$ and other thresholds.

We are now in a position to define what we mean by the solution of spatial interpolation problem that was stated in Section 2. Taking into account the properties (i)–(v) that we imposed and the structure of the energy functional $\mathcal{J} : \Xi \to \mathbb{R}$, we say that a four-band image $I^0 = \left[I^0_R, I^0_G, I^0_B, I^0_{NIR}\right]^t : S_H \to \mathbb{R}^4$ is the result of fusion of MODIS-like multi spectral image $L : S_L \to \mathbb{R}^4$ with the Landsat-like color image $H : S_H \to \mathbb{R}^3$ at higher resolution if:

- the triplet $\left(I^0_R, I^0_G, I^0_B\right)$ is a solution of constrained minimization problem (5.1), i.e.,

$$\left(I^0_R, I^0_G, I^0_B\right) \in \Xi \ \text{ and } \ \mathcal{J}\left(I^0_R, I^0_G, I^0_B\right) = \inf_{(I_R, I_G, I_B)\in\Xi} \mathcal{J}\left(I_R, I_G, I_B\right)$$

- The spectral channel $I^0_{NIR} : \Omega \to \mathbb{R}$ is defined as follows

$$I^0_{NIR}(x,y) = \gamma_R I^0_R(x,y) + \gamma_G I^0_G(x,y) + \gamma_B I^0_B((x,y), \quad \forall\,(x,y) \in \Omega,$$

where

$$\begin{bmatrix} \gamma_R \\ \gamma_G \\ \gamma_B \end{bmatrix} = \left[\int_\Omega \begin{pmatrix} L_R^2 & L_R L_G & L_R L_B \\ L_R L_G & L_R^2 & L_G L_B \\ L_R L_B & L_G L_B & L_B^2 \end{pmatrix} dx\right]^{-1} \int_\Omega \begin{bmatrix} L_{NIR} L_R \\ L_{NIR} L_G \\ L_{NIR} L_B \end{bmatrix} dx. \tag{5.11}$$

Here, the last equality is a formal representation of the solution to the following linear regression problem

$$\int_\Omega \left[\gamma_R L_R + \gamma_G L_G + \gamma_B L_B - L_{NIR}\right]^2 dx \overset{\gamma_R, \gamma_G, \gamma_B}{\longrightarrow} \inf.$$

Remark 5.1. As an alternative way to define the NIR spectral channel I^0_{NIR}, we can propose the following one: define I^0_{NIR} as a solution of the constrained minimization problem

$$\mathcal{Z}\left(I^0_{NIR}\right) = \inf_{I \in \Xi_{NIR}} \mathcal{Z}\left(I\right),$$

where

$$\begin{aligned} \mathcal{Z}\left(I\right) = \int_\Omega \frac{1}{p(x)} |\nabla I(x)|^{p(x)}\, dx + \gamma \int_\Omega \left|\left(\theta^\perp, \nabla I\right)\right|^\alpha dx \\ + \lambda \int_\Omega \left[\gamma_R I^0_R + \gamma_G I^0_G + \gamma_B I^0_B - I\right]^2 dx, \end{aligned}$$

$$\Xi_{NIR} = \left\{ I \in W^{1,p(\cdot)}(\Omega) \ : \ 0 \leqslant I(x,y) \leqslant \max_{(x_i, y_j)\in S_L} L_{NIR}(x_i, y_j) \text{ a.e. in } \ \Omega \right\},$$

and the weight coefficients $\gamma_R, \gamma_G, \gamma_B$ are defined by (5.11).

Remark 5.2. Another variant for the setting of the spatial interpolation problem is to consider, instead of the energy term $\mathcal{J}_1$ in (5.5), the following functional (this approach was firstly proposed in [5])

$$\begin{aligned}\mathcal{J}_1\left(I_R, I_G, I_B\right) = \left(\int_\Omega |\nabla I_R|\,dx + \int_\Omega I_R \operatorname{div}\theta\,dx\right) \\ + \left(\int_\Omega |\nabla I_G|\,dx + \int_\Omega I_G \operatorname{div}\theta\,dx\right) \\ + \left(\int_\Omega |\nabla I_B|\,dx + \int_\Omega I_B \operatorname{div}\theta\,dx\right).\end{aligned}$$

The main motivation for such choice of the functional $\mathcal{J}_1$ is rather clear. Since the geometry of each spectral channel in the retrieved image should be as close as possible to the geometry of the spectral energy of the Landsat image $H : S_H \to \mathbb{R}^3$, it means that the following relations have to be satisfied

$$|\nabla I_R| = (\theta, \nabla I_R)\,,\ |\nabla I_G| = (\theta, \nabla I_G)\,,\ |\nabla I_B| = (\theta, \nabla I_B)\,,\ \text{a.e. in}\ \ \Omega.$$

Hence, the magnitude

$$\int_\Omega \left[\left(|\nabla I_R| - (\theta, \nabla I_R)\right) + \left(|\nabla I_G| - (\theta, \nabla I_G)\right) + \left(|\nabla I_B| - (\theta, \nabla I_B)\right)\right]\,dx$$

must be small enough, where $\theta = \theta(x, y)$ stands for the vector field of unit normals to the topographic map of the spectral energy $Y_H = \alpha_R H_R + \alpha_G H_G + \alpha_B H_B$. By default, we assume that this field is zero along the boundary $\partial\Omega$. Then, making use of the Green's formula, we deduce:

$$\begin{aligned}\int_\Omega \left(|\nabla I_R| - \theta\cdot\nabla I_R\right)\,dx &= \int_\Omega |\nabla I_R|\,dx + \int_\Omega I_R \operatorname{div}\theta\,dx,\\ \int_\Omega \left(|\nabla I_G| - \theta\cdot\nabla I_G\right)\,dx &= \int_\Omega |\nabla I_B|\,dx + \int_\Omega I_B \operatorname{div}\theta\,dx,\\ \int_\Omega \left(|\nabla I_B| - \theta\cdot\nabla I_B\right)\,dx &= \int_\Omega |\nabla I_B|\,dx + \int_\Omega I_B \operatorname{div}\theta\,dx.\end{aligned}$$

6. Existence Result and Optimality Conditions

6.1. On Existence and Uniqueness of Retrieved Image at High Resolution

We begin this section with the following existence result.

Theorem 6.1. *Let $H : S_H \to \mathbb{R}^3$ and $L : S_L \to \mathbb{R}^4$ be given images such that their spectral energies satisfy conditions* (4.1)*. Then, under Assumptions 1–4, there exists a unique triplet $(I_R, I_G, I_B) \in \Xi \subset BV(\Omega; \mathbb{R}^3)$ such that (I_R, I_G, I_B) is a minimizer to constrained minimization problem* (5.1)*.*

Proof. First of all, we notice that minimization problem (5.1) is consistent, moreover, $\mathcal{J}(I_R, I_G, I_B) < +\infty$ for each feasible triplet $(I_R, I_G, I_B) \in \Xi$. Indeed, in view of the pointwise estimates (5.2)–(5.4), we have $I_R, IG, I_B \in L^2(\Omega)$. Hence,

$$\mathcal{J}_2\left(I_R, I_G, I_B\right) < +\infty.$$

It remains to notice that the inclusion $I \in W^{1,p(\cdot)}(\Omega;\mathbb{R}^4)$ and the estimates

$$\begin{aligned}\int_\Omega \left|\left(\theta^\perp, \nabla I_A\right)\right|^\alpha dx &\leqslant \|\theta\|^\alpha_{L^\infty(\Omega;\mathbb{R}^2)}\|\nabla I_A\|^\alpha_{L^\alpha(\Omega;\mathbb{R}^2)}\\ &\overset{\text{by (3.13)–(3.15)}}{\leqslant} (1+|\Omega|)\ \|\theta\|^\alpha_{L^\infty(\Omega;\mathbb{R}^2)}\|\nabla I_A\|_{L^{p(\cdot)}(\Omega;\mathbb{R}^2)}\\ &\leqslant (1+|\Omega|)\ \|\theta\|^\alpha_{L^\infty(\Omega;\mathbb{R}^2)}\|I_A\|_{W^{1,p(\cdot)}(\Omega;\mathbb{R}^2)}, \quad A \in \{R, G, B\}\end{aligned}$$

imply $\mathcal{J}_1\left(I_R, I_G, I_B\right) < +\infty$. As a result, consistency of the problem (5.1) immediately follows from (5.5)–(5.9) and definition of the set Ξ.

Let $\left\{(I_R^k, I_G^k, I_B^k)\right\}_{k\in\mathbb{N}} \subset \Xi$ be a minimizing sequence to the problem (5.1). i.e.,

$$\lim_{k\to\infty} \mathcal{J}(I_R^k, I_G^k, I_B^k) = \inf_{(I_R, I_G, I_B)\in\Xi} \mathcal{J}\left(I_R, I_G, I_B\right).$$

Then there exists a constant $\widehat{C} > 0$ such that

$$\sup_{k\in\mathbb{N}} \mathcal{J}(I_R^k, I_G^k, I_B^k) \leqslant \widehat{C}.$$

From this and (5.5), we deduce that

$$\int_\Omega \frac{1}{p(x)}\left[|\nabla I_R(x)|^{p(x)} + |\nabla I_G(x)|^{p(x)} + |\nabla I_B(x)|^{p(x)}\right] dx \leqslant \widehat{C}, \tag{6.1}$$

$$\int_\Omega \left[\alpha_R I_R^k + \alpha_G I_G^k + \alpha_B I_B^k - Y_H\right]^2 dx \leqslant \widehat{C}. \tag{6.2}$$

Since $\alpha := 1+\delta \leqslant p(x) \leqslant \beta := 2$ for all $x \in \Omega$, it follows from (6.1) and (3.11) that

$$\sup_{k\in\mathbb{N}}\left[\|\nabla I_R\|^\alpha_{L^{p(\cdot)}(\Omega;\mathbb{R}^2)} + \|\nabla I_G\|^\alpha_{L^{p(\cdot)}(\Omega;\mathbb{R}^2)} + \|\nabla I_B\|^\alpha_{L^{p(\cdot)}(\Omega;\mathbb{R}^2)}\right] \leqslant \alpha\left(\widehat{C}+3\right). \tag{6.3}$$

On th other hand, utilizing estimate (6.2) and non-negativity of I_R^k, I_G^k, I_B^k, and Y_H, we obtain

$$\int_\Omega \left[\alpha_R I_R^k + \alpha_G I_G^k + \alpha_B I_B^k\right]^2 dx \leqslant 2\widehat{C} + 2\int_\Omega Y_H^2\, dx.$$

Hence,

$$\begin{aligned}(1+|\Omega|)^{-1}\sup_{k\in\mathbb{N}}\|I_R^k\|^2_{L^{p(\cdot)}(\Omega)} &\overset{\text{by (3.14)}}{\leqslant} \sup_{k\in\mathbb{N}}\|I_R^k\|^2_{L^2(\Omega)} \leqslant 2\alpha_R^{-2}\left[\widehat{C} + \|Y_H\|^2_{L^2(\Omega)}\right],\\ (1+|\Omega|)^{-1}\sup_{k\in\mathbb{N}}\|I_G^k\|^2_{L^{p(\cdot)}(\Omega)} &\overset{\text{by (3.14)}}{\leqslant} \sup_{k\in\mathbb{N}}\|I_G^k\|^2_{L^2(\Omega)} \leqslant 2\alpha_G^{-2}\left[\widehat{C} + \|Y_H\|^2_{L^2(\Omega)}\right],\\ (1+|\Omega|)^{-1}\sup_{k\in\mathbb{N}}\|I_B^k\|^2_{L^{p(\cdot)}(\Omega)} &\overset{\text{by (3.14)}}{\leqslant} \sup_{k\in\mathbb{N}}\|I_B^k\|^2_{L^2(\Omega)} \leqslant 2\alpha_B^{-2}\left[\widehat{C} + \|Y_H\|^2_{L^2(\Omega)}\right].\end{aligned} \tag{6.4}$$

As a result, it follows from (6.3) and (6.4) that

$$
\begin{aligned}
\sup_{k\in\mathbb{N}} \|I_R^k\|_{W^{1,p(\cdot)}(\Omega)} &= \sup_{k\in\mathbb{N}} \left[\|I_R^k\|_{L^{p(\cdot)}(\Omega)} + \|\nabla I_R^k\|_{L^{p(\cdot)}(\Omega;\mathbb{R}^2)}\right] \leqslant \mathcal{Q}_R,\\
\sup_{k\in\mathbb{N}} \|I_G^k\|_{W^{1,p(\cdot)}(\Omega)} &= \sup_{k\in\mathbb{N}} \left[\|I_G^k\|_{L^{p(\cdot)}(\Omega)} + \|\nabla I_G^k\|_{L^{p(\cdot)}(\Omega;\mathbb{R}^2)}\right] \leqslant \mathcal{Q}_G,\\
\sup_{k\in\mathbb{N}} \|I_B^k\|_{W^{1,p(\cdot)}(\Omega)} &= \sup_{k\in\mathbb{N}} \left[\|I_B^k\|_{L^{p(\cdot)}(\Omega)} + \|\nabla I_B^k\|_{L^{p(\cdot)}(\Omega;\mathbb{R}^2)}\right] \leqslant \mathcal{Q}_B
\end{aligned}
$$

with $\mathcal{Q}_A = \left[2\left(1+|\Omega|\right)\alpha_A^{-2}\left(\widehat{C} + \|Y_H\|^2_{L^2(\Omega)}\right)\right]^{1/2} + \left[\alpha\left(\widehat{C}+3\right)\right]^{1/\alpha}$, $A \in \{R, G, B\}$.

Thus, the sequence $\left\{(I_R^k, I_G^k, I_B^k)\right\}_{k\in\mathbb{N}} \subset \Xi$ is bounded in $W^{1,p(\cdot)}(\Omega;\mathbb{R}^3)$. Therefore, in view of Proposition 3.3, there exists a subsequence of

$$
\left\{(I_R^k, I_G^k, I_B^k)\right\}_{k\in\mathbb{N}} \subset \Xi,
$$

still denoted by the same index, and functions $(I_R^0, I_G^0, I_B^0) \in W^{1,p(\cdot)}(\Omega;\mathbb{R}^3)$ such that

$$
(I_R^k, I_G^k, I_B^k) \rightharpoonup (I_R^0, I_G^0, I_B^0) \text{ weakly in } W^{1,p(\cdot)}(\Omega;\mathbb{R}^3), \tag{6.5}
$$
$$
(I_R^k, I_G^k, I_B^k) \rightharpoonup (I_R^0, I_G^0, I_B^0) \text{ weakly in } W^{1,\alpha}(\Omega;\mathbb{R}^3), \tag{6.6}
$$
$$
(I_R^k, I_G^k, I_B^k) \to (I_R^0, I_G^0, I_B^0) \text{ strongly in } L^{\alpha}(\Omega;\mathbb{R}^3), \tag{6.7}
$$

and

$$
\int_\Omega \frac{1}{p(x)}|\nabla I_R^0|^{p(x)}\,dx \leqslant \liminf_{k\to\infty} \int_\Omega \frac{1}{p(x)}|\nabla I_R^k|^{p(x)}\,dx, \tag{6.8}
$$
$$
\int_\Omega \frac{1}{p(x)}|\nabla I_G^0|^{p(x)}\,dx \leqslant \liminf_{k\to\infty} \int_\Omega \frac{1}{p(x)}|\nabla I_G^k|^{p(x)}\,dx, \tag{6.9}
$$
$$
\int_\Omega \frac{1}{p(x)}|\nabla I_B^0|^{p(x)}\,dx \leqslant \liminf_{k\to\infty} \int_\Omega \frac{1}{p(x)}|\nabla I_B^k|^{p(x)}\,dx. \tag{6.10}
$$

Moreover, passing to a subsequence if necessary and taking into account the inequalities (5.2)–(5.4) and (3.13), we have:

$$
(I_R^k(x,y), I_G^k(x), I_B^k(x)) \to (I_R^0(x), I_G^0(x), I_B^0(x)) \quad \text{for a.e. } x \in \Omega, \tag{6.11}
$$
$$
(I_R^k, I_G^k, I_B^k) \rightharpoonup (I_R^0, I_G^0, I_B^0) \quad \text{weakly in } L^2(\Omega;\mathbb{R}^3), \tag{6.12}
$$
$$
\left(\theta^\perp, \nabla I_A^k\right) \rightharpoonup \left(\theta^\perp, \nabla I_A^0\right) \quad \text{weakly in } L^\alpha(\Omega) \text{ for } A \in \{R, G, B\}. \tag{6.13}
$$

Hence, without loss of generality, we can suppose that the limit triplet (I_R^0, I_G^0, I_B^0) satisfies the pointwise restrictions (5.2)–(5.4), and, as a consequence, we deduce: $(I_R^0, I_G^0, I_B^0) \in \Xi$ is a feasible solution to the problem (5.1).

Let us show that $(I_R^0, I_G^0, I_B^0) \in \Xi$ is a minimizer to the problem (5.1). Indeed, utilizing convergence properties (6.5)–(6.12), we get

$$\liminf_{k\to\infty} \mathcal{J}_0(I_R^k, I_G^k, I_B^k) \overset{\text{by (6.8)–(6.10)}}{\geqslant} \mathcal{J}_0(I_R^0, I_G^0, I_B^0),$$
$$\liminf_{k\to\infty} \mathcal{J}_1(I_R^k, I_G^k, I_B^k) \overset{\text{by (6.13)}}{\geqslant} \mathcal{J}_1(I_R^0, I_G^0, I_B^0),$$
$$\liminf_{k\to\infty} \mathcal{J}_2(I_R^k, I_G^k, I_B^k) \overset{\text{by (6.12)}}{\geqslant} \mathcal{J}_2(I_R^0, I_G^0, I_B^0),$$
$$\liminf_{k\to\infty} \mathcal{J}_3(I_R^k, I_G^k, I_B^k) \overset{\text{by (6.11),(6.12)}}{\geqslant} \mathcal{J}_3(I_R^0, I_G^0, I_B^0).$$

Hence, $\liminf_{k\to\infty} \mathcal{J}(I_R^k, I_G^k, I_B^k) \geqslant \mathcal{J}(I_R^0, I_G^0, I_B^0)$, and, therefore,

$$\begin{aligned}\inf_{(I_R,I_G,I_B)\in\Xi} \mathcal{J}\left(I_R, I_G, I_B\right) &= \lim_{k\to\infty} \mathcal{J}(I_R^k, I_G^k, I_B^k) = \liminf_{k\to\infty} \mathcal{J}(I_R^k, I_G^k, I_B^k) \\ &\geqslant \mathcal{J}(I_R^0, I_G^0, I_B^0) \geqslant \inf_{(I_R,I_G,I_B)\in\Xi} \mathcal{J}\left(I_R, I_G, I_B\right).\end{aligned}$$

Thus, (I_R^0, I_G^0, I_B^0) is a minimiser to the problem (5.1).

It remains to show that (I_R^0, I_G^0, I_B^0) is a unique minimizer for this problem. Indeed, let us assume the converse. Let $(I_R^0, I_G^0, I_B^0) \in \Xi$ and $(I_R^*, I_G^*, I_B^*) \in \Xi$ be two minimizers for the problem (5.1). Then by the strict convexity of norm $\|\cdot\|_{L^2(\Omega)}$ and convexity of the set of feasible solutions Ξ, we have

$$\begin{aligned}\mathcal{J}\left(\frac{I_R^0+I_R^*}{2}, \frac{I_G^0+I_G^*}{2}, \frac{I_B^0+I_B^*}{2}\right) &< \frac{1}{2}\mathcal{J}(I_R^0, I_G^0, I_B^0) + \frac{1}{2}\mathcal{J}(I_R^*, I_G^*, I_B^*) \\ &= \inf_{(I_R,I_G,I_B)\in\Xi} \mathcal{J}\left(I_R, I_G, I_B\right)\end{aligned}$$

which brings us into a conflict with the initial assumptions. Thus, (I_R^0, I_G^0, I_B^0) is a unique minimizer to the problem (5.1). The proof is complete. □

For further convenience, we rewrite the energy functional $\mathcal{J} : \Xi \to \mathbb{R}$ in the integral form. To this end, we set: let $\delta_{(i,j)}$ be the Dirac's delta on the point $(i.j) \in \Omega$. Let $\Pi_L = \sum_{(i,j)\in S_L} \delta_{(i,j)}$ be the Dirac's comb on Ω defined by the grid S_L. Then we may write $\mathcal{J}_3$ in integral terms

$$\mathcal{J}_3\left(I_R, I_G, I_B\right) = \sum_{A\in\{R,G.B\}} \int_\Omega \Pi_L \left(\left[\mathcal{K} * I_A\right](x) - L_A(x)\right)^2 \, dx, \tag{6.14}$$

where L_A, $A \in \{R, G.B\}$ denotes an arbitrary extension of $L_A(i,j)$ as continuous functions from S_L to Ω. Since the terms above are multiplied by Π_L, the integral terms in (6.14) do not depend on the particular extensions of L_A, $A \in \{R, G.B\}$.

6.2. Optimality Conditions

In order to derive some optimality conditions to the problem (5.1) and characterize its solution (I_R^0, I_G^0, I_B^0), we check that the functional $\mathcal{J} : \Xi \to \mathbb{R}$ is Gâteaux differentiable. To this end, we note that

$$\frac{|\nabla I_A^0(x) + t\nabla h_A(x)|^{p(x)} - |\nabla I_A^0(x)|^{p(x)}}{p(x)t} \\ \to \Big(|\nabla I_A^0(x)|^{p(x)-2}\nabla I_A^0(x), \nabla h_A(x)\Big) \quad \text{as} \quad t \to 0$$

almost everywhere in Ω for all $A \in \{R, G.B\}$ and $h = (h_R, h_G, h_B) \in W^{1,p(\cdot)}(\Omega)^3$. Indeed, by convexity, we have $|\xi|^p - |\eta|^p \leqslant 2p\left(|\xi|^{p-1} + |\eta|^{p-1}\right)|\xi - \eta|$. Then

$$\left|\frac{|\nabla I_A^0(x) + t\nabla h_A(x)|^{p(x)} - |\nabla I_A^0(x)|^{p(x)}}{p(x)t}\right| \\ \leqslant 2\Big(|\nabla I_A^0(x) + t\nabla h_A(x)|^{p(x)-1} + |\nabla I_A^0(x)|^{p(x)-1}\Big)|\nabla h_A(x)| \\ \leqslant \text{const}\Big(|\nabla I_A^0(x)|^{p(x)-1} + |\nabla h_A(x)|^{p(x)-1}\Big)|\nabla h_A(x)|. \quad (6.15)$$

Taking into account that

$$\||\nabla I_A^0(x)|^{p(\cdot)-1}\|_{L^{p'(\cdot)}(\Omega;\mathbb{R}^2)} \overset{\text{by (3.11) and (3.7)}}{\leqslant} \left(\int_\Omega |\nabla I_A^0(x)|^{p(x)}\,dx + 1\right)^{\frac{1}{2}} \\ \overset{\text{by (3.11)}}{\leqslant} \left(\|\nabla I_A^0|^2_{L^{p(\cdot)}(\Omega;\mathbb{R}^2)} + 2\right)^{\frac{1}{2}},$$

$$\int_\Omega |\nabla I_A^0(x)|^{p(x)-1}|\nabla h_A(x)|\,dx \overset{\text{by (3.19)}}{\leqslant} 2\||\nabla I_A^0(x)|^{p(x)-1}\|_{L^{p'(\cdot)}(\Omega)}\|h_A(x)|\|_{L^{p(\cdot)}(\Omega)},$$

and $\int_\Omega |\nabla h_A(x)|^{p(x)}\,dx \overset{\text{by (3.11)}}{\leqslant} \|\nabla h_A\|^2_{L^{p(\cdot)}(\Omega)} + 1$, we see that the right hand side of inequality (6.15) is an $L^1(\Omega)$ function. Therefore,

$$\int_\Omega \frac{|\nabla I_A^0(x) + t\nabla h_A(x)|^{p(x)} - |\nabla I_A^0(x)|^{p(x)}}{p(x)t}\,dx \\ \to \int_\Omega \Big(|\nabla I_A^0(x)|^{p(x)-2}\nabla I_A^0(x), \nabla h_A(x)\Big)\,dx \quad \text{as} \quad t \to 0$$

by the Lebesgue dominated convergence theorem for each $h = (h_R, h_G, h_B) \in$

$W^{1,p(\cdot)}(\Omega;\mathbb{R}^3)$ and $A \in \{R, G.B\}$. Thus,

$$\lim_{t\to 0}\frac{\mathcal{J}_0\left(I_R^0+th_R, I_G^0+th_G, I_B^0+th_B\right)-\mathcal{J}_0\left(I_R^0, I_G^0, I_B^0\right)}{t}$$
$$=\int_\Omega \left(|\nabla I_R^0(x)|^{p(x)-2}\nabla I_R^0(x), \nabla h_R(x)\right)\,dx$$
$$+\int_\Omega \left(|\nabla I_G^0(x)|^{p(x)-2}\nabla I_G^0(x), \nabla h_G(x)\right)\,dx$$
$$+\int_\Omega \left(|\nabla I_B^0(x)|^{p(x)-2}\nabla I_B^0(x), \nabla h_B(x)\right)\,dx. \quad (6.16)$$

Arguing in a similar manner, it can be shown that (see [2, Section A 14] for the details)

$$\lim_{t\to 0}\frac{\mathcal{J}_1\left(I_R^0+th_R, I_G^0+th_G, I_B^0+th_B\right)-\mathcal{J}_1\left(I_R^0, I_G^0, I_B^0\right)}{t}$$
$$=\alpha\int_\Omega \left|\left(\theta^\perp, \nabla I_R^0\right)\right|^{\alpha-2}\left(\theta^\perp, \nabla I_R^0\right)\left(\theta^\perp, \nabla h_R\right)\,dx$$
$$+\alpha\int_\Omega \left|\left(\theta^\perp, \nabla I_G^0\right)\right|^{\alpha-2}\left(\theta^\perp, \nabla I_G^0\right)\left(\theta^\perp, \nabla h_G\right)\,dx$$
$$+\alpha\int_\Omega \left|\left(\theta^\perp, \nabla I_B^0\right)\right|^{\alpha-2}\left(\theta^\perp, \nabla I_B^0\right)\left(\theta^\perp, \nabla h_B\right)\,dx. \quad (6.17)$$

Setting
$$\Lambda = \theta^\perp\left(\theta^\perp\right)^t = \begin{bmatrix}\theta_1^\perp\,\theta_1^\perp & \theta_1^\perp\,\theta_2^\perp\\ \theta_2^\perp\,\theta_1^\perp & \theta_2^\perp\,\theta_2^\perp\end{bmatrix},$$
the Gâteaux differential of $\mathcal{J}_1$ can be rewritten as follows

$$\lim_{t\to 0}\frac{\mathcal{J}_1\left(I_R^0+th_R, I_G^0+th_G, I_B^0+th_B\right)-\mathcal{J}_1\left(I_R^0, I_G^0, I_B^0\right)}{t}$$
$$=\alpha\int_\Omega \left|\left(\theta^\perp, \nabla I_R^0\right)\right|^{\alpha-2}\left(\Lambda\nabla I_R^0, \nabla h_R\right)\,dx$$
$$+\alpha\int_\Omega \left|\left(\theta^\perp, \nabla I_G^0\right)\right|^{\alpha-2}\left(\Lambda\nabla I_G^0, \nabla h_G\right)\,dx$$
$$+\alpha\int_\Omega \left|\left(\theta^\perp, \nabla I_B^0\right)\right|^{\alpha-2}\left(\Lambda\nabla I_B^0, \nabla h_B\right)\,dx. \quad (6.18)$$

As for the rest terms in the cost functional $\mathcal{J} : \Xi \to \mathbb{R}$, we have the following representation for their Gâteaux derivatives (for the proof and its substantiation we refer to [13, Section 3]).

Proposition 6.1. Let $H : S_H \to \mathbb{R}^3$ and $L : S_L \to \mathbb{R}^4$ be given images such that their spectral energies satisfy conditions (4.1) Then the functionals $\mathcal{J}_2, \mathcal{J}_3$:

$L^2(\Omega;\mathbb{R}^3) \to \mathbb{R}$ are convex and Gâteaux differentiable in $L^2(\Omega;\mathbb{R}^3)$ with

$$\mathcal{J}_2'(I^0)[h] = 2 \sum_{A\in\{R,G.B\}} \int_\Omega \alpha_A \left(\alpha_R I_R^0 + \alpha_G I_G^0 + \alpha_B I_B^0 - Y_H\right) h_A \, dx, \tag{6.19}$$

$$\begin{aligned}\mathcal{J}_3'(I^0)[h] &= 2 \sum_{A\in\{R,G.B\}} \int_\Omega \Pi_L \left(\left[\mathcal{K} * I_A^0\right] - L_A\right) \left[\mathcal{K} * h_A\right] dx \\ &= 2 \sum_{A\in\{R,G.B\}} \int_\Omega \Pi_L \left[\mathcal{K}^* * \left(\left[\mathcal{K} * I_A^0\right] - L_A\right)\right] h_A \, dx,\end{aligned} \tag{6.20}$$

for all $h = (h_R, h_G, h_B) \in L^2(\Omega;\mathbb{R}^3)$.

We are now in a position to derive an optimality system for a unique minimizer $(I_R^0, I_G^0, I_B^0) \in \Xi \subset BV(\Omega;\mathbb{R}^3)$ to constrained minimization problem (5.1). Following the standard technique which is based on the use of the Lagrange principle [10] and utilizing Proposition 4.4, we arrive at the following result.

Theorem 6.2. *Let $(I_R^0, I_G^0, I_B^0) \in \Xi$ be a minimizer of constrained minimization problem* (5.1). *Then the following relations hold true*

$$\begin{aligned}- \operatorname{div}\left(|\nabla I_A^0(x)|^{p(x)-2} \nabla I_A^0(x)\right) &- \gamma\alpha \operatorname{div}\left(\left|\left(\theta^\perp, \nabla I_A^0\right)\right|^{\alpha-2} \Lambda \nabla I_A^0\right) \\ &+ 2\lambda\alpha_A \left(\alpha_R I_R^0 + \alpha_G I_G^0 + \alpha_B I_B^0 - Y_H\right) \\ &+ 2\mu \Pi_L \left[\mathcal{K}^* * \left(\left[\mathcal{K} * I_A^0\right] - L_A\right)\right] = 0 \quad \text{a.e. in } \Omega,\end{aligned} \tag{6.21}$$

$$0 \leqslant I_A^0 \leqslant \max_{(x_i,y_j)\in S_L} L_A(x_i, y_j) \quad \text{a.e. in } \Omega, \tag{6.22}$$

$$\left(\nabla I_A^0, \nu\right) = 0 \quad \text{on } \partial\Omega, \tag{6.23}$$

for $A \in \{R, G, B\}$.

Remark 6.1. In practical implementation, it is reasonable to define an optimal triplet (I_R^0, I_G^0, I_B^0) using a 'gradient descent' strategy. Following the standard procedure, we can start from some initial RGB-components (I_R^*, I_G^*, I_B^*) and then to solve the following initial value problem for the system of quasi-linear parabolic equations with $2D$ elliptic operators in their principle part and Nuemann boundary conditions

$$\begin{aligned}\frac{\partial I_R^0}{\partial t} - \operatorname{div}\left(|\nabla I_R^0(x)|^{p(x)-2} \nabla I_R^0(x)\right) &= \gamma\alpha \operatorname{div}\left(\left|\left(\theta^\perp, \nabla I_R^0\right)\right|^{\alpha-2} \Lambda \nabla I_R^0\right) \\ &- 2\lambda\alpha_R \left(\alpha_R I_R^0 + \alpha_G I_G^0 + \alpha_B I_B^0 - Y_H\right) - 2\mu \Pi_L \left[\mathcal{K}^* * \left(\left[\mathcal{K} * I_R^0\right] - L_R\right)\right], \\ \frac{\partial I_G^0}{\partial t} - \operatorname{div}\left(|\nabla I_G^0(x)|^{p(x)-2} \nabla I_G^0(x)\right) &= \gamma\alpha \operatorname{div}\left(\left|\left(\theta^\perp, \nabla I_G^0\right)\right|^{\alpha-2} \Lambda \nabla I_G^0\right) \\ &- 2\lambda\alpha_G \left(\alpha_R I_R^0 + \alpha_G I_G^0 + \alpha_B I_B^0 - Y_H\right) - 2\mu \Pi_L \left[\mathcal{K}^* * \left(\left[\mathcal{K} * I_G^0\right] - L_G\right)\right], \\ \frac{\partial I_B^0}{\partial t} - \operatorname{div}\left(|\nabla I_B^0(x)|^{p(x)-2} \nabla I_B^0(x)\right) &= \gamma\alpha \operatorname{div}\left(\left|\left(\theta^\perp, \nabla I_B^0\right)\right|^{\alpha-2} \Lambda \nabla I_B^0\right) \\ &- 2\lambda\alpha_B \left(\alpha_R I_R^0 + \alpha_G I_G^0 + \alpha_B I_B^0 - Y_H\right) - 2\mu \Pi_L \left[\mathcal{K}^* * \left(\left[\mathcal{K} * I_B^0\right] - L_B\right)\right],\end{aligned}$$

$$\begin{aligned}&\left(\nabla I_R^0,\nu\right)=0,\ \left(\nabla I_G^0,\nu\right)=0,\ \left(\nabla I_B^0,\nu\right)=0\quad\text{on }\partial\Omega,\\ 0\leqslant I_A^0\leqslant &\max_{(x_i,y_j)\in S_L} L_A(x_i,y_j)\quad\text{a.e. in }\ \Omega\ \forall\, A\in\{R,G,B\},\\ &I_R^0(0,x)=I_R^*,\ I_G^0(0,x)=I_G^*,\ I_B^0(0,x)=I_B^*,\quad \forall\, x\in\Omega,\end{aligned}$$

where we propose to take the triplet (I_R^*, I_G^*, I_B^*) as a result bicubic interpolation of the MODIS-like image $L : S_L \to \mathbb{R}^4$ onto the entire domain Ω.

7. Numerical Experiments

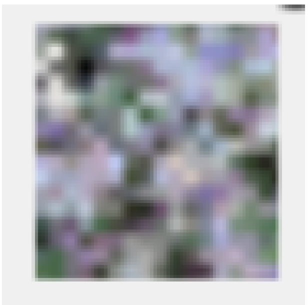

Fig. 7.1. The MODIS image with resolution $350m/pixel$

In order to illustrate the proposed algorithm for the spatial increasing resolution problem of MODIS-like multi-spectral images via their fusion with Lansat-like imagery at higher resolution. As input data we have used a MODIS image of some region with resolution $350m/pixel$ (see Fig. 7.1). This region represents a typical agricultural area with medium sides fields of various shapes.

We also have the image of the same territory with resolution $25m/pixel$ that was made by Lansat satellite at higher resolution. Figure 7.2 shows the spectral channels of this image.

Figure 7.3 displays the reconstructed images corresponding to the data given by Figures 7.1 and 7.2. In order to validate the obtained result, we have provided the following calculations.

- Closednees of the means $\rho_2 = |\mathrm{Mean}\, I - \mathrm{Mean}\, L| = 0$;
- Closedness of the variances $\rho_3 = 100\frac{|\mathrm{Var}\, I - \mathrm{Var}\, L|}{\mathrm{Var}\, L} \approx 6\%$;
- ERGAS metric

$$ERGAS = 100\frac{h}{l}\sqrt{\frac{1}{3}\sum_{k=1}^{3}\left(\frac{\mathrm{RMSE(k)}}{\mu_0(k)}\right)^2} = 2.24,$$

where h/l is the ratio between the size of the high spatial resolution image pixel and the size of the pixel in the MODIS-like image.

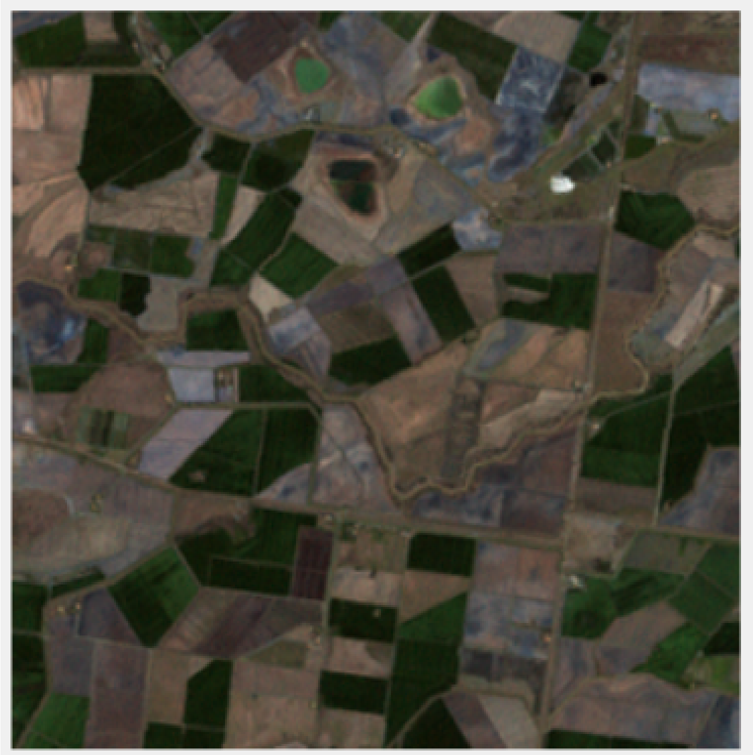

Fig. 7.2. The Lansat image with resolution $25m/pixel$

It is worth to notice that in view of the suggestions of Prof. L. Wald, if the ERGAS value is less than 3, the spectral quality of an image is satisfactory.

References

1. L. Ambrosio, N. Fusco, D. Pallara, *Functions of bounded variation and free discontinuity problems*, Oxford University Press, New York, 2000.
2. A.B. Al'shin, M.O. Korpusov, A.G. Sveshnikov, *Blow-up in Nonlinear Sobolev Type Equations*, De Gruyter series in nonliniear analysis and applications; 15, Walter de Gruyter GmbH & Co, Berlin, 2011.
3. F. Andreu, C. Ballester, V. Caselles, J. M. Mazón, *Minimizing Total Variation Flow*, Diff. and Int. Eq., **14** (2001), 321–360.
4. H. Attouch, G. Buttazzo, G. Michaille, *Variational Analysis in Sobolev and BV Spaces: Applications to PDEs and Optimization*, SIAM, Philadelphia, 2006.
5. C. Ballester, V. Caselles, L. Igual, J. Verdera, B. Rougé, *A Variational Model for P+XS Image Fusion*, International Journal of Computer Vision, **69** (2006), 43–58.
6. G. Crasta, V. De Cicco, *Anzellotti's pairing theory and the Gauss-Green theorem*, Advances in Mathematics, **343** (5) (2019), 935–970.
7. D.V. Cruz-Uribe, A. Fiorenza, *Variable Lebesgue Spaces: Foundations and Harmonic Analysis*, Birkhäuser, New York, 2013.

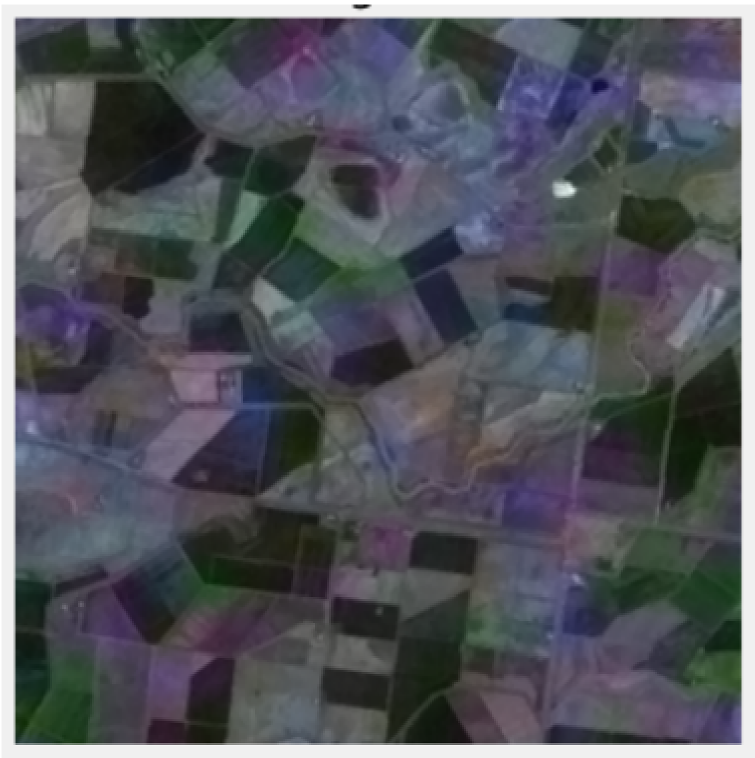

Fig. 7.3. The retrieved image at high resolution $25m/pixel$ following the proposed approach

8. L. Diening, P. Harjulehto, P. Hästö, M. Růžička, *Lebesgue and Sobolev Spaces with Variable Exponents*, Springer, New York, 2011.
9. D. Frantz, *Landsat+ Sentinel-2 analysis ready data and beyond*, Remote Sens., **11**, 1124, 2019.
10. A.D. Ioffe, V.M. Tikhomirov, *Theory of Extremal Problems*, North Holland, Amsterdam, 1979.
11. V.V. Hnatushenko, P.I. Kogut, M.V. Uvarov, *On Flexible Co-Registration of Optical and SAR Satellite Images*, in "Lecture Notes in "Computational Intelligence and Decision Making" (series "Advances in Intelligent Systems and Computing Editors: Babichev, S., Lytvynenko, V., WΓijcik, W., Vyshemyrskaya, S. (Eds.)), Springer, 2021, 515–534.
12. V.V. Hnatushenko, P.I. Kogut, M.V. Uvarov, *Variational Approach for Rigid Co-Registration of Optical/SAR Satellite Images in Agricultural Areas*, Journal of Computational and Applied Mathematics, to appear.
13. V.V. Hnatushenko, P.I. Kogut, M.V. Uvarow, *On optimal* **2**-*D domain segmentation problem via piecewise smooth approximation of a selective target mapping*, J. of Optimization, Differential Equations and Their Applications *(JODEA)*, **27** (2) (2019), 39–74.
14. B. Kawohl, F. Schuricht, *Dirichlet problems for the* 1-*Laplace operator, including the eigenvalue problem*, Communications in Contemporary Mathematics, **9** (4) (2007), 515–543.

15. P.I. Kogut, G. Leugering, *Optimal Control Problems for Partial Differential Equations on Reticulated Domains. Approximation and Asymptotic Analysis*, Series: Systems and Control, Birkhäuser Verlag, Boston, 2011.
16. D.P. Roy, J. Li, H.K. Zhang, L. Yan, *Best practices for the reprojection and resampling of Sentinel-2 Multi Spectral Instrument Level 1C data*, Remote Sens. Lett., **7** (2016), 1023–1032.
17. D.P. Roy, H. Huang, L. Boschetti, L. Giglio, H.K. Zhang, J. Li, *Landsat-8 and Sentinel-2 burned area mapping — a combined sensor multi-temporal change detection approach*, Remote Sens. Environ., **231**, 111254, 2019.
18. L.I. Rudin, S. Osher, E. Fatemi, *Nonlinear total variation based noise removal algorithms*, Physica, **60**(D) (1992), 259–268.
19. L. Yan, D.P. Roy, H. Zhang, J. Li, H. Huang, *An automated approach for sub-pixel registration of Landsat-8 Operational Land Imager (OLI) and Sentinel-2 Multi Spectral Instrument (MSI) imagery*, Remote Sens., **8**, 520, 2016.
20. V.V. Zhikov, *Solvability of the three-dimensional thermistor problem*, Proceedings of the Steklov Institute of Mathematics, **281** (2008), 98–111.
21. V.V. Zhikov, *On variational problems and nonlinear elliptic equations with nonstandard growth conditions*, Journal of Mathematical Sciences, **173**(5) (2011), 463–570.

Received 10.05.2021

JOURNAL OF OPTIMIZATION, DIFFERENTIAL EQUATIONS AND THEIR APPLICATIONS (JODEA)
Volume **29**, Issue **1**, June **2021**, pp. 79–95, DOI 10.15421/142105

ISSN (print) 2617–0108
ISSN (on-line) 2663–6824

MATHEMATICAL SIMULATIONS OF DEFORMATION FOR THE ROTATION SHELLS WITH VARIABLE WALL THICKNESS

Aleksandr A. Dzyuba[*], Anatoliy P. Dzyuba[†], Larisa D. Levitina[‡], Inga A. Safronova[§]

Communicated by Prof. V.V. Loboda

Abstract. Well-posed boundary value problems are constructed for calculating rotation shells of with a stiffness variable along the meridian in two directions, and also with variable bilateral with respect to the reference surface with the shell wall thickness. Algorithms for the numerical integration of systems of differential equations with variable coefficients are discussed.

Key words: Boundary value problem, system of differential equations, shells of revolution, variable wall thickness, straight line method, Fourier method, sweep method..

2010 Mathematics Subject Classification: 74K25, 35F45.

1. Introduction

Shell structures are widely used in the creation of structures for modern mechanical engineering, in the oil and gas, chemical and other industries. At the same time, the requirements for ensuring the strength reliability while reducing the weight indicators lead to the need to build more and more reliable models and methods for calculating shell structures with non-homogeneous parameters (in particular, with variable stiffness) [4, 6–8, 10, 13–15, 17].

In the problems of determining the optimal distribution of material [9] or calculating the durability of shells taking into account the degradation of their surface in an aggressive environment [16], the stiffness parameters change at each step of successive approximations. This leads to the necessity of restructuring the grid at each step of the corresponding iterative computational (search) algorithm using the known finite element analysis packages [1, 5].

[*]Department of Theoretical and Computational Mechanics, Oles Honchar Dnipro National University, 72, Gagarin av., Dnipro, 49010, Ukraine,

[†]Department of Theoretical and Computational Mechanics, Oles Honchar Dnipro National University, 72, Gagarin av., Dnipro, 49010, Ukraine, dzb@ua.fm

[‡]Department of Theoretical and Computational Mechanics, Oles Honchar Dnipro National University, 72, Gagarin av., Dnipro, 49010, Ukraine,

[§]Department of Computer Technologies, Oles Honchar Dnipro National University, 72, Gagarin av., Dnipro, 49010, Ukraine,

An effective approach to the study of the behavior of such structural elements with irregular parameters remains the direct solution of boundary value problems for systems of differential equations describing their state, where the components of the stress-strain state are unknown. In this case, the parameters of non-homogeneity (change in the thickness of the shell wall) are taken into account quite simply, since they turn out to be components of the coefficients of these systems and the computational costs when using this approach are mainly associated only with the need to solve the corresponding boundary value problems [3, 12, 15].

This paper presents general information about the exact mathematical models of shells with rigidity, in two directions, as well as with a two-sided change in the shell wall thickness with respect to the reference surface.

2. Basic Relations

The basic equations of the moment theory of shells are obtained under the assumption that shells of revolution (with an arbitrary meridian shape in the general case) and circular (annular) plates are homogeneous, isotropic, thin and elastic. The validity of Kirchhoff's hypotheses is accepted, as well as the smallness of deformations and angles of rotation in comparison with unity. The shell wall thickness is generally considered arbitrary $h = h\,(s, \varphi)$.

Deformation of the middle surface ε_1, ε_2, γ_{12} the angles of rotation of the normal to the surface ϑ_1, ϑ_2 and the parameters of the change in curvature χ_1, χ_2, χ_{12} are associated with the displacements u, v, w (Fig. 1) by the dependencies [3]:

$$\begin{aligned}
\varepsilon_1 &= \frac{\partial u}{\partial s} + \frac{w}{R_1}; \qquad \varepsilon_2 = \frac{\partial v}{r\partial\varphi} + \frac{\cos\theta}{r}u + \frac{\sin\theta}{r}w;\\
\vartheta_1 &= \frac{u}{R_1} - \frac{\partial w}{\partial s}; \qquad \vartheta_2 = \frac{\sin\theta}{r}v - \frac{\partial w}{r\partial\varphi};\\
\gamma_{12} &= r\frac{\partial}{\partial s}\left(\frac{v}{r}\right) + \frac{\partial u}{r\partial\varphi};\\
\chi_1 &= -\frac{\partial}{\partial s}\left(\frac{\partial w}{\partial s} - \frac{u}{R_1}\right) = \frac{\partial\vartheta_1}{\partial s};\\
\chi_2 &= \frac{\partial\vartheta_2}{r\partial\varphi} + \frac{\cos\theta}{r}\vartheta_1 = \frac{\sin\theta}{r^2}\frac{\partial v}{\partial\varphi} - \frac{1}{r^2}\frac{\partial^2 w}{\partial\varphi^2} + \frac{\cos\theta}{r}\vartheta_1;\\
\chi_{12} &= \frac{1}{r}\frac{\partial\vartheta_1}{\partial\varphi} - \frac{\cos\theta}{r}\vartheta_2 + \frac{\sin\theta}{r}\frac{\partial v}{\partial s},
\end{aligned} \tag{2.1}$$

where $\theta(s)$ is the angle between the normal to the median surface and the shell rotation axis; $r(s)$ is the radius of the parallel circle.

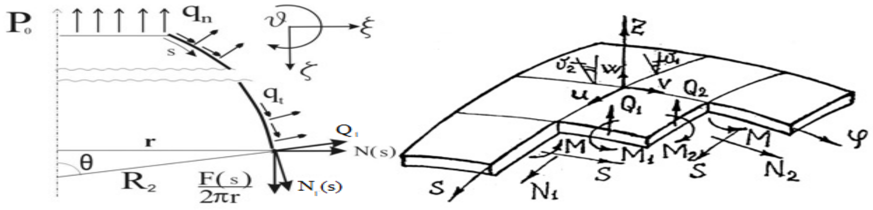

Fig. 2.1. Efforts and displacements in the shell

Elastic ratios are taken in the usual form

$$\begin{aligned}
N_1 &= \frac{Eh}{1-\mu^2}(\varepsilon_1+\mu\varepsilon_2); \qquad M_1 = D(\chi_1+\mu\chi_2);\\
N_2 &= \frac{Eh}{1-\mu^2}(\varepsilon_2+\mu\varepsilon_1); \qquad M_2 = D(\chi_2+\mu\chi_1);\\
S &= \frac{Eh}{2(1+\mu)}\gamma_{12}; \qquad M = D(1-\mu)\chi_{12},
\end{aligned} \tag{2.2}$$

where $D = Eh^3/(12(1-\mu^2))$ is the cylindrical stiffness; R_1, R_2 are thr radii of curvature of the surface; E, μ are the modulus of elastic and Poisson's ratio, respectively. As a result, the equations of forces and moments can be written as follows:

$$\begin{aligned}
\frac{\partial}{\partial s}(rN_1)+\frac{\partial}{\partial\varphi}\left(S+\frac{M}{R_1}\right)-\cos\theta\cdot N_2+\frac{r}{R_1}Q_1+rq_1 &= 0;\\
\frac{\partial N_2}{\partial\varphi}+\frac{\partial}{\partial s}\left[r\left(S+\frac{M}{R_2}\right)\right]+\cos\theta\left(S+\frac{M}{R_1}\right)+\sin\theta\cdot Q_2+rq_2 &= 0;\\
\frac{\partial}{\partial s}(rQ_1)+\frac{\partial Q_2}{\partial\varphi}-\frac{r}{R_1}N_1-\sin\theta\cdot N_2+rq_3 &= 0;\\
\frac{1}{r}\left[\frac{\partial}{\partial s}(rM)+\frac{\partial M_2}{\partial\varphi}+\cos\theta\cdot M\right]-Q_2 &= 0;\\
\frac{1}{r}\left[\frac{\partial M}{\partial\varphi}+\frac{\partial}{\partial s}(rM_1)-\cos\theta\cdot M_2\right]-Q_1 &= 0,
\end{aligned} \tag{2.3}$$

Here, for the force factors, the generally accepted designations are introduced [3]: $N_1, N_2, S, M_1, M_2, M, Q_1, Q_2$, P° q_1, q_2, q_3 are the meridional, circumferential and normal components of the intensity of the external load, respectively.

As the main variables with respect to which the system is written, four quantities u, v, w, ϑ_1 are selected, which characterize the displacements and the four force factors N_1, S^*, Q_1^*, M_1 corresponding to them, where $S^* = S + \frac{2M}{R_2}$; $Q_1^* = Q_1 + \frac{1}{r}\frac{\partial M}{\partial\varphi}$ are reduced efforts. After appropriate transformations, the equations of the moment theory for homogeneous isotropic elastic thin-walled shells of variable thickness under asymmetric loading can be, as is known [3, 12], reduced to a system of eight partial differential equations, which can be written in the form:

$$
\begin{aligned}
\frac{\partial u}{\partial s} &= -\mu\frac{\cos\theta}{r}u-\left(\mu\frac{\sin\theta}{r}+\frac{1}{R_1}\right)w+\frac{1}{Kr}\left(N_1r\right)-\mu\frac{1}{r}\frac{\partial v}{\partial\varphi};\\
\frac{\partial v}{\partial s} &= \frac{\cos\theta}{r}v+\frac{2}{K\left(1-\mu\right)}\frac{1}{r}\left(S^{*}r\right)-\left(\frac{1}{r}+\frac{4D}{KR_2}\frac{\sin\theta}{r^2}\right)\frac{\partial u}{\partial\varphi}\\
&\quad+\frac{4D}{KR_2}\frac{\cos\theta}{r^2}\frac{\partial w}{\partial\varphi}+\frac{4D}{KR_2}\frac{\partial\vartheta_1}{r\partial\varphi};\\
\frac{\partial w}{\partial s} &= \frac{u}{R_1}-\vartheta_1;\\
\frac{\partial\vartheta_1}{\partial s} &= -\mu\frac{\cos\theta}{r}\vartheta_1+\frac{1}{Dr}\left(M_1r\right)-\mu\frac{\sin\theta}{r^2}\frac{\partial v}{\partial\varphi}+\mu\frac{1}{r^2}\frac{\partial^2 w}{\partial\varphi^2};\\
\frac{\partial\left(N_1r\right)}{\partial s} &= K\left(1-\mu^2\right)\frac{\cos^2\theta}{r}u-K\left(1-\mu^2\right)\frac{\cos\theta\sin\theta}{r}w+\mu\frac{\cos\theta}{r}\left(N_1r\right)\\
&\quad-\frac{1}{R_1}\left(Q_1^{*}r\right)+\frac{2\left(1-\mu\right)}{R_2}\frac{\sin\theta}{r^2}\frac{\partial D}{\partial\varphi}\frac{\partial u}{\partial\varphi}+K\left(1-\mu^2\right)\frac{\cos\theta}{r}\frac{\partial v}{\partial\varphi}\\
&\quad-\frac{2\left(1-\mu\right)}{R_2}\frac{\cos\theta}{r^2}\frac{\partial D}{\partial\varphi}\frac{\partial w}{\partial\varphi}-\frac{2\left(1-\mu\right)}{R_2}\frac{1}{r}\frac{\partial D}{\partial\varphi}\frac{\partial\vartheta_1}{\partial\varphi}\\
&\quad+\frac{2D\left(1-\mu\right)}{R_2}\frac{\sin\theta}{r^2}\frac{\partial^2 u}{\partial\varphi^2}-\frac{2D\left(1-\mu\right)}{R_2}\frac{\cos\theta}{r^2}\frac{\partial^2 w}{\partial\varphi^2}\\
&\quad-\frac{2D\left(1-\mu\right)}{R_2}\frac{1}{r}\frac{\partial^2\vartheta_1}{\partial\varphi^2}-\frac{1}{r}\frac{\partial}{\partial\varphi}\left(S^{*}r\right)-rq_1; \qquad (2.4)\\
\frac{\partial\left(S^{*}r\right)}{\partial s} &= -\frac{\partial K}{\partial\varphi}\left(1-\mu^2\right)\frac{\cos\theta}{r}u-\frac{\partial K}{\partial\varphi}\left(1-\mu^2\right)\frac{\sin\theta}{r}w\\
&\quad-\frac{\partial D}{\partial\varphi}\left(1-\mu^2\right)\frac{\sin\theta\cos\theta}{r^2}\vartheta_1-\frac{\cos\theta}{r}\left(S^{*}r\right)-K\left(1-\mu^2\right)\frac{\cos\theta}{r}\frac{\partial u}{\partial\varphi}\\
&\quad-\left(1-\mu^2\right)\left(\frac{1}{r}\frac{\partial K}{\partial\varphi}+\frac{\sin^2\theta}{r^3}\frac{\partial D}{\partial\varphi}\right)\frac{\partial v}{\partial\varphi}-K\left(1-\mu^2\right)\frac{\sin\theta}{r}\frac{\partial w}{\partial\varphi}\\
&\quad-D\left(1-\mu^2\right)\frac{\sin\theta\cos\theta}{r^2}\frac{\partial\vartheta_1}{\partial\varphi}-\mu\frac{1}{r}\frac{\partial\left(N_1r\right)}{\partial\varphi}\\
&\quad-\mu\frac{\sin\theta}{r^2}\frac{\partial\left(M_1r\right)}{\partial\varphi}-\left(1-\mu^2\right)\left(K\frac{1}{r}-D\frac{\sin^2\theta}{r^3}\right)\frac{\partial^2 v}{\partial\varphi^2}\\
&\quad+\frac{\sin\theta}{r^3}\left(1-\mu^2\right)\frac{\partial D}{\partial\varphi}\frac{\partial^2 w}{\partial\varphi^2}+\left(1-\mu^2\right)D\frac{\sin\theta}{r^3}\frac{\partial^3 w}{\partial\varphi^3}-rq_2;\\
\frac{\partial\left(Q_1^{*}r\right)}{\partial s} &= \left(\frac{1}{R_1}+\mu\frac{\sin\theta}{r}\right)\left(N_1r\right)+K\left(1-\mu^2\right)\frac{\cos\theta\sin\theta}{r}u\\
&\quad+K\left(1-\mu^2\right)\frac{\sin^2\theta}{r}w-\frac{\partial^2 D}{\partial\varphi^2}\left(1-\mu^2\right)\frac{\cos\theta}{r^2}\vartheta_1\\
&\quad+\frac{\partial D}{\partial\varphi}\left(1-\mu\right)\frac{2\cos\theta\sin\theta}{r^3}\frac{\partial u}{\partial\varphi}-\left(1-\mu^2\right)\frac{\sin\theta}{r}\left(\frac{\partial^2 D}{\partial\varphi^2}\frac{1}{r^2}-K\right)\frac{\partial v}{\partial\varphi}\\
&\quad-\frac{\partial D}{\partial\varphi}\left(1-\mu\right)\frac{2\cos^2\theta}{r^3}\frac{\partial w}{\partial\varphi}-\frac{\partial D}{\partial\varphi}\frac{2\cos\theta}{r^2}\left(\left(1-\mu\right)+\left(1-\mu^2\right)\right)\frac{\partial\vartheta_1}{\partial\varphi}\\
&\quad+D\left(1-\mu\right)\frac{2\cos\theta\sin\theta}{r^3}\frac{\partial^2 u}{\partial\varphi^2}-\frac{\partial D}{\partial\varphi}\left(1-\mu^2\right)\frac{2\sin\theta}{r^3}\frac{\partial^2 v}{\partial\varphi^2}
\end{aligned}
$$

$$
\begin{aligned}
& -\left(D\left(1-\mu\right)\frac{2\cos^2\theta}{r^3}-\frac{\partial^2 D}{\partial\varphi^2}\left(1-\mu^2\right)\frac{1}{r^3}\right)\frac{\partial^2 w}{\partial\varphi^2} \\
& -D\left(1-\mu\right)\frac{2\cos\theta}{r^2}\frac{\partial^2\vartheta_1}{\partial\varphi^2}-\frac{\mu}{r^2}\frac{\partial^2\left(M_1 r\right)}{\partial\varphi^2}-D\left(1-\mu^2\right)\frac{\sin\theta}{r^3}\frac{\partial^3 v}{\partial\varphi^3} \\
& +\frac{\partial D}{\partial\varphi}\left(1-\mu^2\right)\frac{2}{r^3}\frac{\partial^3 w}{\partial\varphi^3}+D\left(1-\mu^2\right)\frac{1}{r^3}\frac{\partial^4 w}{\partial\varphi^4}-rq_3; \\
\frac{\partial\left(M_1 r\right)}{\partial s} = \; & D\left(1-\mu^2\right)\frac{\cos^2\theta}{r}\vartheta_1+\left(Q_1^* r\right)+\mu\frac{\cos\theta}{r}\left(M_1 r\right) \\
& +2\left(1-\mu\right)\frac{\partial D}{\partial\varphi}\frac{\sin\theta}{r^2}\frac{\partial u}{\partial\varphi}+D\left(1-\mu^2\right)\frac{\cos\theta\sin\theta}{r^2}\frac{\partial v}{\partial\varphi} \\
& -2\left(1-\mu\right)\frac{\partial D}{\partial\varphi}\frac{\cos\theta}{r^2}\frac{\partial w}{\partial\varphi}-2\left(1-\mu\right)\frac{\partial D}{\partial\varphi}\frac{1}{r}\frac{\partial\vartheta_1}{\partial\varphi} \\
& +2D\left(1-\mu\right)\frac{\sin\theta}{r^2}\frac{\partial^2 u}{\partial\varphi^2} \\
& -\left(2D\left(1-\mu\right)\frac{\cos\theta}{r^2}+D\left(1-\mu^2\right)\frac{\cos\theta}{r^2}\right)\frac{\partial^2 w}{\partial\varphi^2}-2D\left(1-\mu\right)\frac{1}{r}\frac{\partial^2\vartheta_1}{\partial\varphi^2}.
\end{aligned}
$$

3. Shells with Stiffness, Variable in two Directions

To solve system (2.4) in the case $h = h\left(s, \varphi\right)$, it is proposed to use the method of straight lines [2,4,7,12], the essence of which is to replace the derivatives in the direction of the circumferential coordinate by difference relations, which allows one to obtain a set of one-dimensional boundary value problems along each i-th meridian ($i = \overline{1, m}$), which are subsequently solved by the sweep method with orthogonalization according to S.K. Godunov [11] along the nodal points j ($j = \overline{1, n}$).

Assuming that the shell state parameters are sufficiently smooth in the circumferential direction, the partial derivatives with respect to the variable $\varphi = \varphi_i$, ($i = 1, 2, ..., m$) equations (2.4) are replaced by finite differences of the fourth order of accuracy [2]:

$$
\begin{aligned}
y' &= \left(y_{i-2}-8y_{i-1}+8y_{i+1}-y_{i+2}\right)/\left(12\Delta\right); \\
y'' &= \left(-y_{i-2}+16y_{i-1}-30y_i+16y_{i+1}-y_{i+2}\right)/\left(12\Delta^2\right); \\
y''' &= \left(y_{i-3}-8y_{i-2}+13y_{i-1}-13y_{i+1}+8y_{i+2}-y_{i+3}\right)/\left(8\Delta^3\right); \\
y'^{v} &= \left(-y_{i-3}+12y_{i-2}-39y_{i-1}+56y_i-39y_{i+1}+12y_{i+2}-y_{i+3}\right)/\left(6\Delta^4\right),
\end{aligned} \tag{3.1}
$$

where $\Delta = \Delta\varphi_i$ is the step of the difference grid in the circumferential direction with the approximation error $O\left(\Delta^4\right)$.

It should be noted that, depending on the method of replacing derivatives with finite differences, different systems of the method of lines are possible, which may differ in the accuracy of the approximating relations for the corresponding derivatives.

After replacing the derivatives with respect to the coordinate φ in the system of equations (2.4) and reducing similar terms for the components of the stress-strain state vector $\overline{Y} = (u,\, v,\, w,\, \vartheta_1,\, N_1 r,\, S_1^* r,\, Q_1^* r,\, M_1 r)^T$ for each i-th strip $(i = 1, 2, ..., m)$, we can obtain a boundary value problem for a system of ordinary differential equations.

Further (in order to avoid cumbersome presentation) such a system for the case of a cylindrical shell is given ($\sin\theta = 1,\ \cos\theta = 0, R_1 = \infty,\ R_2 = R$):

$$
\begin{aligned}
\frac{du_i}{ds} &= -\mu\frac{1}{r}w_i + \frac{1}{K_i r}(N_1 r)_i - \mu\frac{1}{r}\frac{1}{12\Delta}\left(v_{i-2} - 8v_{i-1} + 8v_{i+1} - v_{i+2}\right);\\
\frac{dv_i}{ds} &= \frac{2}{K_i\,(1-\mu)}\frac{1}{r}(S_1{}^* r)_i\\
&\quad -\left(\frac{1}{r} + \frac{4D_i}{K_i r^3}\right)\frac{1}{12\Delta}\left(u_{i-2} - 8u_{i-1} + 8u_{i+1} - u_{i+2}\right)\\
&\quad +\frac{4D_i}{K_i r^2}\frac{1}{12\Delta}\left(\vartheta_{1i-2} - 8\vartheta_{1i-1} + 8\vartheta_{1i+1} - \vartheta_{1i+2}\right);\\
\frac{dw_i}{ds} &= -\vartheta_{1i};\\
\frac{d\vartheta_{1i}}{ds} &= -\mu\frac{1}{r^2}\frac{30}{12\Delta^2}w_i + \frac{1}{D_i r}(M_1 r)_i\\
&\quad -\mu\frac{1}{r^2}\frac{1}{12\Delta}\left(v_{i-2} - 8v_{i-1} + 8v_{i+1} - v_{i+2}\right)\\
&\quad +\mu\frac{1}{r^2}\frac{1}{12\Delta^2}\left(-w_{i-2} + 16w_{i-1} + 16w_{i+1} - w_{i+2}\right);\\
\frac{d(N_1 r)_i}{ds} &= -\frac{2D_i\,(1-\mu)}{r^3}\frac{30}{12\Delta^2}u_i - \frac{2D_i\,(1-\mu)}{r^2}\frac{30}{12\Delta^2}\vartheta_{1i}\\
&\quad +\frac{2\,(1-\mu)}{r^3}\left(\frac{\partial D}{\partial\varphi}\right)_i\frac{1}{12\Delta}\left(u_{i-2} - 8u_{i-1} + 8u_{i+1} - u_{i+2}\right)\\
&\quad -\frac{2\,(1-\mu)}{r^2}\left(\frac{\partial D}{\partial\varphi}\right)_i\frac{1}{12\Delta}\left(\vartheta_{1i-2} - 8\vartheta_{1i-1} + 8\vartheta_{1i+1} - \vartheta_{1i+2}\right)\\
&\quad -\frac{1}{r}\frac{1}{12\Delta}(S^*{}_1)_{i-2}\\
&\quad +\frac{2D_i\,(1-\mu)}{r^3}\frac{1}{12\Delta^2}\left(-u_{i-2} + 16u_{i-1} + 16u_{i+1} - u_{i+2}\right)\\
&\quad -\frac{2D_i\,(1-\mu)}{r^2}\frac{1}{12\Delta^2}\left(-\vartheta_{1i-2} + 16\vartheta_{1i-1} + 16\vartheta_{1i+1} - \vartheta_{1i+2}\right) - rq_{1i};
\end{aligned}
\tag{3.2}
$$

$$
\begin{aligned}
\frac{\partial(S_1{}^* r)_i}{\partial s} &= -\left(\frac{\partial K}{\partial\varphi}\right)_i\left(1-\mu^2\right)\frac{1}{r}w - \left(1-\mu^2\right)\left(\frac{1}{r}\left(\frac{\partial K}{\partial\varphi}\right)_i + \frac{1}{r^3}\left(\frac{\partial D}{\partial\varphi}\right)_i\right)\\
&\quad \times\frac{1}{12\Delta}\left(v_{i-2} - 8v_{i-1} + 8v_{i+1} - v_{i+2}\right)\\
&\quad -K_i\left(1-\mu^2\right)\frac{1}{r}\frac{1}{12\Delta}\left(w_{i-2} - 8w_{i-1} + 8w_{i+1} - w_{i+2}\right)
\end{aligned}
$$

$$
\begin{aligned}
&-\mu\frac{1}{r}\frac{1}{12\Delta}\left((N_1r)_{i-2}-8(N_1r)_{i-1}+8(N_1r)_{i+1}-(N_1r)_{i+2}\right)\\
&-\mu\frac{1}{r^2}\frac{1}{12\Delta}\left((M_1r)_{i-2}-8(M_1r)_{i-1}+8(M_1r)_{i+1}-(M_1r)_{i+2}\right)\\
&-\left(1-\mu^2\right)\left(K_i\frac{1}{r}-D_i\frac{1}{r^3}\right)\frac{1}{12\Delta^2}\\
&\times\left(-v_{i-2}+16v_{i-1}-30v_i+16v_{i+1}-v_{i+2}\right)\\
&+\frac{1}{r^3}\left(1-\mu^2\right)\left(\frac{\partial D}{\partial\varphi}\right)_i\frac{1}{12\Delta^2}\\
&\times\left(-w_{i-2}+16w_{i-1}-30w_i+16w_{i+1}-w_{i+2}\right)+\\
&+\left(1-\mu^2\right)D_i\frac{1}{r^3}\frac{1}{8\Delta^3}\\
&\times\left(w_{i-3}-8w_{i-2}+16w_{i-1}-13w_{i+1}+8w_{i+2}-w_{i+3}\right)-rq_{2i};
\end{aligned}
$$

$$
\begin{aligned}
\frac{d(Q_1^*r)_i}{ds} \;=\;& \left(\frac{\partial D}{\partial\varphi}\right)_i\left(1-\mu^2\right)\frac{2}{r^3}\frac{30}{12\Delta^2}v_i+\left(1-\mu^2\right)\\
&\times\left(K_i\frac{1}{r}+\left(\frac{\partial^2 D}{\partial\varphi^2}\right)_i\frac{1}{r^3}\frac{1}{12\Delta^2}+D_i\frac{1}{r^3}\frac{56}{6\Delta^4}\right)w_i+\mu\frac{1}{r}(N_1r)_i\\
&+\frac{\mu}{r^2}\frac{30}{12\Delta}(M_1r)_i-\left(1-\mu^2\right)\frac{1}{r}\left(\left(\frac{\partial^2 D}{\partial\varphi^2}\right)_i\frac{1}{r^2}-K_i\right)\\
&\times\frac{1}{12\Delta}\left(v_{i-2}-8v_{i-1}+8v_{i+1}-v_{i+2}\right)\\
&-\left(\frac{\partial D}{\partial\varphi}\right)_i\left(1-\mu^2\right)\frac{2}{r^3}\frac{1}{12\Delta^2}\left(-v_{i-2}+16v_{i-1}+16v_{i+1}-v_{i+2}\right)\\
&-\left(\frac{\partial^2 D}{\partial\varphi^2}\right)_i\left(1-\mu^2\right)\frac{1}{r^3}\frac{1}{12\Delta^2}\left(-w_{i-2}+16w_{i-1}+16w_{i+1}-w_{i+2}\right)\\
&-\frac{\mu}{r^2}\frac{1}{12\Delta}\left((M_1r)_{i-2}+16(M_1r)_{i-1}+16(M_1r)_{i+1}-(M_1r)_{i+2}\right)\\
&-D_i\left(1-\mu^2\right)\frac{1}{r^3}\frac{1}{8\Delta^3}\\
&\times\left(v_{i-3}-8v_{i-2}+13v_{i-1}-13v_{i+1}+8v_{i+2}-v_{i+3}\right)\\
&+\left(\frac{\partial D}{\partial\varphi}\right)_i\left(1-\mu^2\right)\frac{2}{r^3}\frac{1}{8\Delta^3}\\
&\times\left(w_{i-3}-8w_{i-2}+13w_{i-1}-13w_{i+1}+8w_{i+2}-w_{i+3}\right)\\
&+D_i\left(1-\mu^2\right)\frac{1}{r^3}\frac{1}{6\Delta^4}\\
&\times\left(-w_{i-3}+12w_{i-2}-39w_{i-1}-39w_{i+1}+12w_{i+2}-w_{i+3}\right)-rq_{3i};
\end{aligned}
$$

$$
\begin{aligned}
\frac{d\left(M_1r\right)}{ds} \;=\;& -2D\left(1-\mu\right)\frac{1}{r^2}\frac{30}{12\Delta^2}u_i+2D\left(1-\mu\right)\frac{1}{r}\frac{30}{12\Delta^2}\vartheta_{1i}+(Q_1^*r)\\
&+2\left(1-\mu\right)\left(\frac{\partial D}{\partial\varphi}\right)_i\frac{1}{r^2}\frac{1}{12\Delta}\left(u_{i-2}-8u_{i-1}+8u_{i+1}-u_{i+2}\right)
\end{aligned}
$$

$$
\begin{aligned}
&-2\,(1-\mu)\left(\frac{\partial D}{\partial\varphi}\right)_i \frac{1}{r}\frac{1}{12\Delta}\left(\vartheta_{1i-2}-8\vartheta_{1i-1}+8\vartheta_{1i+1}-\vartheta_{1i+2}\right)\\
&+2D\,(1-\mu)\,\frac{1}{r^2}\frac{1}{12\Delta^2}\left(-u_{i-2}+16u_{i-1}+16u_{i+1}-u_{i+2}\right)\\
&-2D\,(1-\mu)\,\frac{1}{r}\frac{1}{12\Delta^2}\left(-\vartheta_{1i-2}+16\vartheta_{1i-1}+16\vartheta_{1i+1}-\vartheta_{1i+2}\right).
\end{aligned}
$$

Here,

$$
\begin{aligned}
\Delta=\Delta\varphi_i;\qquad \Delta\varphi_i&=2\pi/m;\qquad \varphi_i=\Delta\varphi_i\,(i-1)\,;\\
\left(\frac{\partial K}{\partial\varphi}\right)_i&=\frac{K_{i-2}-8K_{i-1}+8K_{i+1}-K_{i+2}}{12\Delta};\\
\left(\frac{\partial D}{\partial\varphi}\right)_i&=\frac{D_{i-2}-8D_{i-1}+8D_{i+1}-D_{i+2}}{12\Delta};\\
\left(\frac{\partial^2 D}{\partial\varphi^2}\right)_i&=\frac{-D_{i-2}+16D_{i-1}-30D_i+16D_{i+1}-D_{i+2}}{12\Delta^2}.
\end{aligned}
$$

As for the fulfillment of the boundary conditions, for the case of an open shell at the ends of the variation interval φ, one-sided differences are used, where for the straight lines 0 and m, the values of the parameters specified in accordance with the conditions for fixing the contour are taken into account. For a closed cylindrical shell, when the derivatives in the circumferential direction are replaced by their finite-difference expressions, only the central differences are used. The boundary conditions at the meridional edges of the shell ($s=0,\ s=L$ where L is the shell length) are taken into account when solving boundary value problems along the meridian $s=s_i$, $(i=1,2,...,n)$, using the sweep method with orthogonalization according to S.K. Godunov [11].

4. Rotational Shells with a Stiffness Variable Along Meridian

In the case $h=h\,(s)$ of separating variables, the Fourier method is used. At the same time, the problem of solving the system of partial differential equations (2.4) by expanding the components of the stress-strain state and load into trigonometric series in the circular coordinate [3,10,12,15], reduces, in the general case, to solving systems of $t+1$ ordinary differential equations for finding harmonics of expansions of the sought functions in Fourier series.

The decomposition of the load, displacements and forces acting in the shell into Fourier series [3, 15] along the circumferential coordinate φ is carried out in the form

$$
f=\sum_{k=0}^{\infty} f_k^c\cos k\varphi+\sum_{k=1}^{\infty} f_k^t\sin k\varphi;\qquad \psi=\sum_{k=1}^{\infty}\psi_k^c\sin k\varphi-\sum_{k=0}^{\infty}\psi_k^t\cos k\varphi \tag{4.1}
$$

where f, in the generally accepted notation [3], stands for the functions $u,\ w,$ $\varepsilon_1,\ \varepsilon_2,\ \vartheta_1,\ \chi_1,\ \chi_2,\ N_1, N_2, Q_1, M_1, M_2, q_1, q_3$, whereas ψ can be substituted by functions v, γ_{12}, ϑ_2, χ_{12}, $S, Q_2, M, q_2, f_k^c, f_k^t$, ψ_k^c, ψ_k^t, and f_k^c, f_k^t , ψ_k^c, ψ_k^t are the coefficients of their expansions in trigonometric series.

With this choice of functions, the expansion coefficients with the superscript t, which correspond to the skew-symmetric deformation of the shell with respect to the zero meridian, are determined by exactly the same system of equations as the coefficients with the index c, which correspond to the symmetric deformation. Therefore, the results of further transformations for these coefficients coincide, which allows them to be carried out only for functions with the index c, omitting this sign.

In this case, the displacements and forces that correspond to the k-th term of the expansion are determined by the formulas [3]

$$\begin{gathered}
u = u_k(s)\cos k\varphi; \qquad v = v_k(s)\sin k\varphi; \qquad w = w_k(s)\cos k\varphi;\\
\vartheta_1 = \vartheta_{1k}(s)\cos k\varphi; \qquad \vartheta_2 = \vartheta_{2k}(s)\sin k\varphi; \qquad N_1 = N_{1k}(s)\cos k\varphi;\\
S^* = S_k^*(s)\sin k\varphi; \qquad Q_1^* = Q_{1k}^*(s)\cos k\varphi; \qquad N_2 = N_{2k}(s)\cos k\varphi;\\
M_1 = M_{1k}(s)\cos k\varphi; \qquad M_2 = M_{2k}(s)\cos k\varphi; \qquad M = M_k(s)\sin k\varphi.
\end{gathered} \tag{4.2}$$

The use of the Fourier method (and this is possible only in the case when the shell wall thickness changes only in the meridional direction $h = h(s)$, and remains constant in the circumferential direction) makes it possible to reduce the adopted system of equations of state of the shell in partial derivatives to a system of ordinary differential equations with respect to the coefficients expansions in trigonometric series of the main variables of the stress-strain state, which are the coefficients of the expansion of displacements and force factors. In this case, it is convenient to take for the main unknowns their product by the radius r of the parallel circle $N_{1k}r(s),\ S_k^*r(s),\ Q_{1k}^*r(s),\ M_{1k}r(s))$:

$$\begin{aligned}
\frac{du_k}{ds} &= -\mu\frac{\cos\theta}{r}u_k - \mu\frac{k}{r}v_k - \left(\frac{1}{R_1} + \mu\frac{\sin\theta}{r}\right)w_k + \frac{1-\mu^2}{Ehr}(N_{1k}r);\\
\frac{dv_k}{ds} &= \frac{k}{r}u_k + \frac{\cos\theta}{r}v_k + \frac{2(1+\mu)}{Ehr}(S_k^*r);\\
\frac{dw_k}{ds} &= \frac{1}{R_1}u_k - \vartheta_{1k};\\
\frac{d\vartheta_{1k}}{ds} &= -\mu\frac{k}{r^2}\sin\theta v_k - \mu\frac{k^2}{r^2}w_k - \mu\frac{\cos\theta}{r}\vartheta_{1k} + \frac{12(1-\mu^2)}{Eh^3r}(M_{1k}r);\\
\frac{d(N_{1k}r)}{ds} &= -\frac{Eh}{r}\left[\cos^2\theta + \frac{k^2h^2\sin^2\theta}{6(1+\mu)r^2}\right]u_k + k\frac{Eh}{r}\cos\theta\nu_k\\
&\quad + \frac{Eh}{r}\sin\theta\cos\theta\left[1 - \frac{k^2h^2}{6(1+\mu)r^2}\right]w_k - \frac{k^2Eh^3}{6(1+\mu)r^2}\sin\theta\cdot\vartheta_{1k}\\
&\quad + \frac{\mu}{r}\cos\theta(N_{1k}r) - \frac{k}{r}\left(S_k^*r\right) - \frac{1}{R_1}\left(Q_{1k}^*r\right) - q_{1k}r;
\end{aligned}$$

$$\begin{aligned}
\frac{d\left(S_k^* r\right)}{ds} &= \frac{Eh}{r}k\cos\theta u_k + \frac{Eh}{r}k^2 v_k + \frac{Eh}{r}k\sin\theta\left(1+\frac{k^2h^2}{12r^2}\right)w_k \\
&+\frac{Eh^3}{12r^2}k\sin\theta\cos\theta\cdot\vartheta_{1k} + \mu\frac{k}{r}\left(N_{1k}r\right) - \frac{\cos\theta}{r}\left(S_k^* r\right) \\
&+\mu\frac{k}{r^2}\sin\theta\left(M_{1k}r\right) - q_{2k}r;
\end{aligned} \tag{4.3}$$

$$\begin{aligned}
\frac{d\left(Q_{1k}^* r\right)}{ds} &= \frac{Eh}{r}\sin\theta\cos\theta\left[1-\frac{k^2h^2}{6(1+\mu)r^2}\right]u_k + \frac{Eh}{r}k\sin\theta\left(1+\frac{k^2h^2}{12r^2}\right)v_k \\
&+\frac{Eh}{r}\left[\sin^2\theta + \frac{k^4h^2}{12r^2} + \frac{k^2h^2\cos^2\theta}{6(1+\mu)r^2}\right]w_k \\
&+\frac{3+\mu}{1+\mu}\cdot\frac{Eh^3}{12r^2}k^2\cos\theta\cdot\vartheta_{1k} + \left(\frac{1}{R_1}+\mu\frac{\sin\theta}{r}\right)\left(N_{1k}r\right) \\
&+\mu\frac{k^2}{r^2}\left(M_{1k}r\right) - q_{3k}r; \\
\frac{d\left(M_{1k}\cdot r\right)}{ds} &= -\frac{k^2Eh^3}{6(1+\mu)r^2}\sin\theta\cdot u_k + \frac{Eh^3}{12r^2}k\sin\theta\cos\theta\cdot v_k \\
&+\frac{3+\mu}{1+\mu}\frac{Eh^3}{12r^2}k^2\cos\theta\cdot w_k + \frac{Eh^3}{12r}\left(\cos^2\theta+\frac{12k^2}{1+\mu}\right)\vartheta_{1k} \\
&+\left(Q_{1k}^* r\right) + \mu\frac{\cos\theta}{r}\left(M_{1k}\cdot r\right).
\end{aligned}$$

The expansion coefficients of displacements and forces for each harmonic number k, which are not the main variables, using the relations of the theory of elasticity and the dependences between displacements and deformations, are expressed in terms of the main variables as follows:

$$\begin{aligned}
\vartheta_{2k} &= \left(\frac{\sin\theta}{r}v_k + \frac{k}{r}w_k\right)\sin k\varphi; \\
N_{2k} &= \left[\mu N_{1k} + Eh\left(\frac{k}{r}v_k + \frac{\cos\theta}{r}u_k + \frac{\sin\theta}{r}w_k\right)\right]\cos k\varphi; \\
M_{2k} &= \left[\mu M_{1k} + \frac{Eh^3}{12}\left(\frac{\cos\theta}{r}\vartheta_{1k} + \frac{k}{r^2}\sin\theta v_k + \frac{k^2}{r^2}w_k\right)\right]\cos k\varphi; \\
M_k &= D\left(-\frac{k}{r}\vartheta_{1k} - \frac{k\cos\theta}{r^2}w_k + \frac{k\sin\theta}{r^2}u_k\right)\sin k\varphi.
\end{aligned} \tag{4.4}$$

The inconvenience of the system of equations (4.3) is that the forces and displacements are related to the local coordinate system associated with the normal and tangent to the shell meridian. Therefore, the coefficients of the system have discontinuities when the shell meridian consists of several sections with corner points between them. In this case, it turns out to be necessary to draw up compatibility equations for different areas.

These difficulties, in accordance with [3], can be circumvented by passing to global coordinates. For this, forces and displacements are projected onto the normal to the shell's symmetry axis and onto the axis itself. In this case, instead of displacements $u,\ w$, displacements $\xi,\ \zeta$ are introduced, and instead of forces $N_1,\ Q_1^*,\ X,\ Z$ forces are introduced as follows:

$$\begin{aligned} \xi &= u\cos\theta + w\sin\theta; \qquad & \zeta &= u\sin\theta - w\cos\theta; \\ X &= N_1\cos\theta + Q_1^*\sin\theta; \qquad & Z &= N_1\sin\theta - Q_1^*\cos\theta. \end{aligned} \tag{4.5}$$

The same dependencies are also related to the coefficients of the expansion in the Fourier series of the corresponding functions. Substitution of $u_k,\ w_k,\ N_{1k},\ Q_{1k}^*$ and their derivatives through $\xi_k,\ \zeta_k,\ X_k,\ Z_k$ into system (4.3) brings it to the form:

$$\begin{aligned}
\frac{d\xi_k}{ds} &= -\mu\frac{\cos\theta}{r}\xi_k - \mu\frac{k\cos\theta}{r}v_k - \sin\theta\cdot\vartheta_{1k} + \frac{1-\mu^2}{Eh}\frac{\cos^2\theta}{r}(X_k r) \\
&\quad + \frac{1-\mu^2}{Eh}\frac{\sin\theta\cos\theta}{r}(Z_k r); \\
\frac{d\zeta_k}{ds} &= -\mu\frac{\sin\theta}{r}\xi_k - \mu\frac{k\sin\theta}{r}v_k + \cos\theta\cdot\vartheta_{1k} \\
&\quad + \frac{1-\mu^2}{Eh}\frac{\sin\theta\cdot\cos\theta}{r}(X_k r) + \frac{1-\mu^2}{Eh}\frac{\sin^2\theta}{r}(Z_k r); \\
\frac{dv_k}{ds} &= k\frac{\cos\theta}{r}\xi_k + k\frac{\sin\theta}{r}\zeta_k + \frac{\cos\theta}{r}v_k + \frac{2(1+\mu)}{Ehr}(S_k^*\cdot r); \\
\frac{d\vartheta_{1k}}{ds} &= -\mu k^2\frac{\sin\theta}{r^2}\xi_k + \mu k^2\frac{\cos\theta}{r^2}\zeta_k - \mu k\frac{\sin\theta}{r^2}v_k - \mu\frac{\cos\theta}{r}\vartheta_{1k} \\
&\quad + \frac{12(1-\mu^2)}{Eh^3 r}(M_{1k}\cdot r); \\
\frac{d\,(X_k\cdot r)}{ds} &= \frac{Eh}{r}\left(1 + \frac{h^2k^4}{12r^2}\sin^2\theta\right)\xi_k - \frac{Eh^3}{12}\cdot\frac{k^4\sin\theta\cdot\cos\theta}{r^3}\zeta_k \\
&\quad + \frac{Ehk}{r}\left(1 + \frac{h^2k^2}{12r^2}\sin^2\theta\right)v_k + \frac{Eh^3k^2}{12}\cdot\frac{\sin\theta\cdot\cos\theta}{r^2}\vartheta_{1k} \\
&\quad + \mu\frac{\cos\theta}{r}(X_k\cdot r) + \mu\frac{\sin\theta}{r}(Z_k\cdot r) - k\frac{\cos\theta}{r}(S_k^*\cdot r) \\
&\quad + \mu k^2\frac{\sin\theta}{r^2}(M_{1k}\cdot r) - rq_{xk};
\end{aligned}$$

$$\begin{aligned}
\frac{d\,(Z_k\cdot r)}{ds} &= -k^4\frac{Eh^3}{12}\cdot\frac{\sin\theta\cdot\cos\theta}{r^3}\xi_k + \frac{Eh^3}{12r^3}\left(\frac{2k^2}{1+\mu} + k^4\cos^2\theta\right)\zeta_k \\
&\quad - \frac{Eh^3k^3}{12}\cdot\frac{\sin\theta\cdot\cos\theta}{r^3}v_k - \frac{Eh^3k^2}{12}\cdot\frac{2+(1+\mu)\cos^2\theta}{(1+\mu)r^2}\vartheta_{1k} \\
&\quad - k\frac{\sin\theta}{r}(S_k^*\cdot r) - \mu k^2\frac{\cos\theta}{r^2}(M_{1k}\cdot r) - rq_{zk};
\end{aligned} \tag{4.6}$$

$$
\begin{aligned}
\frac{d\left(S_k^{*}\cdot r\right)}{ds} \quad = \quad & \frac{Ehk}{r}\left(1+\frac{h^2k^2}{12r^2}\sin^2\theta\right)\xi_k-\frac{Eh^3k^3}{12}\cdot\frac{\sin\theta\cdot\cos\theta}{r^3}\zeta_k \\
& +\frac{Ehk^2}{r}\upsilon_k+\frac{Eh^3k}{12r^2}\cdot\sin\theta\cdot\cos\theta\cdot\vartheta_{1k}+\mu k\frac{\cos\theta}{r}(X_kr) \\
& +\mu\frac{k\sin\theta}{r}(Z_k\cdot r)-\frac{\cos\theta}{r}(S_k\cdot r)+\mu\frac{k\sin\theta}{r^2}(M_{1k}\cdot r)-rq_{2k};
\end{aligned}
$$

$$
\begin{aligned}
\frac{d\left(M_{1k}\cdot r\right)}{ds} \quad = \quad & \frac{Eh^3k^2}{12}\cdot\frac{\sin\theta\cdot\cos\theta}{r^2}\xi_k-\frac{Eh^3k^2}{12}\frac{2+(1+\mu)\cos^2\theta}{(1+\mu)r^2}\zeta_k \\
& +\frac{Eh^3k}{12}\cdot\frac{\sin\theta\cdot\cos\theta}{r^2}\upsilon_k+\frac{Eh^3}{12r}\left(\cos^2\theta+\frac{2k^2}{1+\mu}\right)\vartheta_{1k} \\
& +\sin\theta(X_kr)-\cos\theta(Z_kr)-\mu\frac{\cos\theta}{r}(M_{1k}\cdot r)
\end{aligned}
$$

where the following designations are introduced for the radial and axial loading components

$$q_{xk}=q_{1k}\cos\theta+q_{3k}\sin\theta;\qquad q_{zk}=q_{1k}\sin\theta-q_{3k}\cos\theta. \tag{4.7}$$

Since the coefficients of the resulting system of equations do not contain the curvature $1/R_1$ of the meridian, they remain continuous even for a shell whose curvature is subject to discontinuity. As a consequence, the main unknowns, referred to a fixed coordinate system, remain continuous for an arbitrary shape of the meridian, including for combined shell, which makes it possible not to compose the docking equations for such cases. As for the force unknowns $X_kr, Z_kr, S_k^{*}r$, $M_{1k}r$, they experience discontinuity of a predetermined magnitude only where concentrated forces are applied to the shells at a specific parallel of the load.

The specified forces and displacements at the ends of the shell are the boundary conditions for the resulting system, which are also decomposed into the corresponding trigonometric series along the circumferential coordinate.

5. Shells with Two-Sided Relative to the Reference Surface Change in Wall Thickness

Let us consider the case of the shell wall thickness $\delta(s)$ variable along the meridian under axisymmetric loading. In this case, both the external and internal components of the shell wall thickness with respect to the reference surface are independent functions of the meridional coordinate s. Let us denote by $H(s)$ and $h(s)$ the distances along the normal direction from the reference surface to the outer and inner surfaces of the shell, respectively, and $h^{*}(s)$ the distance from the middle surface to the reduced surface (Fig. 5.2), so that

$$H(s)-h^{*}(s)=\frac{\delta(s)}{2};\qquad h(s)+h^{*}(s)=\frac{\delta(s)}{2}; \tag{5.1}$$
$$h^{*}(s)=\frac{(H(s)-h(s))}{2}.$$

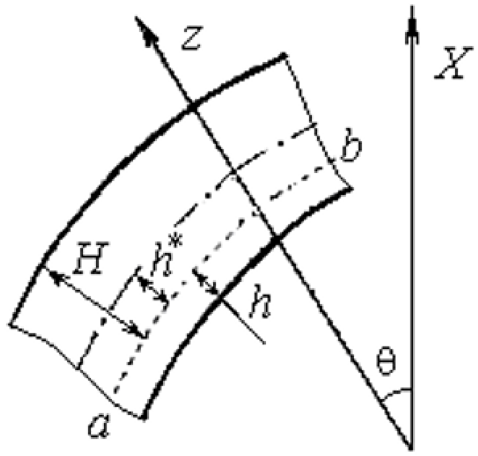

Fig. 5.2. Position of the reference surface (dashed line) relative to the middle surface (dash-dotted line)

It is also assumed that the error associated with the mismatch of the normal to the middle surface and the reference surface can be neglected for thin-walled shells.

Taking into account that the deformations $\varepsilon_1, \varepsilon_2$ and parameters of changing the curvatures χ_1, χ_2 of the reference surface are expressed through the deformations of the middle surface as follows $\varepsilon_1 = \varepsilon_{1cp} - h^*\chi_1$, $\varepsilon_2 = \varepsilon_{2cp} - h^*\chi_2$ (Fig. 5.2), the relationship between stresses and deformations on the reference surface in accordance with Hooke's law will have the form

$$\begin{aligned} \sigma_1 &= \frac{E}{1-\mu^2}\left((\varepsilon_1 + \mu\varepsilon_2) + z\left(\chi_1 + \mu\chi_2\right)\right); \\ \sigma_2 &= \frac{E}{1-\mu^2}\left((\varepsilon_2 + \mu\varepsilon_1) + z\left(\chi_2 + \mu\chi_1\right)\right). \end{aligned} \tag{5.2}$$

Note that expressions (5.2) at $z = h^*$ coincide with the well-known [3] expressions for calculating the stresses on the middle surface.

Internal forces and moments relative to the reference surface, taking into account the known dependencies

$$\begin{aligned} N_1 &= \int_{-h}^{H} \sigma_1 dz; \qquad N_2 = \int_{-h}^{H} \sigma_2 dz; \\ M_1 &= \int_{-h}^{H} \sigma_1 z dz; \qquad M_2 = \int_{-h}^{H} \sigma_2 z dz, \end{aligned} \tag{5.3}$$

and relations (5.2) after introducing the notation

$$K_1 = \frac{E(H+h)}{(1-\mu^2)}; \qquad K_2 = \frac{E(H^2-h^2)}{2(1-\mu^2)}; \qquad D = \frac{E}{1-\mu^2}\frac{H^3+h^3}{3} \tag{5.4}$$

will be next:

$$\begin{aligned} N_1 &= K_1\left(\varepsilon_1+\mu\varepsilon_2\right)+K_2\left(\chi_1+\mu\chi_2\right); \\ N_2 &= K_1\left(\varepsilon_2+\mu\varepsilon_1\right)+K_2\left(\chi_2+\mu\chi_1\right); \end{aligned} \tag{5.5}$$

$$\begin{aligned} M_1 &= K_2\left(\varepsilon_1+\mu\varepsilon_2\right)+D\left(\chi_1+\mu\chi_2\right); \\ M_2 &= K_2\left(\varepsilon_2+\mu\varepsilon_1\right)+D\left(\chi_2+\mu\chi_1\right). \end{aligned} \tag{5.6}$$

Considering that $N_1\sin\theta-Q_1\cos\theta=F(s)$; $N_1\cos\theta+Q_1\sin\theta=N$, (Fig. 2.1) we represent the efforts $N_1$and Q_1 in the form

$$N_1=\frac{F(s)}{2\pi r}\sin\theta+N\cos\theta; \qquad Q_1=-\frac{F(s)}{2\pi r}\cos\theta+N\sin\theta, \tag{5.7}$$

where N is the spacer force; $F(s)=P_0+\int_{s_0}^{s_n}\left(q_n\cos\theta-q_1\sin\theta\right)2\pi r ds$ is total axial loading; P_0 is axial load; $q_n,\ q_1$ is distributed normal and meridian loads, respectively.

We take as the main variables the radial displacement ξ, the angle of rotation of the normal ϑ, the axial displacement ζ, as well as the spacer force Nr and moment M_1r multiplied by the radius of the parallel circle.

Eliminating from (5.5) taking into account

$$\varepsilon_2=\frac{\xi}{r}; \qquad \chi_1=\frac{d\vartheta}{ds}; \quad \chi_2=\frac{\cos\theta}{r}\vartheta; \qquad \frac{1}{R_1}=\frac{d\theta}{ds}; \quad \frac{1}{R_2}=\frac{\sin\theta}{r}. \tag{5.8}$$

we obtain

$$N_2=\mu N_1+K_1(1-\mu^2)\frac{\xi}{r}+K_2(1-\mu^2)\frac{\cos\theta}{r}\vartheta. \tag{5.9}$$

Similarly, relations (5.6) yield the expression for M_2

$$M_2=\mu M_1+K_2(1-\mu^2)\frac{\xi}{r}+D(1-\mu^2)\frac{\cos\theta}{r}\vartheta. \tag{5.10}$$

From equation (5.5), taking into account (5.7), (5.8), we obtain

$$\varepsilon_1=\frac{1}{K_1}\left(\frac{F(s)}{2\pi r}\sin\theta+N\cos\theta\right)-\mu\frac{\xi}{r}-\frac{K_2}{K_1}\left(\frac{d\vartheta}{ds}+\mu\frac{\cos\theta}{r}\vartheta\right). \tag{5.11}$$

Substituting further (5.7), (5.8), (5.11) into (5.6), we obtain

$$M_1=\frac{K_2}{K_1}\left(\frac{\cos\theta}{r}Nr+\frac{\sin\theta}{r}\frac{F(s)}{2\pi}\right)+\left(D-\frac{K_2^2}{K_1}\right)\left(\frac{d\vartheta}{ds}+\mu\frac{\cos\theta}{r}\vartheta\right),$$

from which one of the equations of the system of state follows

$$\begin{aligned} \frac{d\vartheta}{ds} \;=\; & -\mu\frac{\cos\theta}{r}\vartheta-\left(\frac{K_2}{DK_1-K_2^2}\right)\frac{\cos\theta}{r}Nr+ \\ & +\left(\frac{K_1}{DK_1-K_2^2}\right)\frac{M_1r}{r}-\left(\frac{K_2}{DK_1-K_2^2}\right)\frac{\sin\theta}{r}\frac{F(s)}{2\pi}. \end{aligned} \tag{5.12}$$

Next, we take into account the equilibrium equations (2.3), which for the axisymmetric case can be represented in the form

$$\frac{1}{r}\frac{d}{ds}(Q_1 r) - \frac{N_1}{R_1} - \frac{N_2}{R_2} + q_n = 0; \tag{5.13}$$

$$\frac{1}{r}\frac{d}{ds}(N_1 r) - N_2\frac{\cos\theta}{r} + \frac{Q_1}{R_1} + q_1 = 0; \tag{5.14}$$

$$\frac{1}{r}\frac{d}{ds}(M_1 r) - M_2\frac{\cos\theta}{r} - Q_1 = 0. \tag{5.15}$$

Substitution of the found expressions (5.5), (5.7)–(5.9) into equation (5.13) gives one more equation of the system

$$\begin{aligned}\frac{d\xi}{dS} &= -\mu\frac{\cos\theta}{r}\xi - \vartheta\sin\theta + \frac{D}{DK_1 - K_2^2}\frac{\cos^2\theta}{r}Nr \\ &+\frac{K_2}{DK_1 - K_2^2}\frac{\sin\theta}{r}M_1 r + \frac{D}{DK_1 - K_2^2}\frac{\sin\theta\cos\theta}{r}\frac{F(s)}{2\pi}.\end{aligned} \tag{5.16}$$

The following equation is obtained from (5.14) after substituting into it the values of the variables from (5.7)–(5.9), taking into account that

$$\begin{aligned}\frac{d}{ds}\left(\frac{F(s)}{2\pi}\right) &= (q_n\cos\theta - q_1\sin\theta)2\pi r; \\ \frac{d\,(Nr)}{ds} &= K_1(1-\mu^2)\frac{\xi}{r} + K_2(1-\mu^2)\frac{\cos\theta}{r}\vartheta \\ &+\mu\frac{\cos\theta}{r}(Nr) + \mu\frac{\sin\theta}{r}\frac{F(s)}{2\pi} - q_r r\end{aligned} \tag{5.17}$$

where $q_r = q_1\cos\theta + q_n\sin\theta$.

Substituting into (5.15) the expression for and from (5.6), (5.7), we obtain

$$\begin{aligned}\frac{d\,(M_1 r)}{dr} &= K_2\left(1-\mu^2\right)\frac{\cos\theta}{r}\xi + D\left(1-\mu^2\right)\frac{\cos^2\theta}{r}\vartheta \\ &+\sin\theta\,(Nr) + \mu\frac{\cos\theta}{r}(M_1 r) - \cos\theta\frac{F(s)}{2\pi}.\end{aligned} \tag{5.18}$$

To determine the axial displacement, the expression for (5.11) is substituted into the equation of continuity of deformations, which will have the form

$$\begin{aligned}\frac{d\zeta}{ds} &= -\mu\frac{\sin\theta}{r}\xi + \vartheta\cos\theta + \frac{D}{DK_1 - K_2^2}\frac{\sin\theta\cos\theta}{r}(Nr) \\ &-\frac{K_2}{DK_1 - K_2^2}\frac{\sin\theta}{r}(M_1 r) + \frac{D}{DK_1 - K_2^2}\frac{\sin^2\theta}{r}\frac{F(s)}{2\pi}.\end{aligned} \tag{5.19}$$

Thus, the obtained equations (5.14) , (5.12), (5.17) – (5.19) form a system of differential equations with variable coefficients, which describes the stress-strain state of shells of revolution with a two-sided, relative to the reference surface, change along the meridian wall thickness.

For the particular case, when the reference surface coincides with the median, that is $h^*(s) = 0$, it follows that $H(s) = h(s)$. Then (5.4) will have the form $K_1 = E\delta / \left(1-\mu^2\right)$, $K_2 = 0$, $D = E\delta^3 / \left(12\left(1-\mu^2\right)\right)$, where $\delta\left(s\right) = H\left(s\right) + h\left(s\right)$ is the shell thickness, and the system of the obtained equations coincides with the well-known system of equations given in [3].

The boundary conditions are the conditions for fixing the ends of the shell. For the numerical solution of the obtained boundary value problem for a system of ordinary differential equations with variable (due to a change in the shell wall thickness) coefficients under the given boundary conditions, a sufficiently effective and repeatedly tested in the problems of mechanics of thin-walled structures [3, 12, 15] are used the sweep method of S. K. Godunov [11].

Conclusion.

The article presents correct mathematical models describing the state of asymmetrically loaded shells of revolution with variable wall thickness in the meridian and circumferential directions, only along the meridian, as well as with a two-sided change in the wall thickness relative to the reference surface. For all considered cases, boundary value problems for systems of ordinary differential equations with variable coefficients are constructed, the numerical solution of which is carried out by the sweep method.

References

1. A.A. Alyamovsky, *SolidWorks, COSMOSWorks, Finite Element Engineering Analysis*, DMK Press, Moscow, 2004.
2. I. Babushka, E. Vitasek, M. Prager, *Numerical processes for solving differential equations: monograph*, Mir, Moscow, 1996.
3. V.L. Biderman, *Mechanics of thin-walled structures*, Mashinostroenie, Mosscow, (1977).
4. P.I. Bulakaev, A.P. Dzyuba, I.A. Safronova, *Discrete-continuous algorithm for the construction of a stress-strain state of rotation shells variable in two directions of rigidity*, Problems of computational mechanics and strength of structures, Collection of scientific articles, **16** (2011), 69–78.
5. A.F. Dashchenko, D.V. Lazareva, N.G. Suryaninov, *ANSYS in the problems of mechanical engineering: monograph. second ed.*, Burun and Ko., Kharkiv, 2011.
6. A.P. Dzyuba, L.D. Levitina, A.A. Dzyuba, Yu.A. Korennov, *Equations of state for rotaition shells with a two-sided change in wall thickness relative to the reference surface*, Solution methods of applied problems in the mechanics of deforming solid bodies, **12**(2011), 106–112.
7. A.P. Dzyuba, I.A. Safronova, L.D. Levitina, *Calculation algorithm on the basis of a discrete-continuous approach for cylindrical shell of variable rigidity in circular direction*, Problems of computational mechanics and strength of structures, Collection of scientific articles, **30**(2019), 53–67.

8. A.P. Dzyuba, I.A. Safronova, L D. Levitina, *Algorithm for computational costs reducing in problems of calculation of asymmetrically loaded shells of rotation*, J. Strength of Materials and Theory of Structures, **105**(2020), 99–113.
9. A.P. Dzyuba, V.N. Sirenko, A.A. Dzyuba, I.A. Safronova, *Models and algorithms for optimization of elements of nonuniform shell structures in N. V. Polyakov (Eds.), Actual problems of mechanics: Monograph*, Lira, Dnipro,**2018**, 225–242.
10. I.G. Emelyanov, *Application of discrete Fourier series to the stress analysis of shell structures*, J. Computational Continuum Mechanics, **8(3)**(2015), 245–253.
11. S.K. Godunov, *On the numerical solution of boundary value problems for systems of linear ordinary differential equations*, J. Advances in Mathematical Sciences, **16**(3(99))(1961), 171–174.
12. Ya.M. Grigorenko, A.P. Mukoed, *Solving the problems of shell theory on a computer*, High School, Kiev, 1979.
13. Ya.M. Grigorenko, A.T. Vasilenko, *Methods for calculating shells. Theory of shells of variable rigidity*, Naukova Dunka, Kiev, 1981.
14. A.Ya. Grigorenko, N.P. Yaremchenko, C.N. Yaremchenko, *Stress-strain state of shallow rectangular shells of variable thickness under various boundary conditions*, Bul. of NAS Ukraine, **6**(2016), 31–37.
15. V.I. Myachenkov, I.V. Grigoryev, *Calculation of compound shell structures on a computer: Reference*, Mashinostroenie, Moscow, 1981.
16. I.G. Ovchinnikov, Yu.M. Pochtman, *Thin-walled structures under conditions of corrosion wear: Calculation and optimization*, *DNU*, Dnepropetrovsk, 1995.
17. N.F. Sineva, F.S. Selivanov, D.V. Nikityuk, *Calculation of a cylindrical shell of variable stiffness interacting with a nonlinear elastic base*, Bull. Saratov State Techn. Un-ty, Ser.: Construction and architecture, **4(60)** (2)(2011), 15–21.
18. G.P. Tolstov, *Fourier Series*, Fizmatgiz, Moscow, 1960.

Received 22.05.2021

Journal of Optimization, Differential Equations and Their Applications

Volume 29 Issue 1 June 2021

For notes

Journal of Optimization, Differential Equations and Their Applications

---

Volume 29 **Issue 1** **June 2021**

JODEA will publish carefully selected, longer research papers on mathematical aspects of optimal control theory and optimization for partial differential equations and on applications of the mathematic theory to issues arising in the sciences and in engineering. Papers submitted to this journal should be correct, innovative, non-trivial, with a lucid presentation, and of interest to a substantial number of readers. Emphasis will be placed on papers that are judged to be specially timely, and of interest to a substantial number of mathematicians working in this area.

Instruction to Authors:

Manuscripts should be in English and submitted electronically, pdf format to the member of the Editorial Board whose area, in the opinion of author, is most closely related to the topic of the paper and the same time, copy your submission email to the Managing Editor. Submissions can also be made directly to the Managing Editor.

Submission of a manuscript is a representation that the work has not been previously published, has not been copyrighted, is not being submitted for publication elsewhere, and that its submission has been approved by all of the authors and by the institution where the work was carried out. Furthermore, that any person cited as a source of personal communications has approved such citation, and that the authors have agreed that the copyright in the article shall be assigned exclusively to the Publisher upon acceptance of the article.

Manuscript style: Number each page. Page 1 should contain the title, authors names and complete affiliations. Place any footnote to the title at the bottom of Page 1. Each paper requires an abstract not exceeding 200 words summarizing the techniques, methods and main conclusions. AMS subject classification must accompany all articles, placed at Page 1 after Abstract. E-mail addresses of all authors should be placed together with the corresponding affiliations. Each paper requires a running head (abbriviated form of the title) of no more than 40 characters.

Equations should be centered with the number placed in parentheses at the right margin.

Figures must be drafted in high resolution and high contrast on separate pieces of white paper, in the form suitable for photographic reproduction and reduction.

References should be listed alphabetically, typed and punctuated according to the following examples:

1. S. N. Chow, J. K. Hale, *Methods od Bifurcation Theory*, *Springer-Verlad*, New York, 1982.
2. J. Serrin, *Gradient estimates for solutions of nonlinear elliptic and parabolic equations*, in "Contributions to Nonlinear Functional Analysis,"(ed. E.H. Zarantonello), *Academic Press* (1971).
3. S. Smale, *Stable manifolds for differential equations and diffeomorphisms*, *Ann. Scuola Norm. Sup. Pisa Cl.Sci.*, **18** (1963), 97–116.

For journal abbreviations used in bibliographies, consult the list of serials in the latest *Mathematical Reviews* annual index.

Final version of the manuscript should be typeset using LaTeX which can shorten the production process. Files of sample papers can be downloaded from the Journal's home page, where more information on how to prepare TeX files can be found.

Journal of Optimization, Differential Equations and Their Applications

Volume 29 **Issue 1** **June 2021**

ISSN 2617-0108

CONTENTS

V. L. Borsch, P. I. Kogut. Solutions to a Simplified Initial Boundary Value Problem for 1D Hyperbolic Equation with Interior Degeneracy 1

V. V. Pichkur, V. V. Sobchuk. Mathematical Model and Control Design of a Functionally Stable Technological Process 32

E. L. Hart, B. I. Terokhin. Computer Simulation of the Stress-Strain State of the Plate with Circular Hole and Functionally Graded Inclusion 42

P. I. Kogut, O. P. Kupenko, M. V. Uvarov. On Increasing of Resolution of Satellite Images via Their Fusion with Imagery at Higher Resolution 54

A. A. Dzyuba, A. P. Dzyuba, L. D. Levitina, I. A. Safronova. Mathematical Simulations of Deformation for the Rotation Shells with Variable Wall Thickness ... 79